Progress in Vacuum Pressure Measurement

Dr. Martin Wüest

Balzers, Principality of Liechtenstein

Overview

- Historical Development, Drivers
- The most common vacuum gauge types
- Example of improving our product using rarefied gas dynamics
- Optical pressure sensing

What is Vacuum?

Particle density [#/cm^3]

241

2.4 E22

2.4 E25

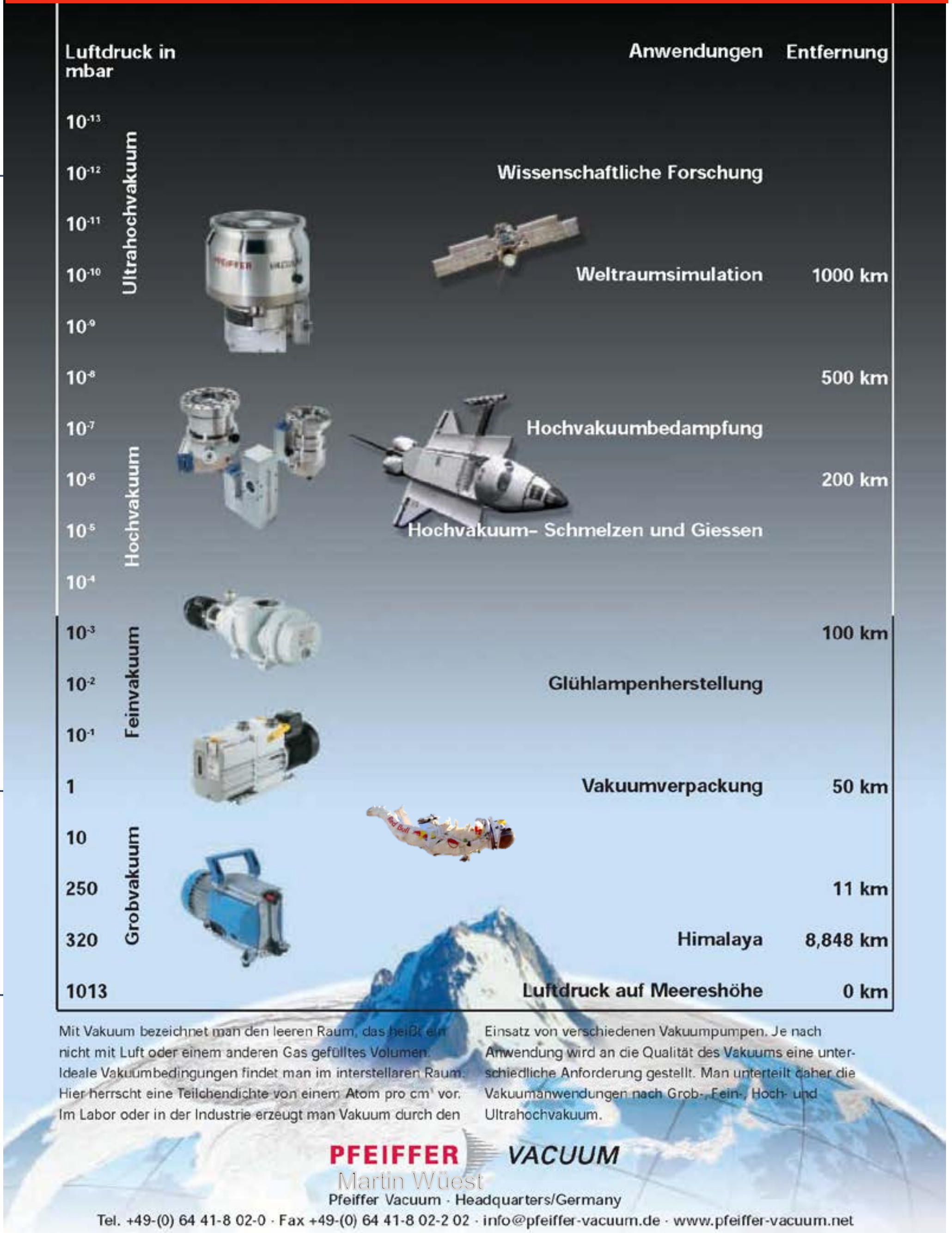

Early History

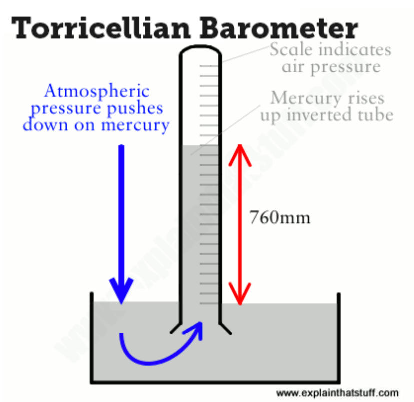

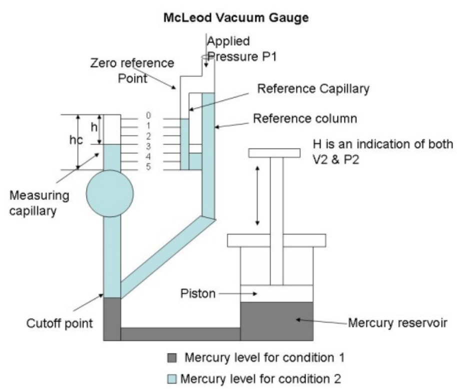

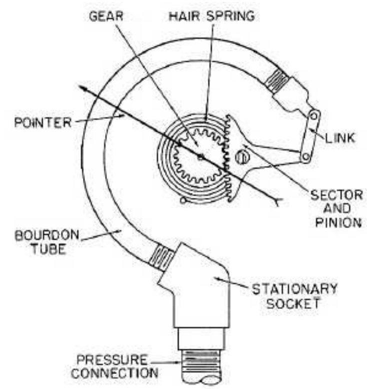

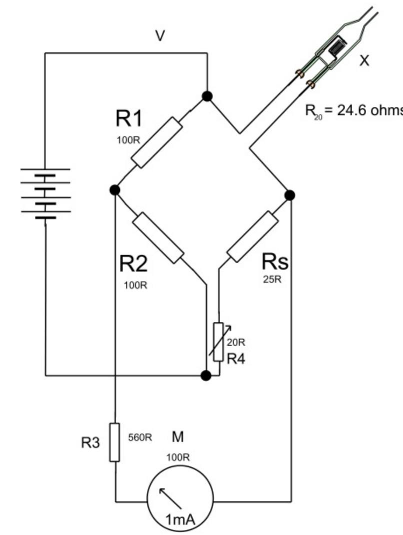

Barometer

1643 – 1860+

McLeod

1874 – 1916+

Bourdon

1849 -

mechanical

Pirani

1906 -

electrical

The Quest for the Ultimate Vacuum

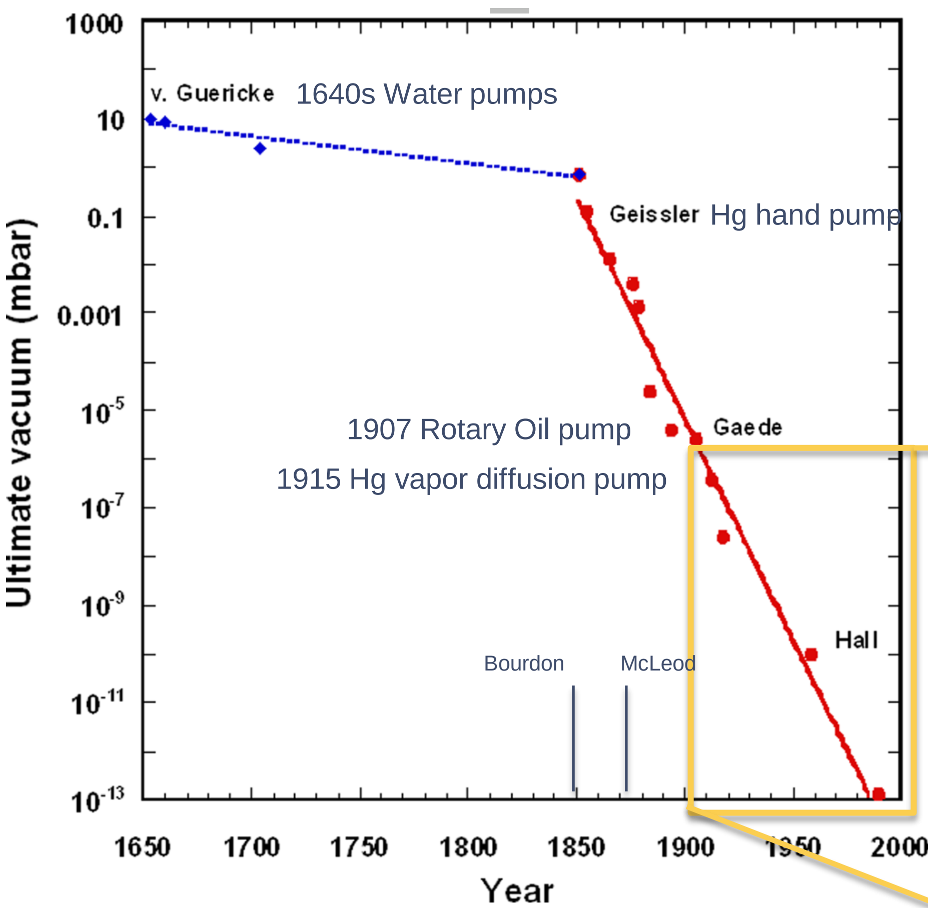

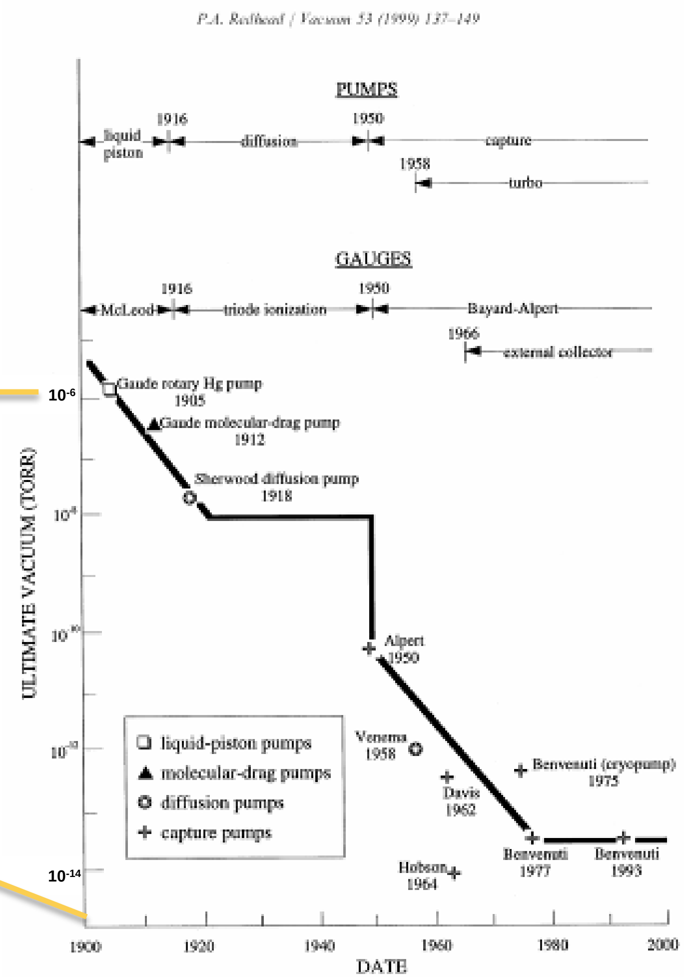

Georg Gaertner
J. Vac. Sci. Technol. B 30, 060801 (2012); doi: 10.1116/1.4747705

P.A. Redhead, Vacuum 53, 137 (1999)

Changing Markets

- Incandescent Lights

- Semiconductor

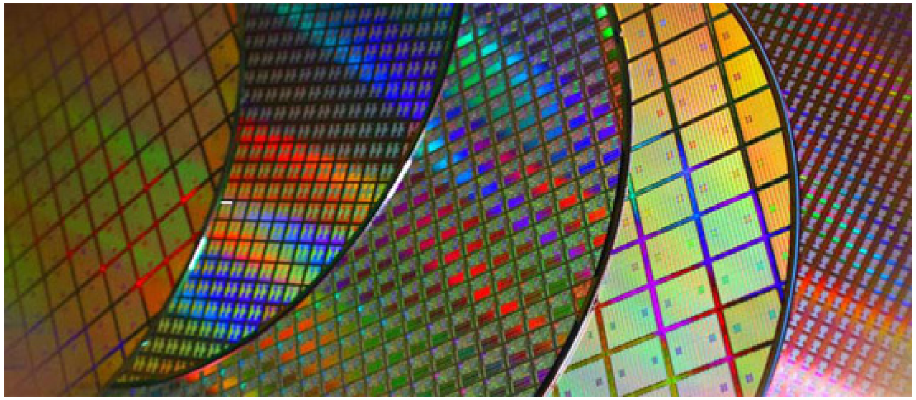

http://www.chineselight.com/uploads/130107/1_114009_1.jpg
http://www.kitguru.net/wp-content/uploads/2014/07/semiconductor_umc_wafers.jpg

The Quest for Reproducibility

Semiconductor Manufacturing

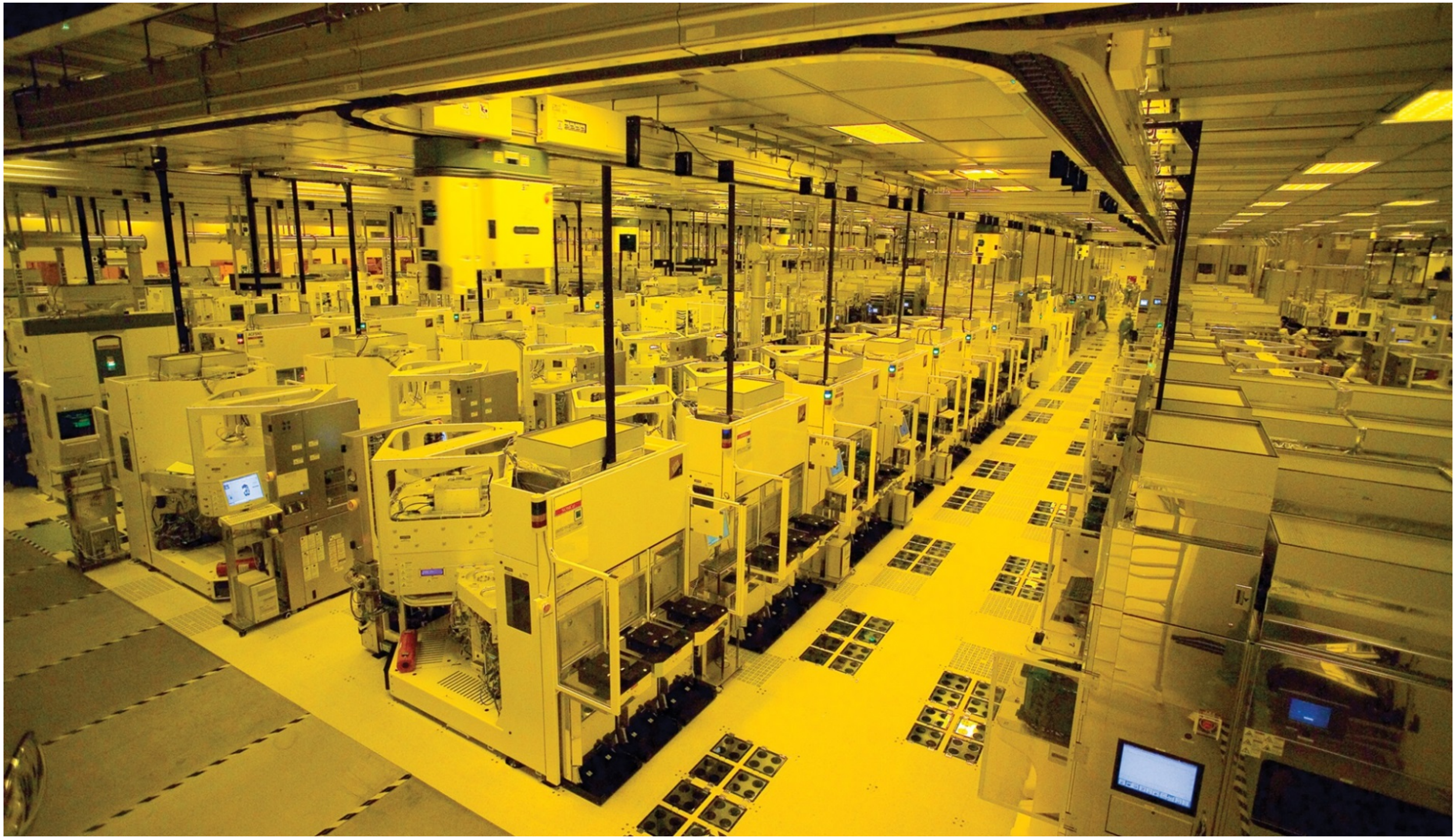

Copy Exactly !
(build exactly the same)

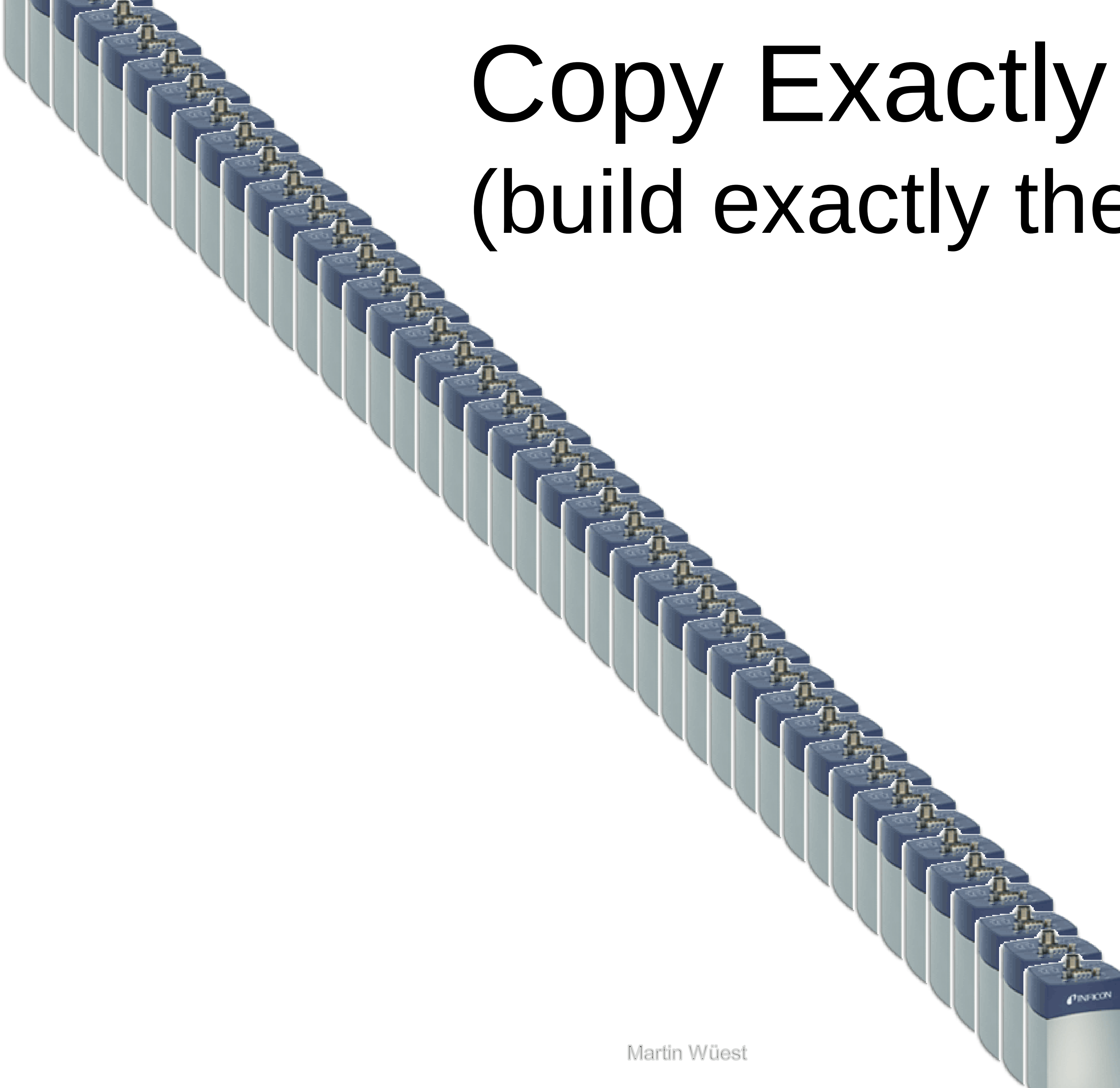

Definitions

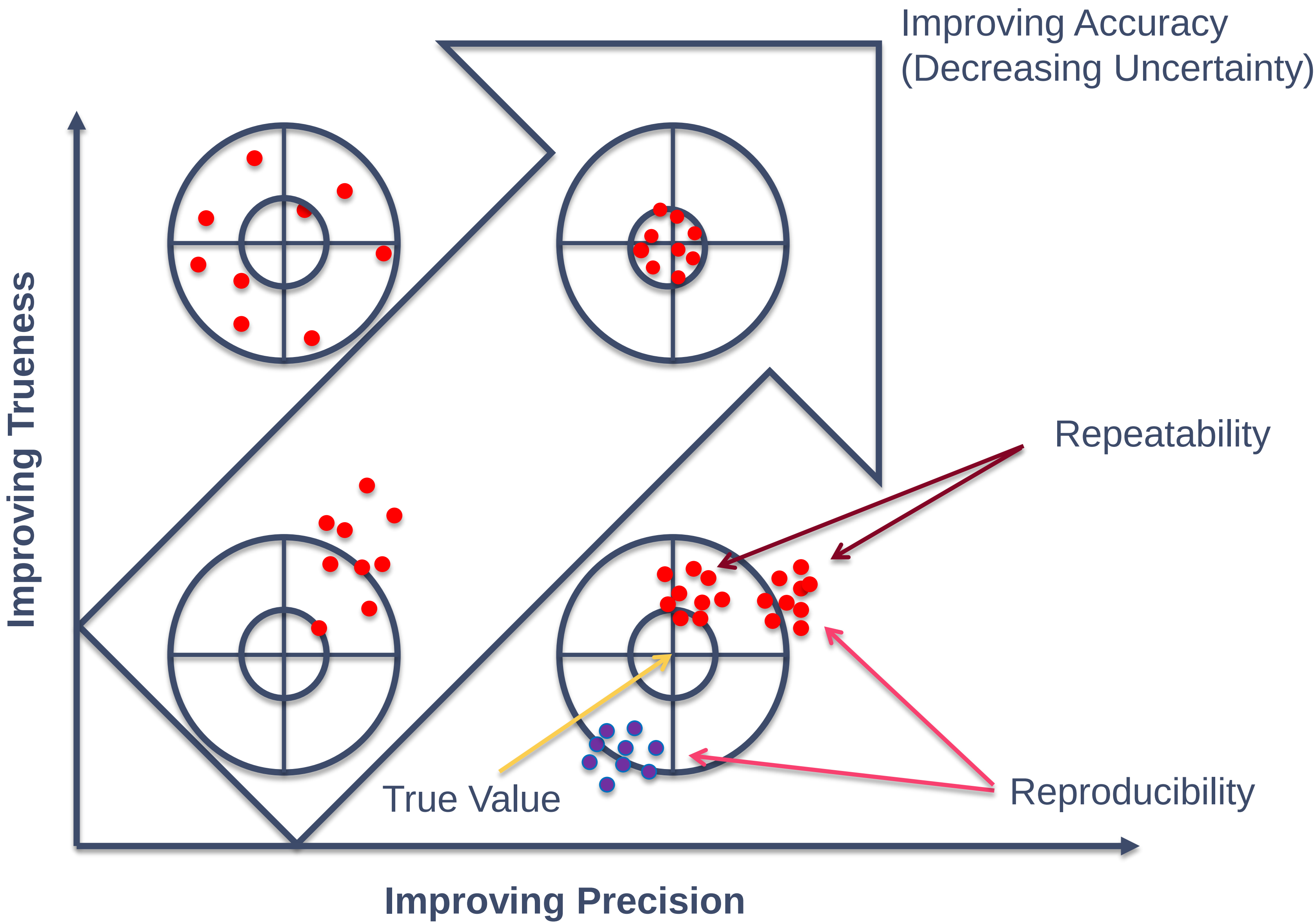

Process Ranges

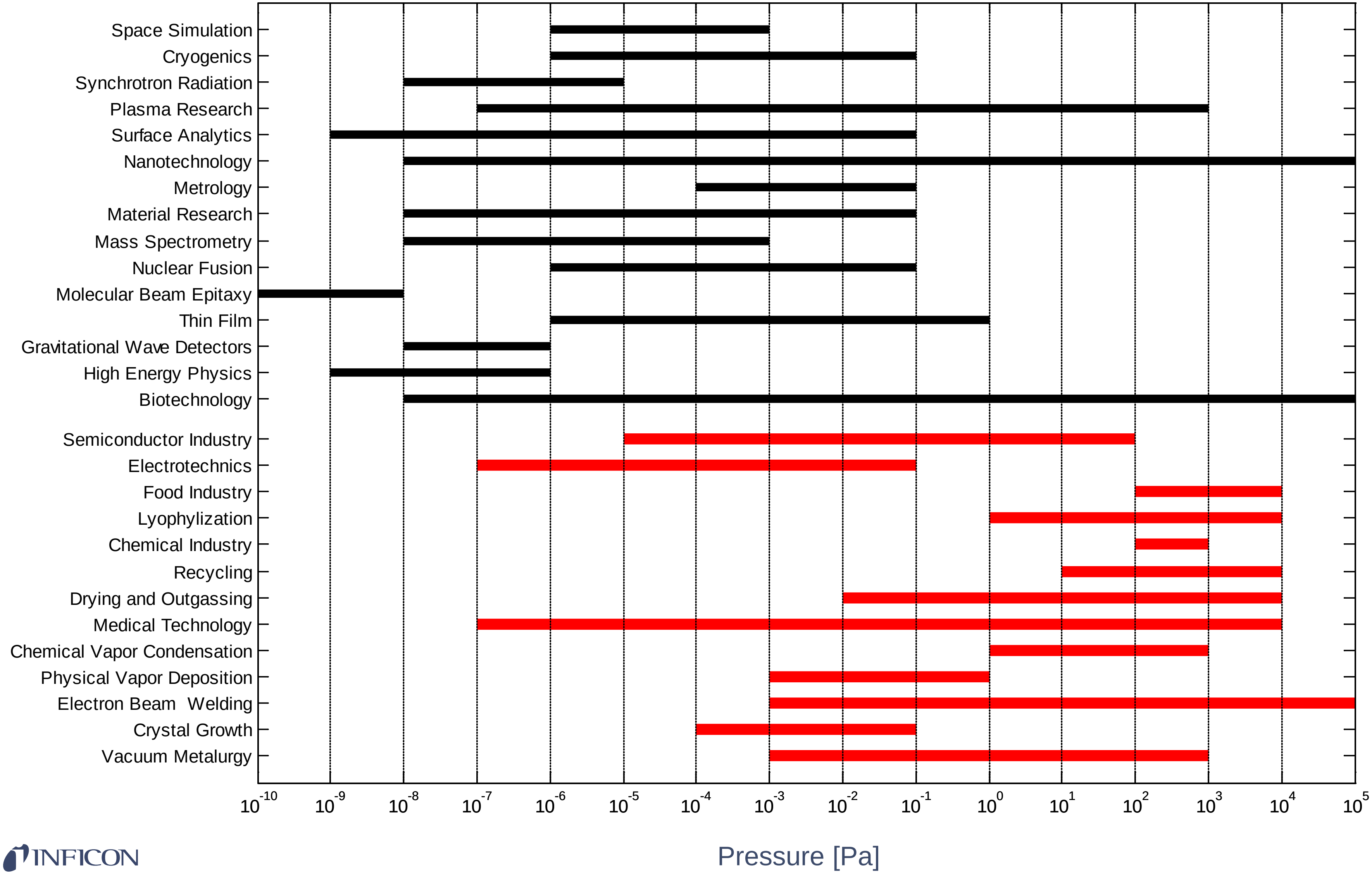

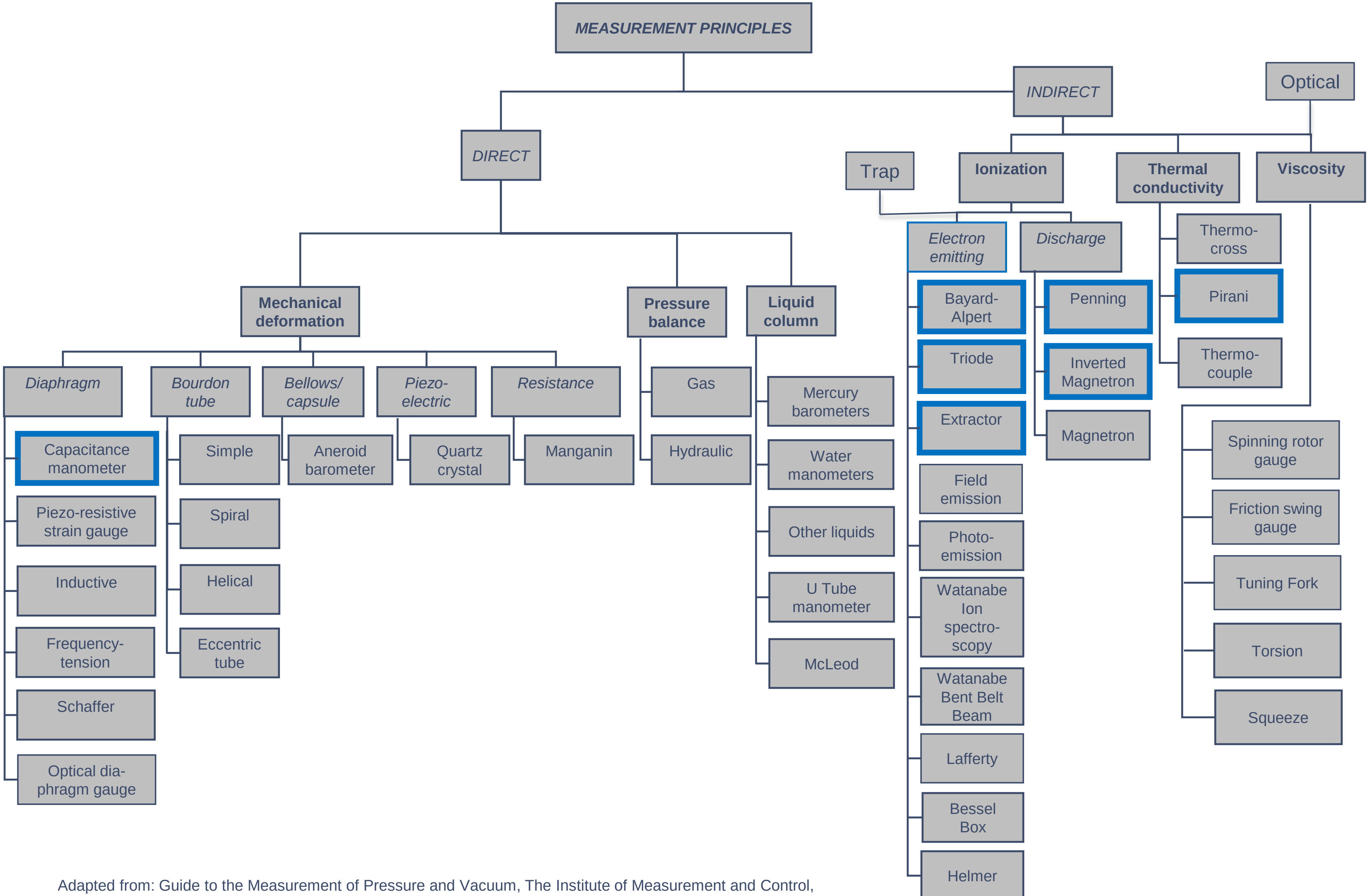

Adapted from: Guide to the Measurement of Pressure and Vacuum, The Institute of Measurement and Control, London, ISBN 0 9044577 29X, 1998

Vacuum Pressure Sensors Ranges

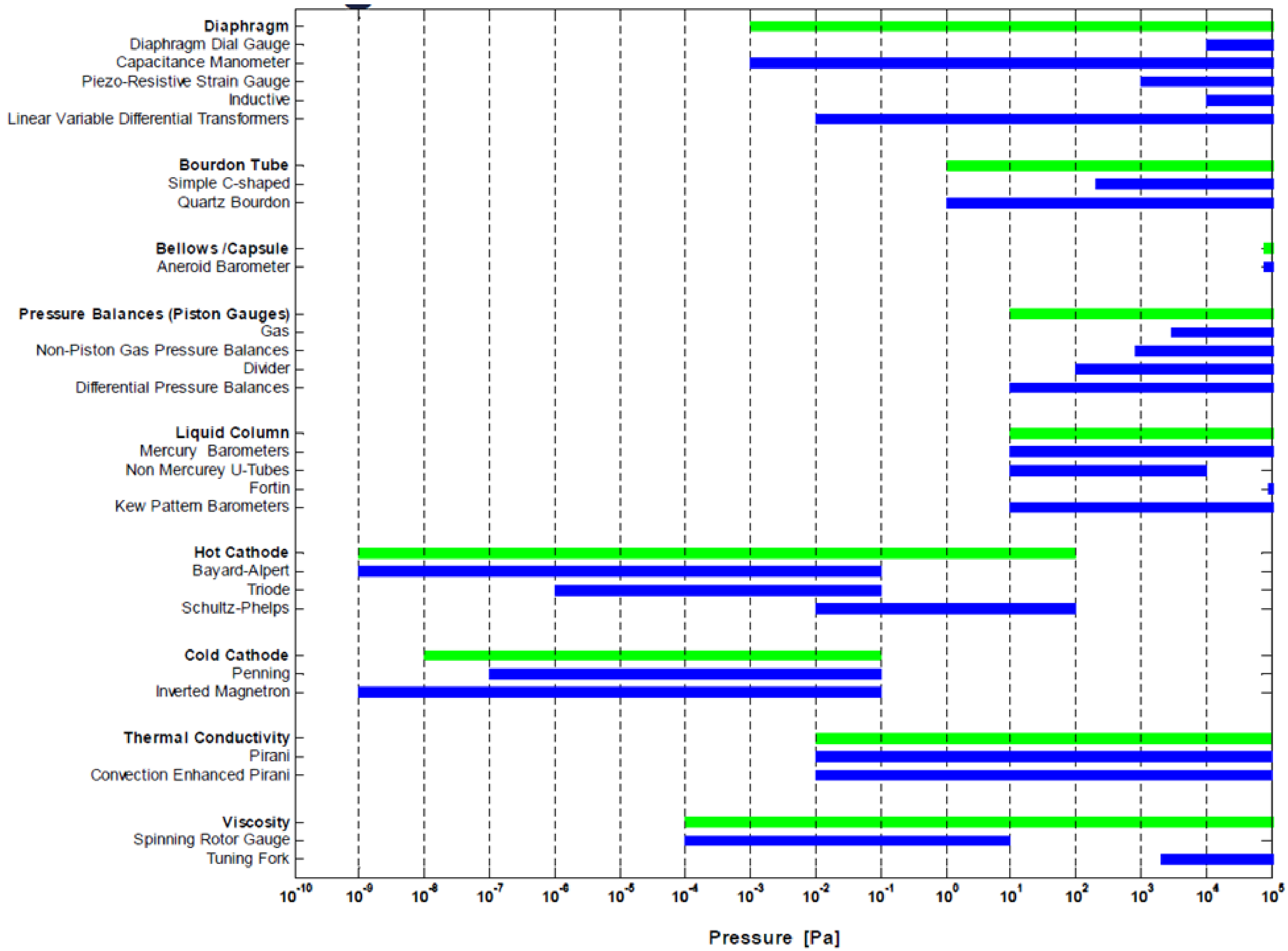

The Ubiquitous Four

- Capacitance Diaphragm Gauge

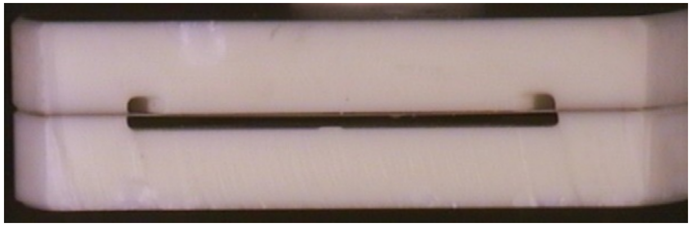

- Pirani

- Hot Ionization Gauge

- Cold Cathode Gauge

Pirani in the Market Place

MARTE, Mars Environment Simulation Chamber

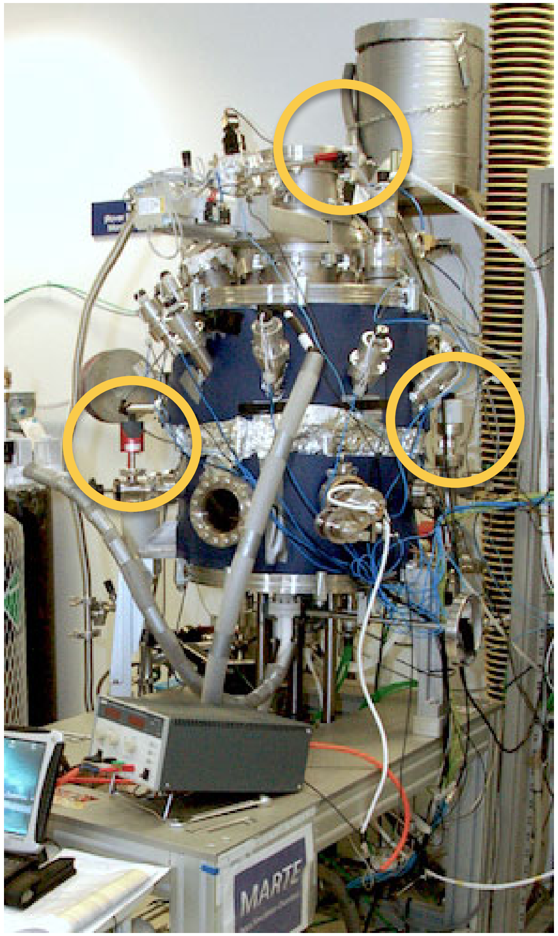

Jesus Sobrado, Juan Manuel Manchado and Jose Angel Martin-Gago
Mimicking the Martian surface, Physics World, Aug 2015

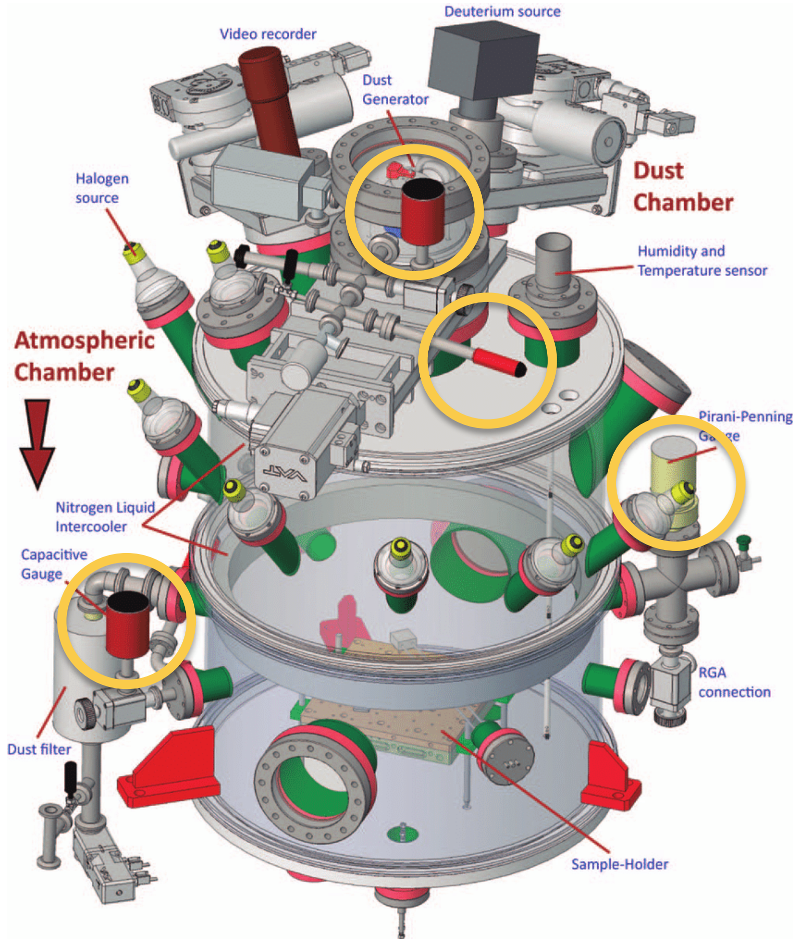

J. M. Sobrado et al., Rev. Sci. Instrum, 85 035111, 2014

Hot Ionization Gauge

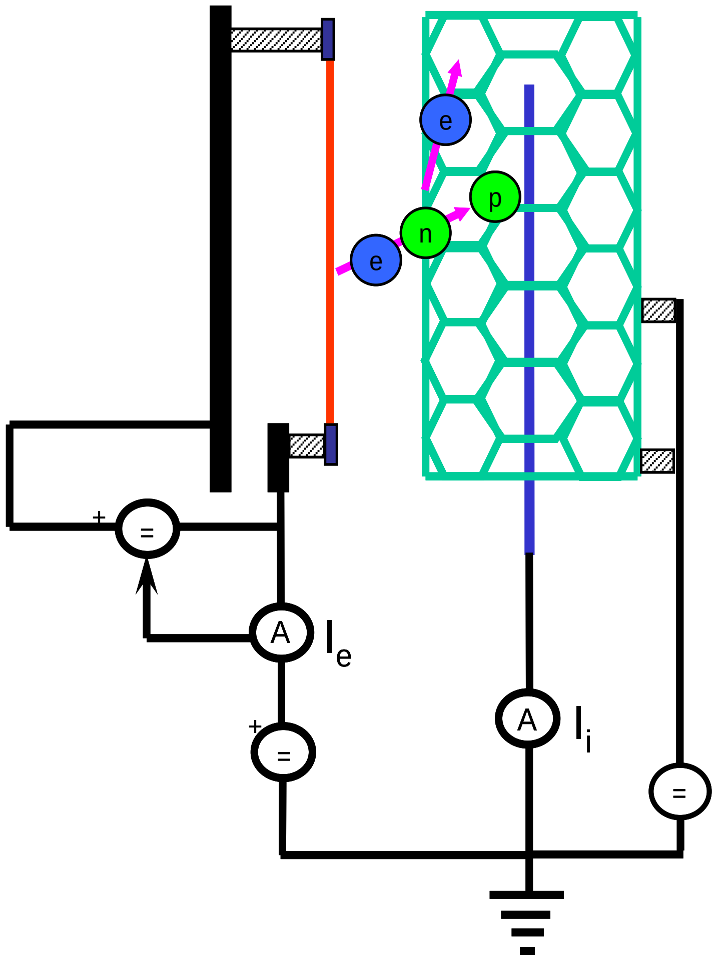

Hot Cathode Ion Gauge

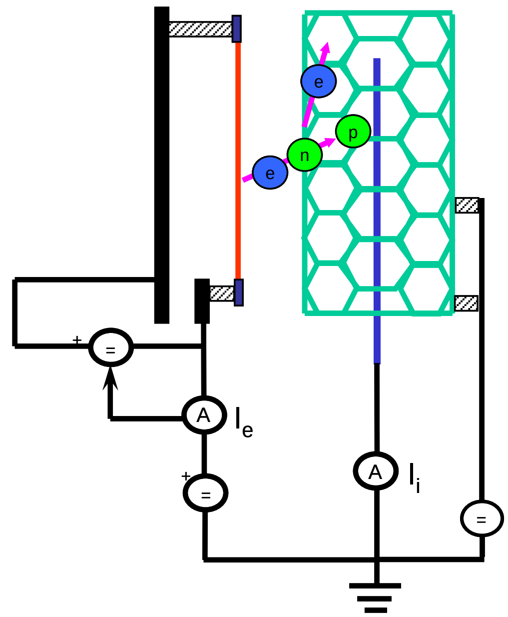

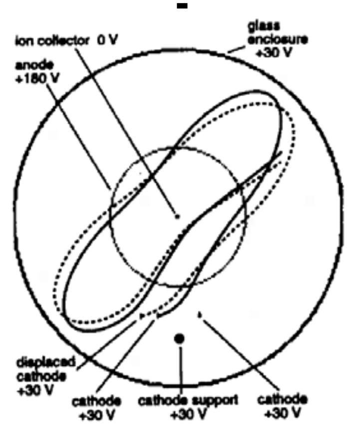

Hot Ionization Ranges

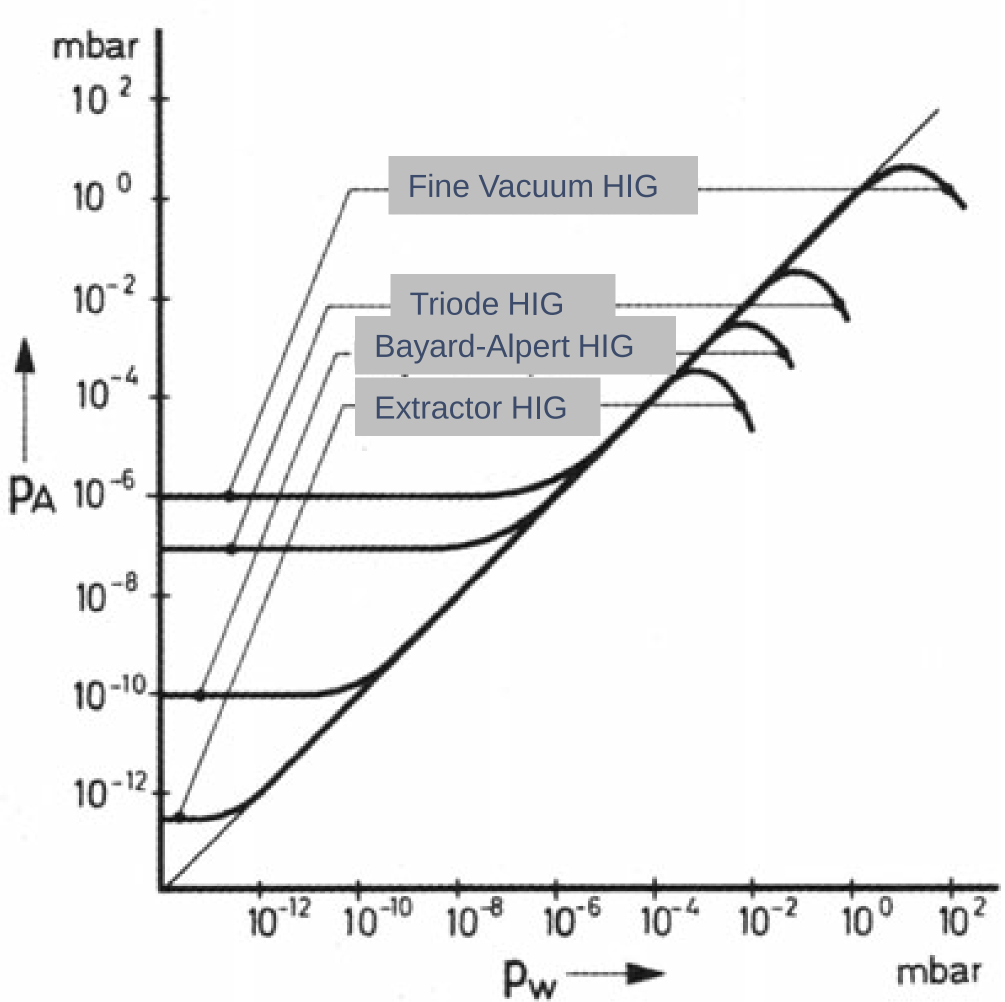

INFICON Manufactured Bayard-Alpert Hot Ionization Gauges

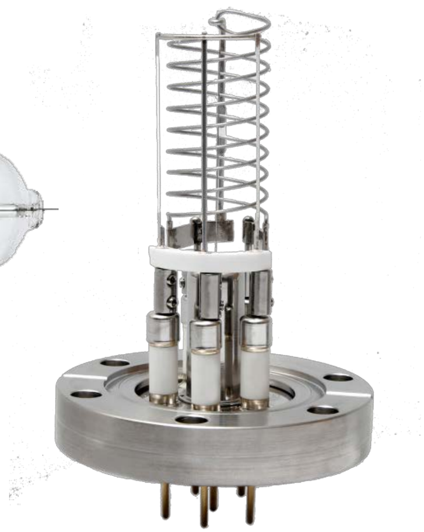

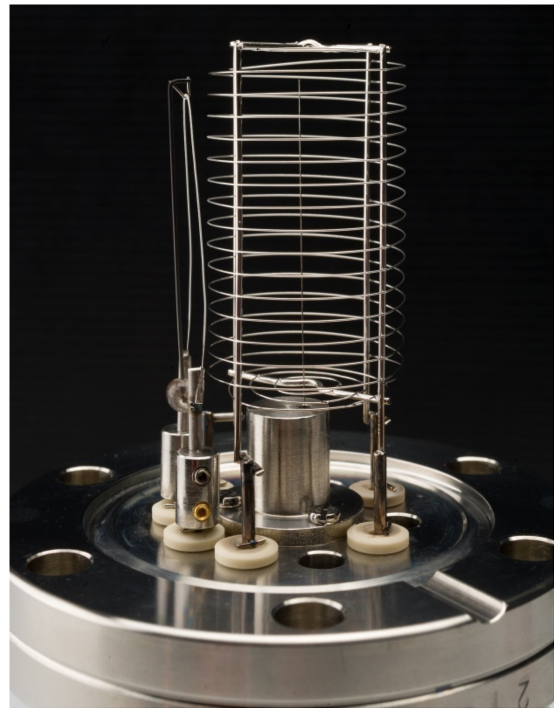

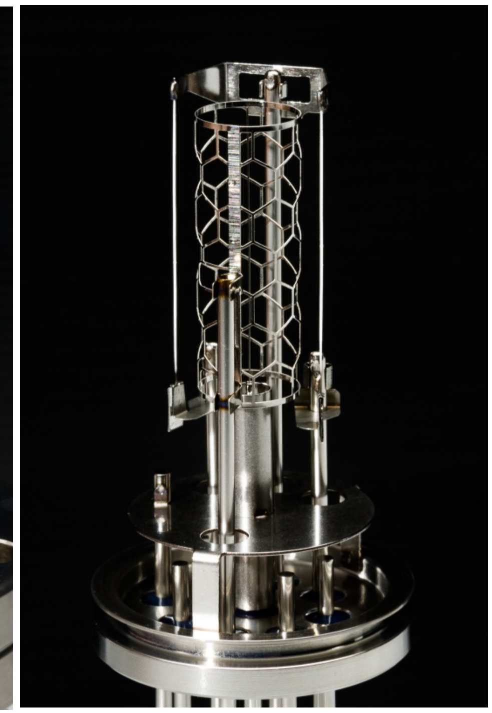

BAG052 BAG051 IE414 BAG402

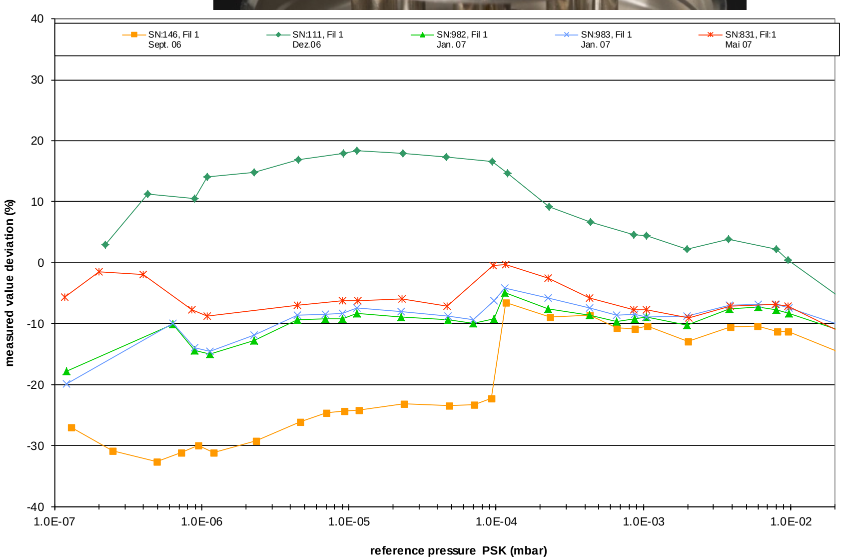
SN:146, Fil 1 Sept. 06
SN:111, Fil 1 Dez.06
SN:982, Fil 1 Jan. 07
SN:983, Fil 1 Jan. 07
SN:831, Fil:1 Mai 07
40
30
20
10
0
-10
-20
-30
-40
measured value deviation (%)
1.0E-07
1.0E-06
1.0E-05
1.0E-04
1.0E-03
1.0E-02
reference pressure PSK (mbar)

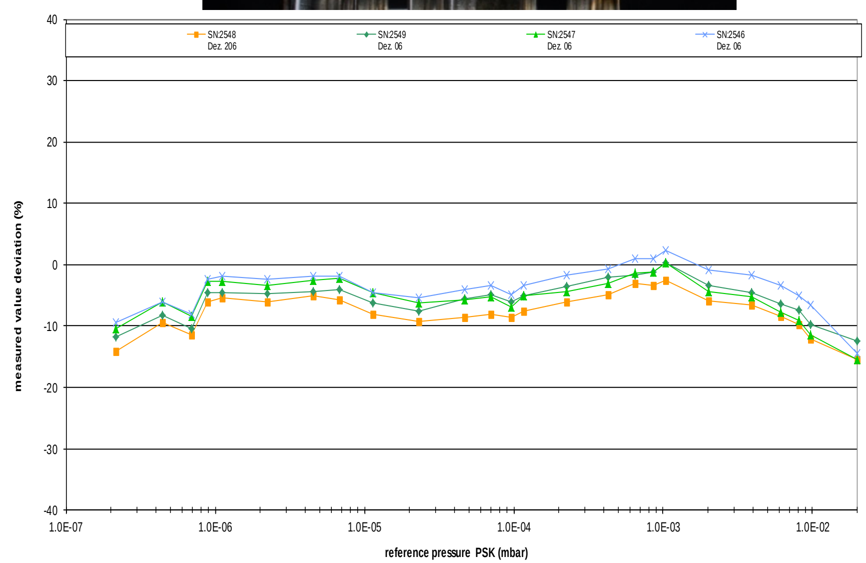
SN:2548 Dez. 206
SN:2549 Dez. 06
SN:2547 Dez. 06
SN:2546 Dez. 06
40
30
20
10
0
-10
-20
-30
-40
measured value deviation (%)
1.0E-07
1.0E-06
1.0E-05
1.0E-04
1.0E-03
1.0E-02
reference pressure PSK (mbar)

Inverted Magnetron

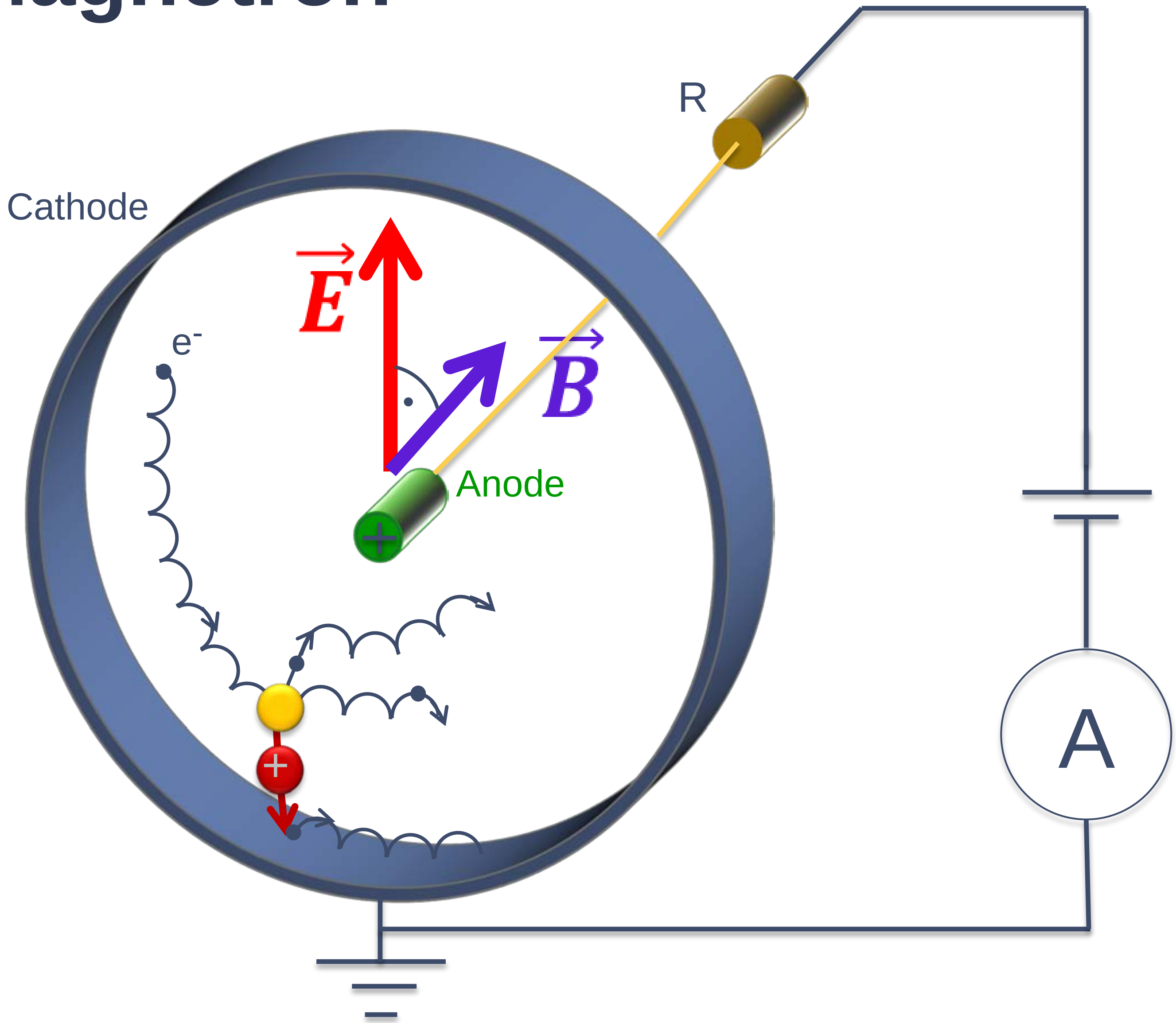

$$I^+ = Cp^n$$

Inverted Magnetron Ion Gauge

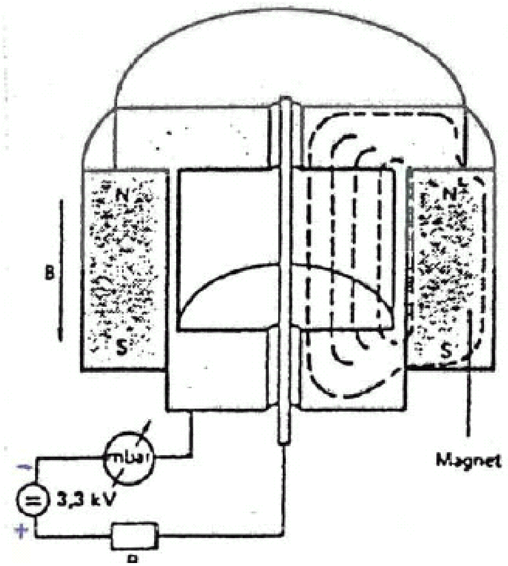

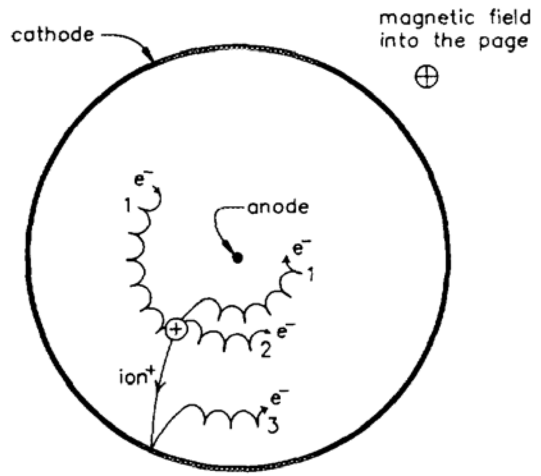

R.N. Peacock et al., JVST A9, 1977, 1991

Inverted Magnetrons

passive — active

HV1	IKR013 (CERN)	IKR010	IKR020	MPG400	MPG500
1960’s	1972 ⟷	1977	1980-1995	1993	2013

Inverted Magnetron MPG550

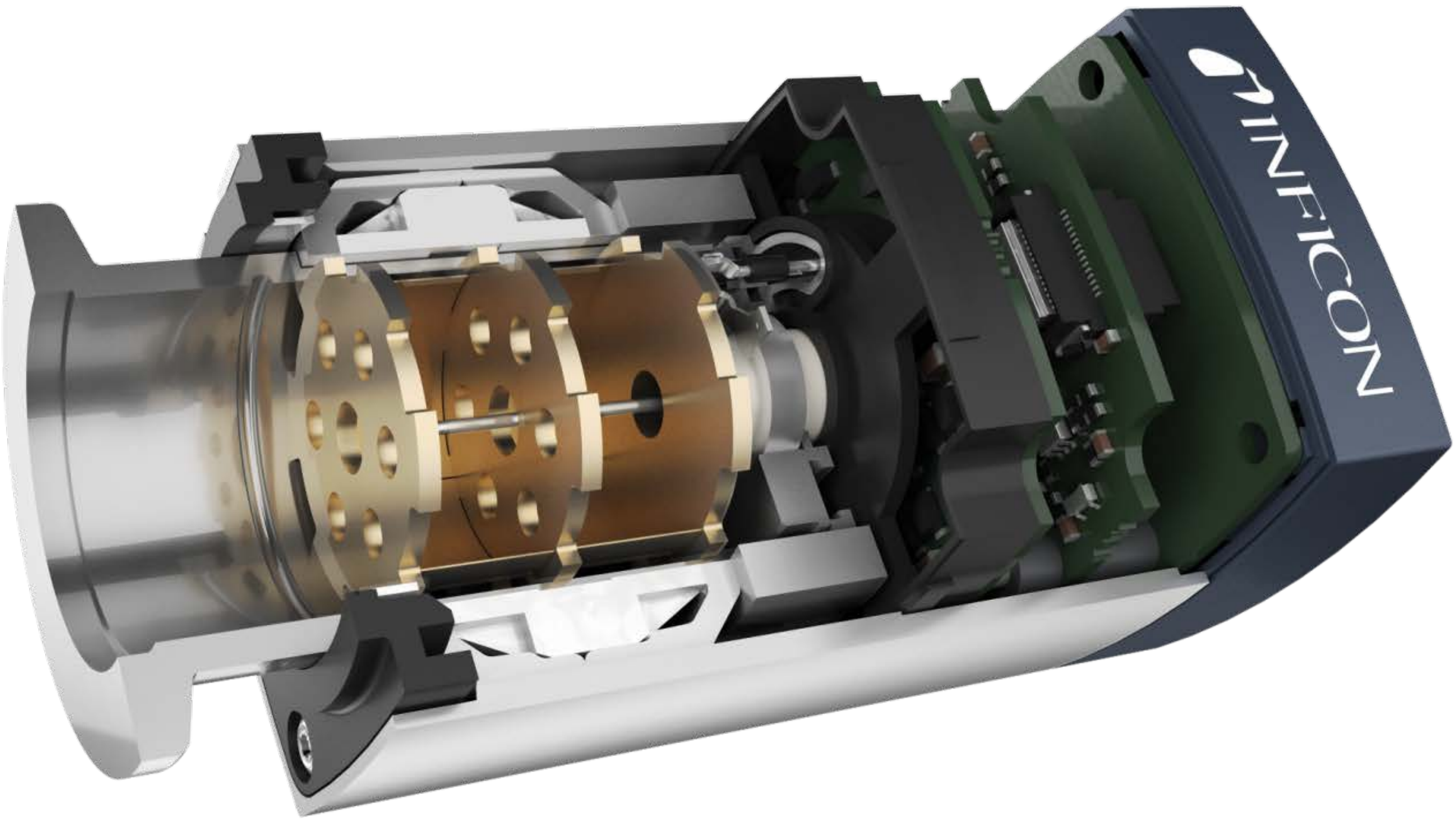

Novel Magnet Design

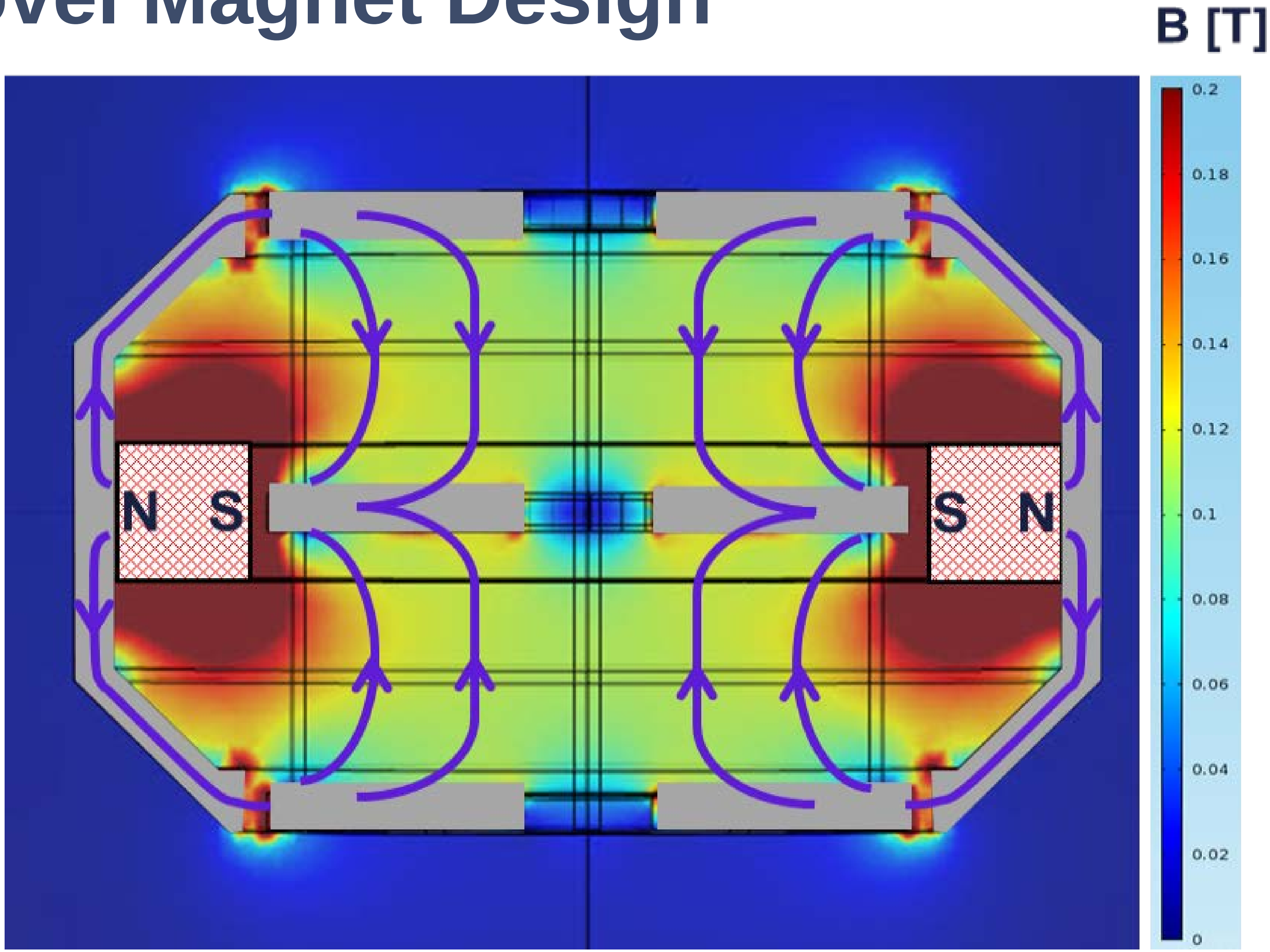

Low Magnetic Stray Field

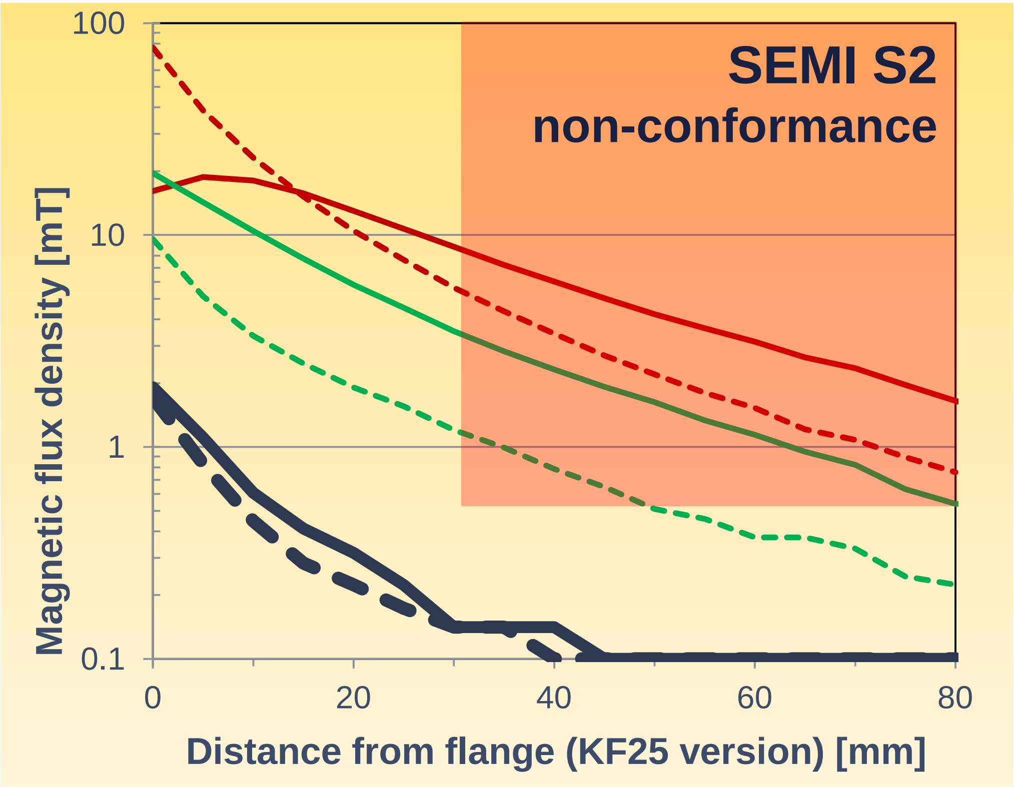

Axial (z) direction
- Gemini MxG50x
- MPG40x
- state-of-art "low-field" design

Radial (r) direction
- Gemini MxG50x
- MPG40x
- state-of-art "low-field" design

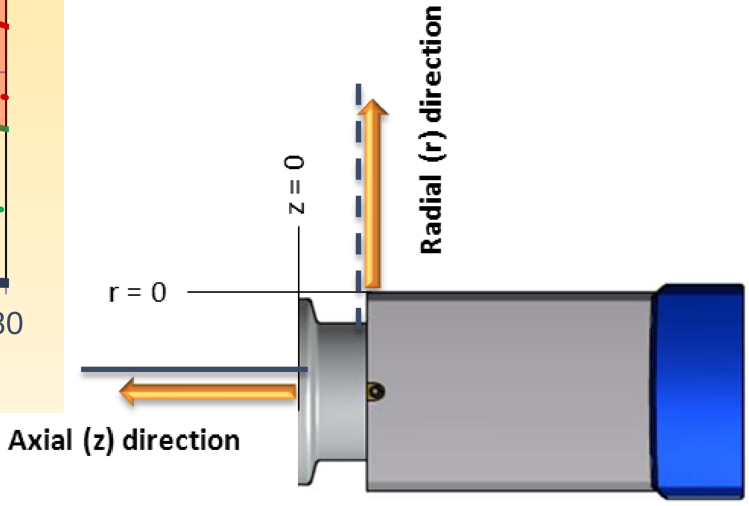


INFICON
INFICON
MPG


INFICON
CDG

Vacuum Measurement

direct

$$p = \frac{F}{A}$$

indirect

Ionisation
Viscosity
Convection
Thermal Conductivity

Direct vacuum measurement (1)

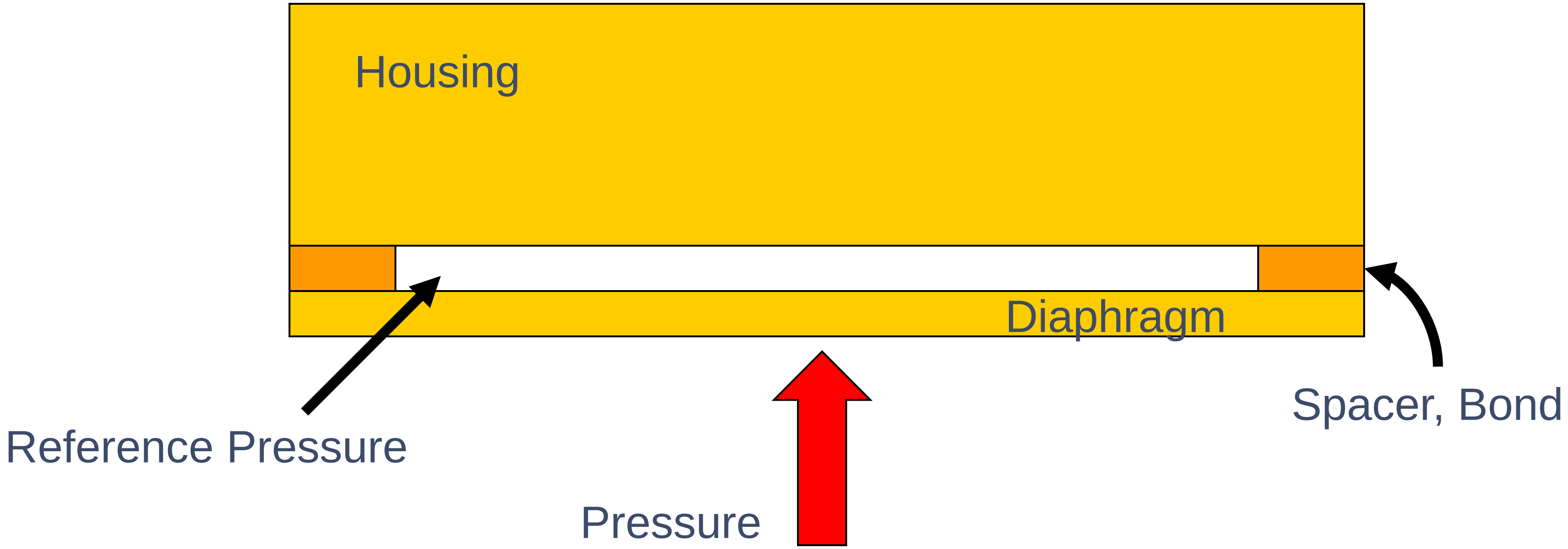

Direct measurement of vacuum (2)

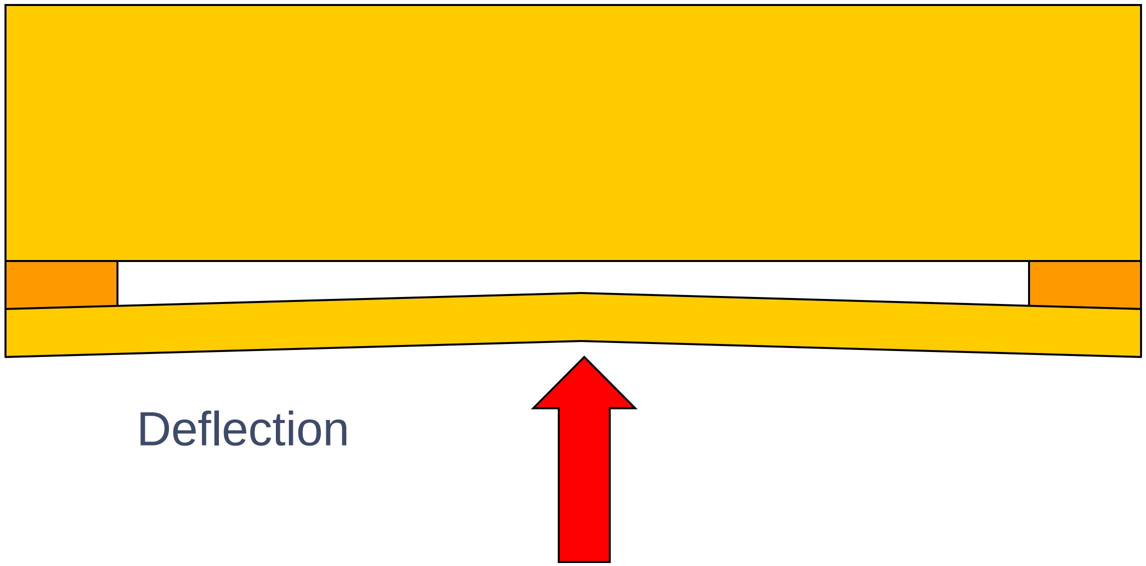

The deflection results from the net force of the pressure difference between the reference pressure (typical 10^{-7} Torr) and the pressure around the cell (outside pressure - inside pressure).

Direct measurement of vacuum

The capacitance C is given by the electrodes having a distance d and area A

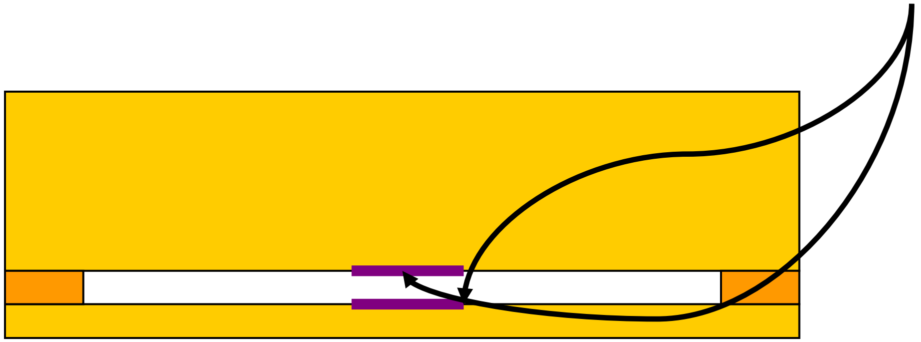

$$C = \varepsilon_0 A / d$$

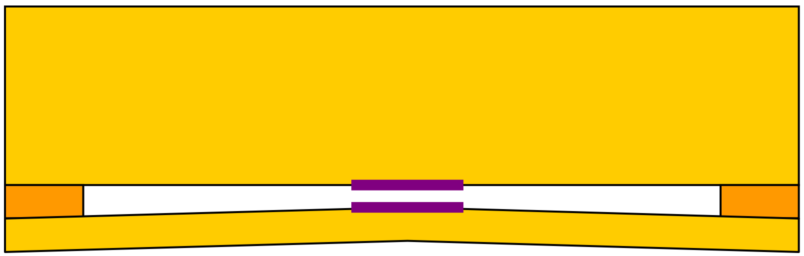

..and in case of deflection we see a change in capacitance, the distance d gets smaller:

$$\partial C / \partial d = -\varepsilon_0 A / d^2$$

The electrical sensitivity of a CDG defined as the relative change of the capacitance depends strongly on the distance d!

Membrane

- Ultrapure Al_2O_3 ceramic
- Polycrystalline
- High corrosion resistance
- Thicknesses down to 30µm
- Thinfilm gold electrode (reference cavity side)

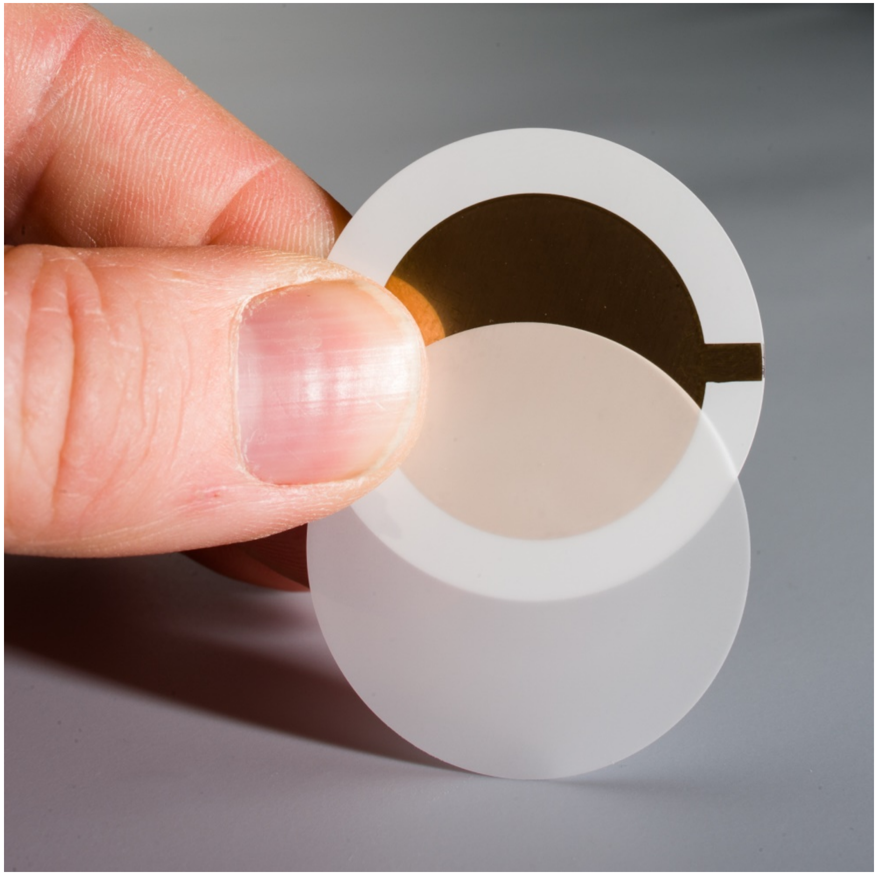

CDG Cell

Capacitance

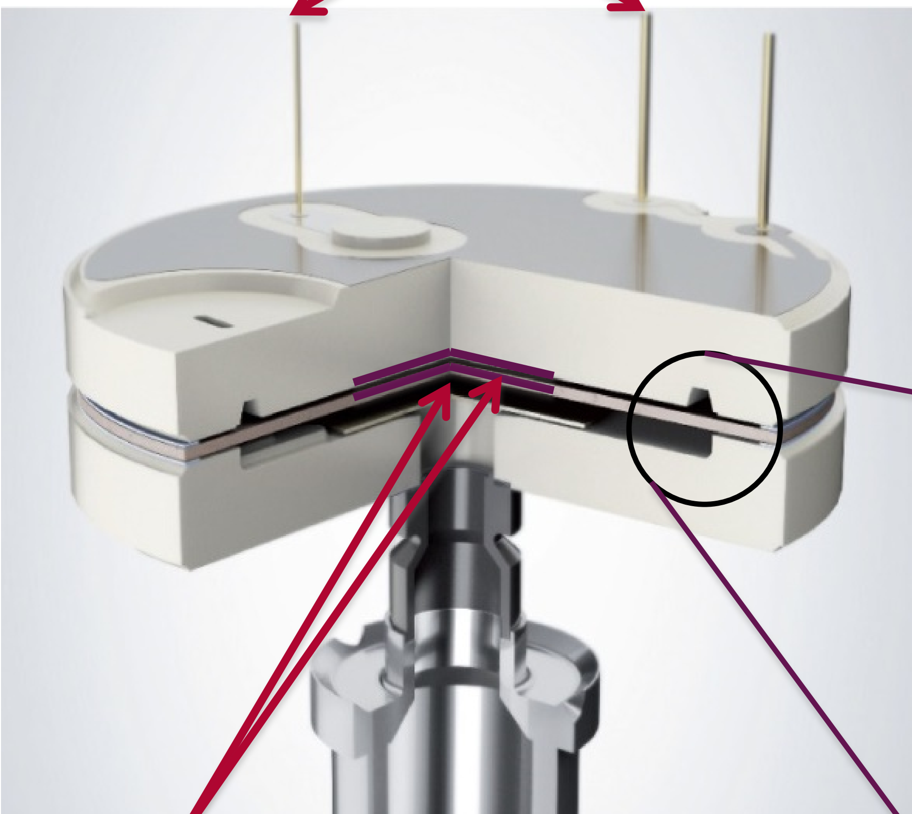

Electrodes

Ceramic CDG cell

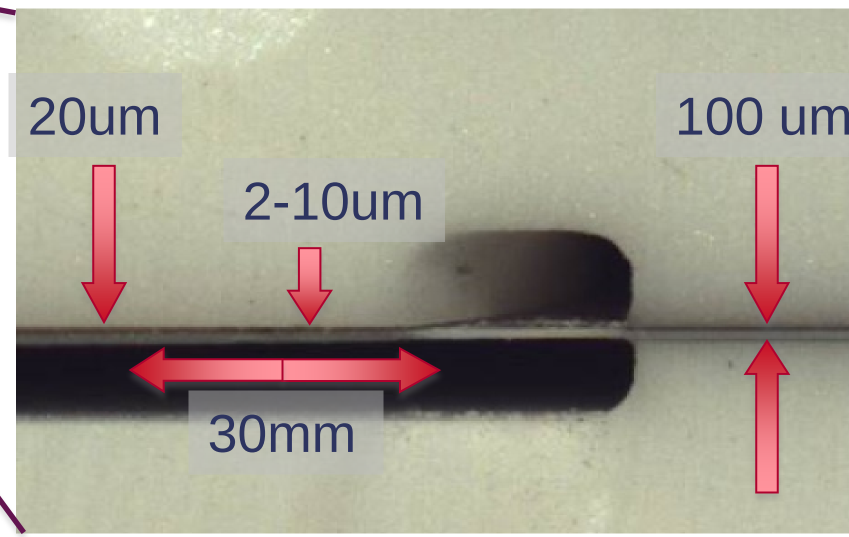

From ΔC to a readout

Change in pressure

Change of capacity

Oszillator

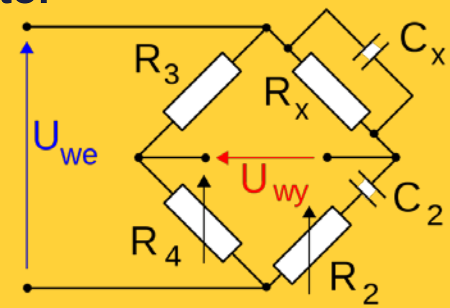

V

Charge Based: Sigma Delta

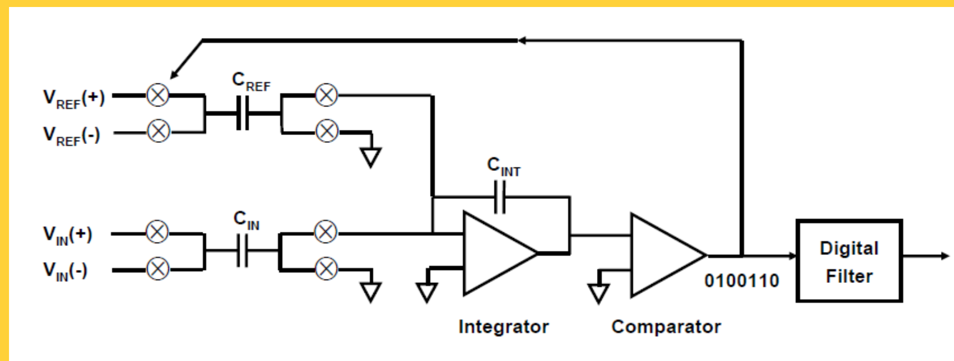

V

bit

Time based: TDC

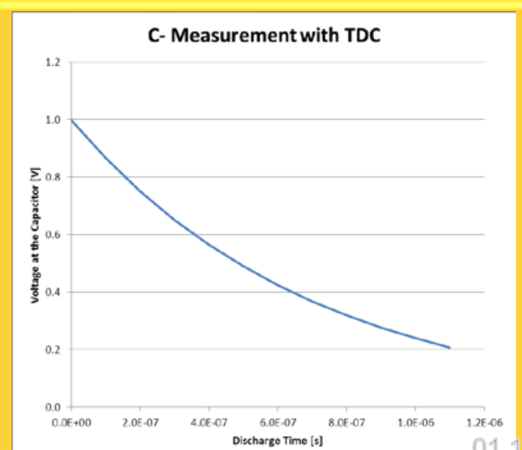

t

From ΔC to a readout

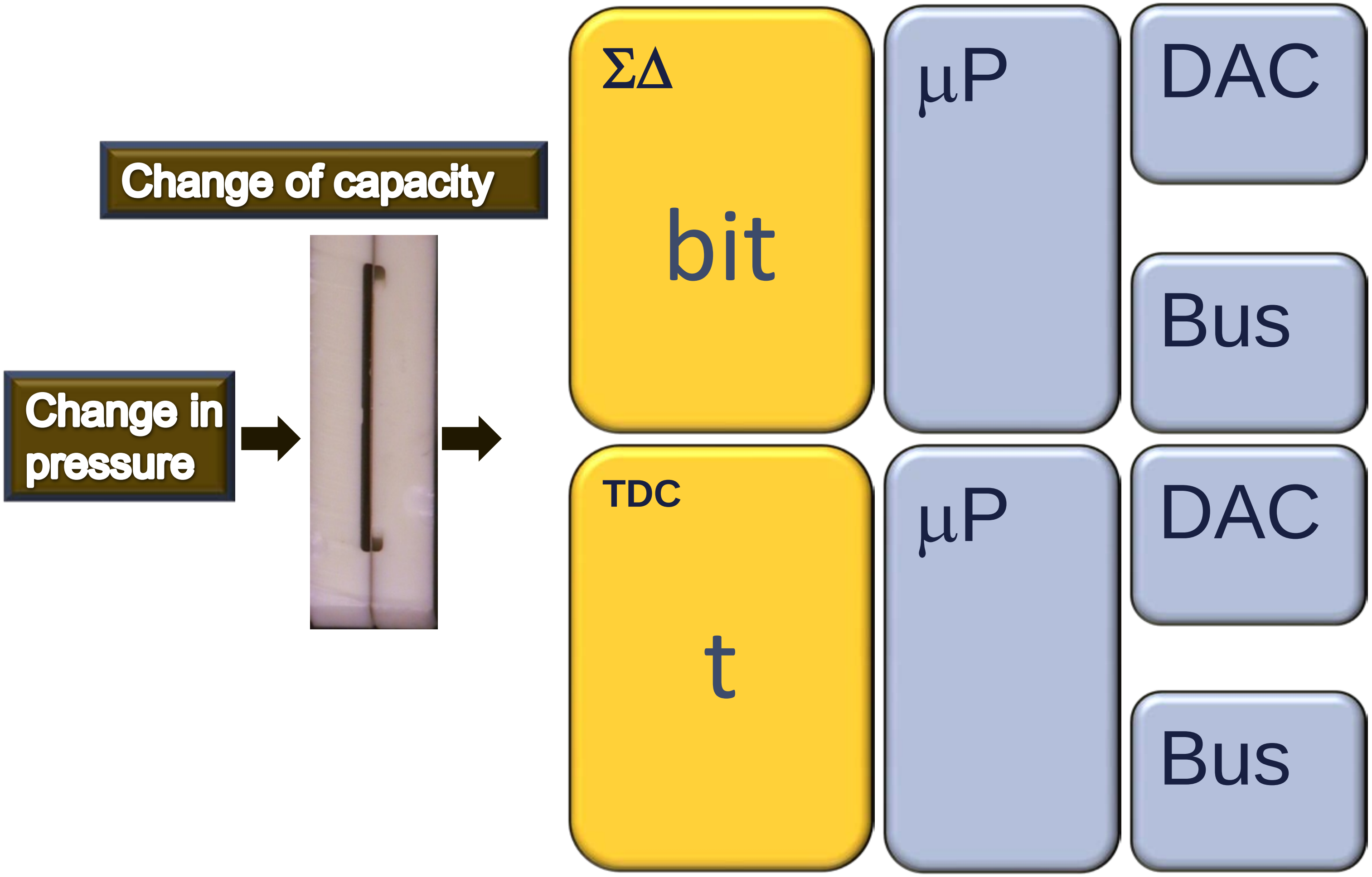

Capacitive Diaphragm Gauges

INCONEL analog	Al_2O_3 analog	Al_2O_3 digital	1ms 10mTorr Al_2O_3 digital

Late 90 s	2000	2006	2014

Innovative Portfolio

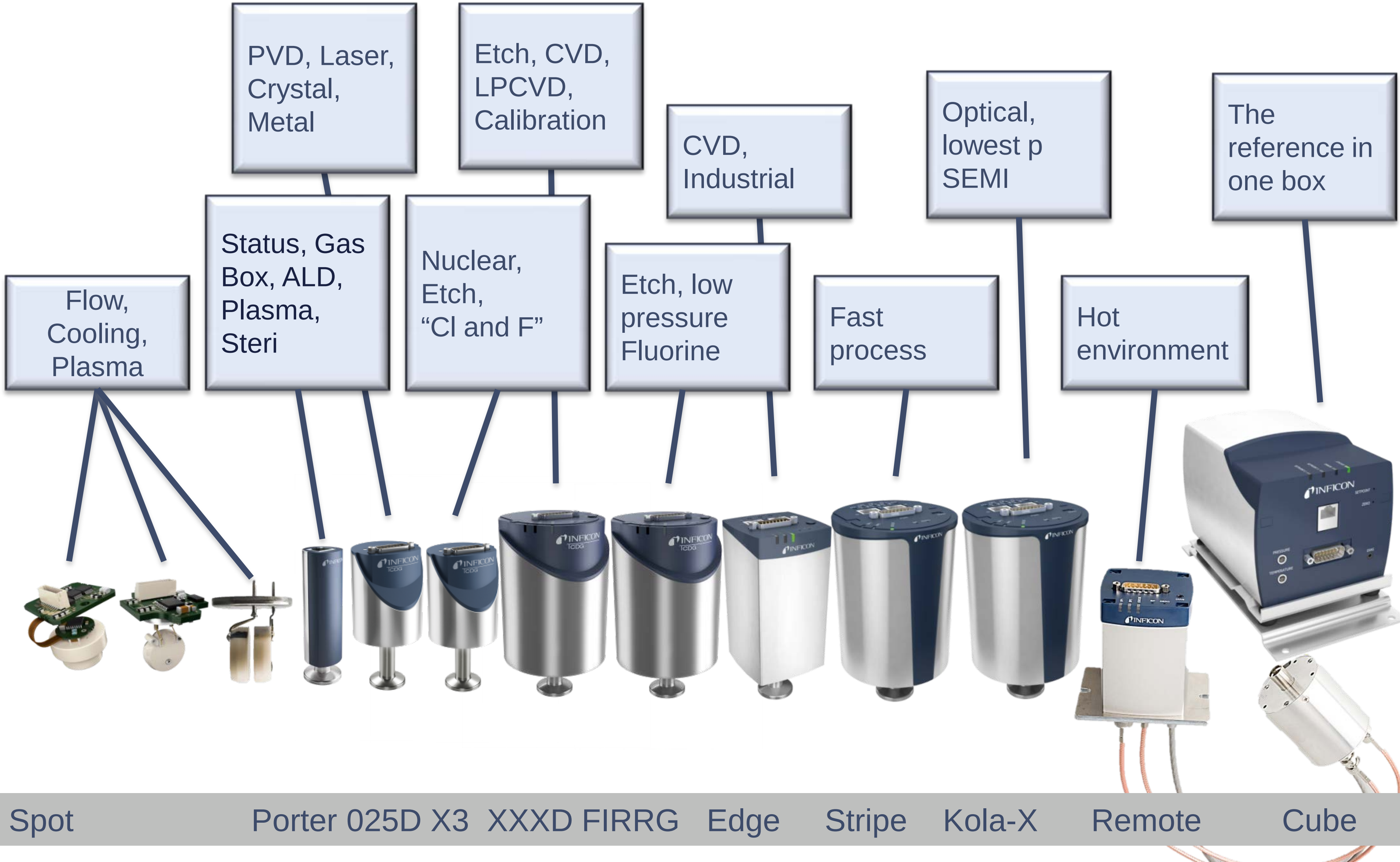

Functional Blocks of a CDG

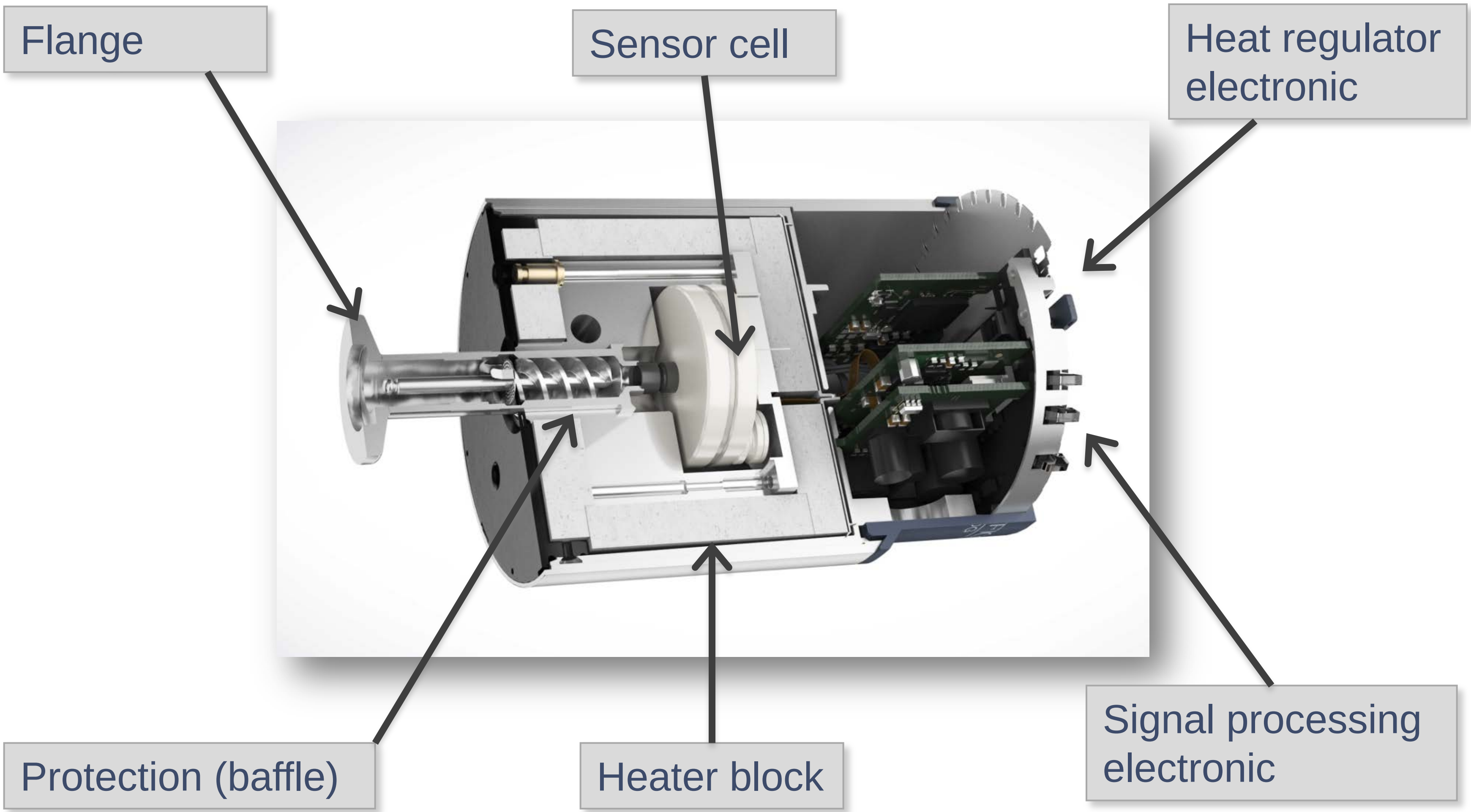

Effect of Process Contamination on CDG’s

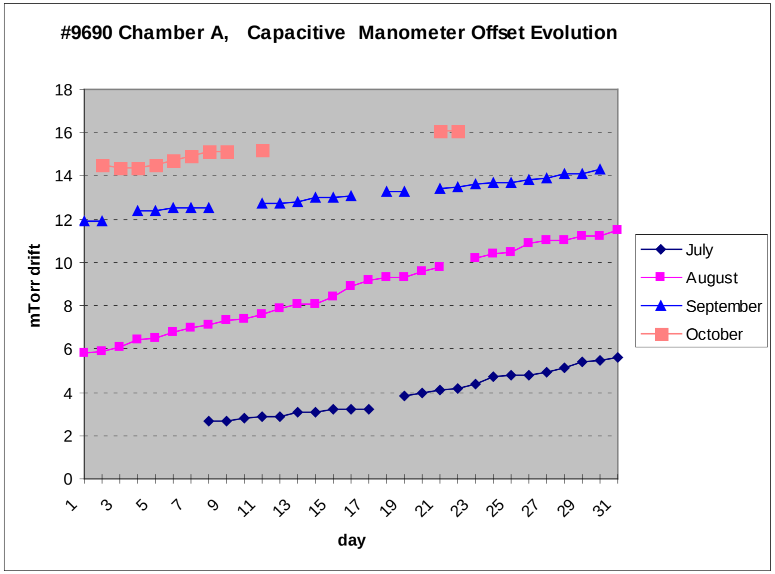

Process byproducts that do not bond to the plasma shield (baffle) will deposit heavily around the center of the diaphragm

This results in uneven tensioning and weighting of the diaphragm causing changes which are typically seen as zero drift

As the deposition continues, the gauge will rapidly run out of zero adjustment and will need to be replaced.

Intentional Cu coating on CTR90, 10 Torr open sensor

Process build-up on CDG’s

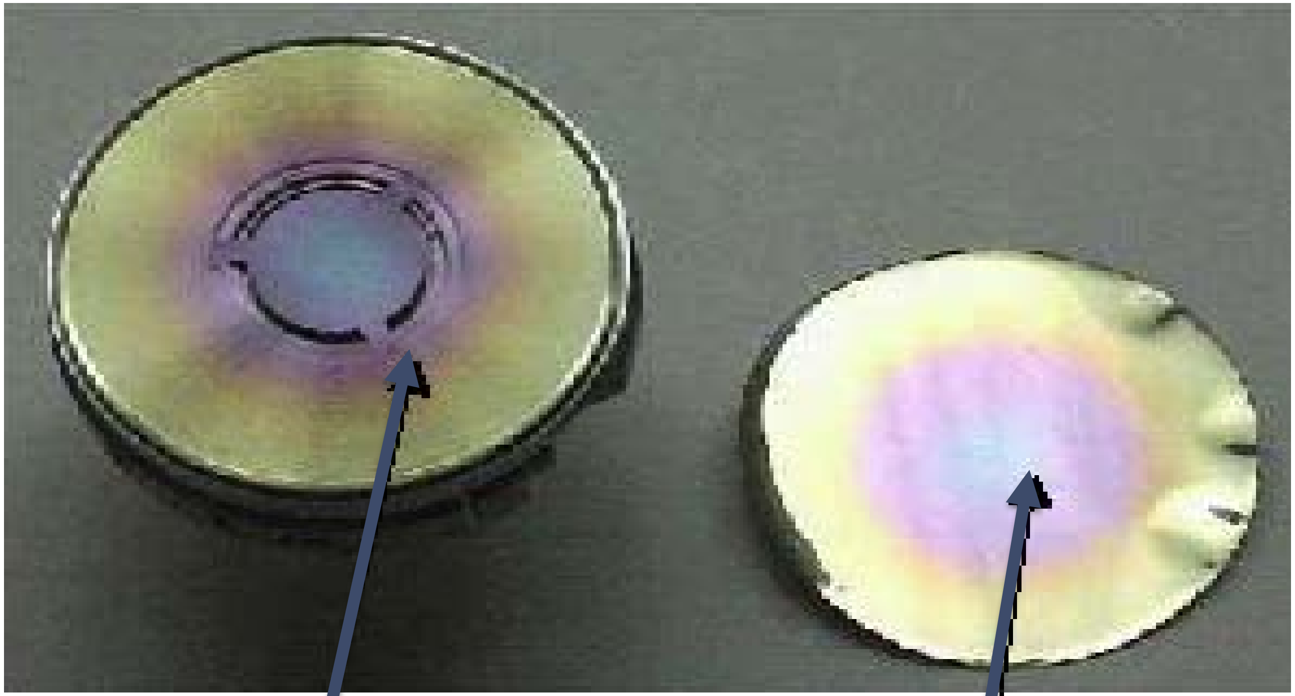

Heavy process build-up on plasma shield

Process build-up around the center of the metallic diaphragm

S.A. Tison, Transition Flow, Applications in Semiconductor Fabrication, Gas Dynamics Workshop, 30. June 2003, Avila, Spain.

Observed Contaminations

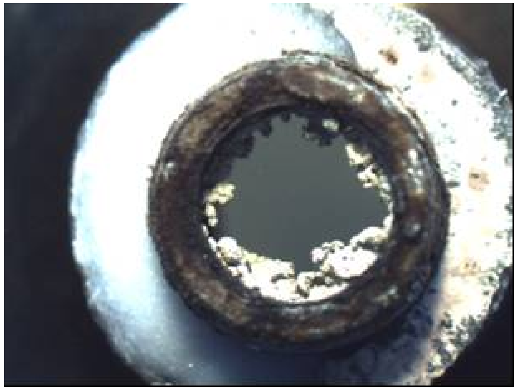

Vacon
CR096 10T_SN333
Ti/TiN

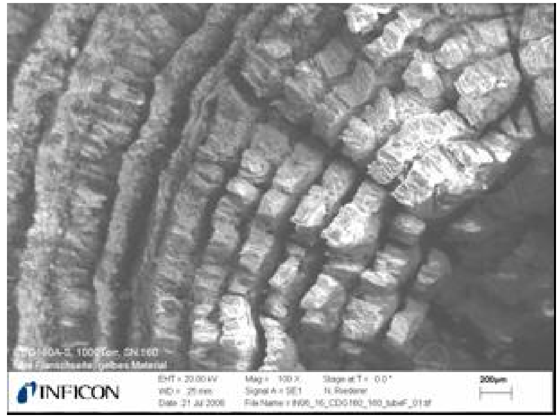

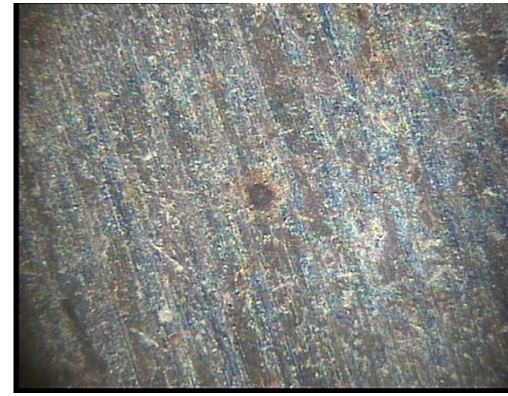

Plasma shield pitting corrosion
CR095-S 1330Pa SN 013 or 105
TiN

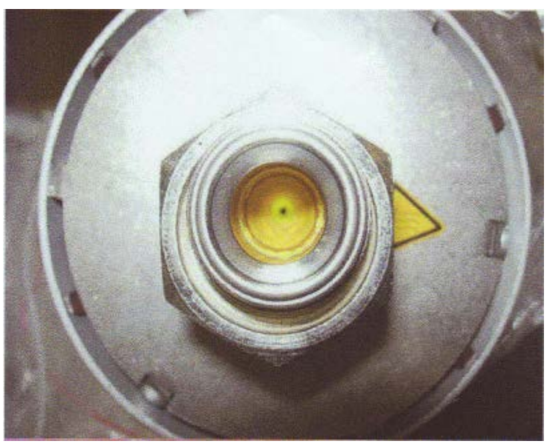

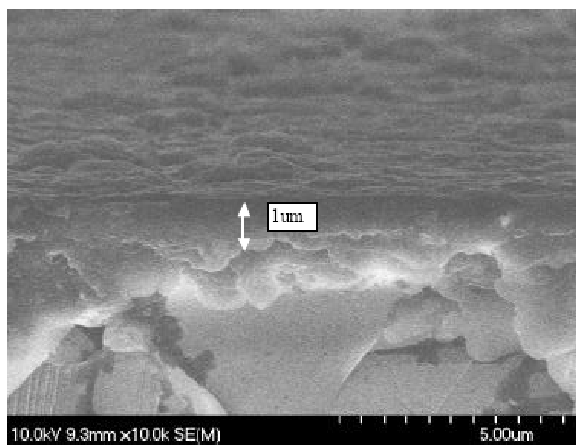

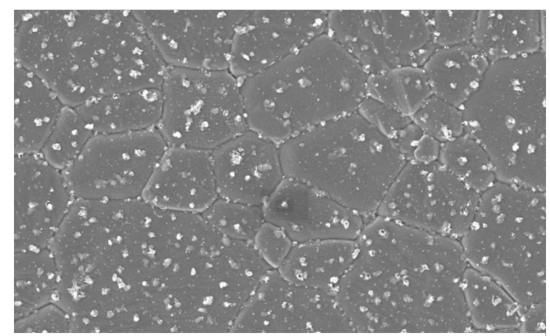

Diaphragm
CR096-S_133Pa SN104
TiN

CR096-S 10T SN225/SN333

Application	Ti/TiN	Ti/TiN
Product	**CR096-S**	**CR096-S**
Range	**10 Torr**	**10 Torr**
Serial number	**225**	**333**
Production / start warranty	**31.5.2002 / ca.Okt.2002**	**12.11.2003 / 11.11.2003**
Return	**27.04.2006**	**27.04.2006**
Precursors	**$TiCl_4$, NH_3 H_2, N_2, Ar ClF_3**	**$TiCl_4$, NH_3 H_2, N_2, Ar ClF_3**
Customer remarks	**long time running**	

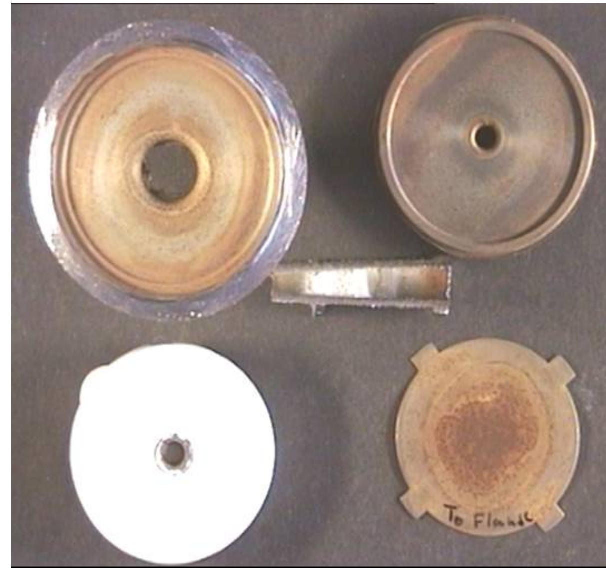

SN 225

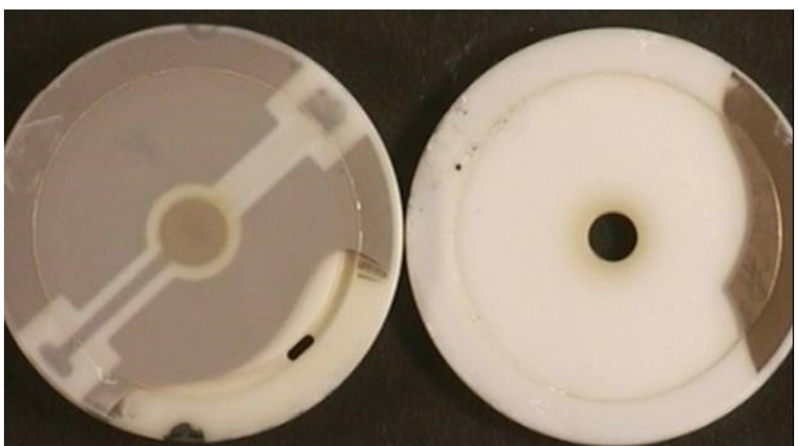

SN 333

Design Improvements

Gauge inherent

Process related

Issues

- A vacuum pressure gauge should accurately measure pressure under all circumstances.
- Processes, in particular coating or etching applications, affect the accuracy of the sensor in the long run by deposition of material or etching of sensor elements.
- Usually this causes sensor signal drift or in the worst case destroys the sensor.

Goal

The goal of this investigation is

- to find methods to protect our gauges from process contamination in order
- to keep accuracy and
- to increase their life time on a process tool.

TiN Uses in Semiconductor Industry

- Contact Liner - Ti / TiN
  - Diffusion barrier material between substrate and metal interconnects
  - Prevent the diffusion of metal ions into the semiconductor material
  - Films in the order of few 100nm

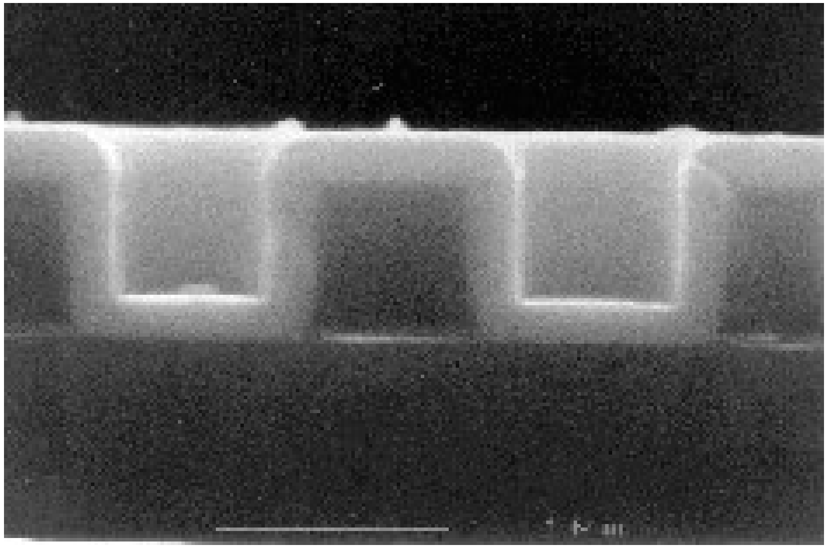

- Capacitor electrodes - TiN

TiN Process Basic Chemistry

Process:

$$6TiCl_4(g) + 8NH_3(g) \longrightarrow 6TiN(b) + 24HCl(g) + N_2(g)$$

Dry clean: (ClF_3 + N_2 or Ar)

$$6TiN(b) + 8ClF_3(g) \longrightarrow 6TiF_4(g) + 4Cl_2(g) + 3N_2(g)$$

Wet clean:

Isopropyl-Alcohol (C_3H_8O) + De-ionized water (H_2O)

By-product Reactions

$$NH_3 + HCl \longrightarrow NH_4Cl$$

= ammonium chloride
is very reactive
has a vapour pressure of 1Torr @160 C
it sublimes and condensates at cold places

$$TiCl_4 + H_2O \longrightarrow TiO_2\,\text{(white powder)} + 4HCl$$

$$2Ti + 6HCl \longrightarrow 2TiCl_3 + 3H_2$$

$$2TiCl_2 + HCl \xrightarrow{>500°C} TiCl_2 + TiCl_3$$

$TiCl_2$ = Very reductive
May reduce water

$$TiCl_4 + 2HCl \longrightarrow H_2[TiCl_6]\text{(yellow)} + 4HCl$$

Surface chemistry mechanism for TiN deposition

Gas:	$TiCl_4$(g) NH_3(g)	HCl(g) N2(g)
Surface:	$TiCl_3$(s) $TiCl_2$(s)	TiCl(s) Ti(s) Ti^*(s) NH_2(s) NH(s) N(s) N^*(s) N^{**}(s)
Bulk:	Ti(b)	N(b)

Titanium deposition:		A	E/R
1.	TiCl(g) + NH_2(s) + Ti*(s) —> $TiCl_3$(s) + NH(s) + HCl(g) + Ti(b)	$1.6\ 10^{24}$	7500
2.	$TiCl_4$(g) + NH(s) + Ti*(s) —> $TiCl_3$(s) + N(s) + HCl(g) + Ti(b)	$1.6\ 10^{24}$	7500
Nitrogen deposition:			
3.	$TiCl_3$(s) + NH_3(g) + N(s) —> $TiCl_2$(s) + NH_2(s) + HCl(g) + N(b)	$2.5\ 10^{22}$	7000
4.	$TiCl_2$(s) + NH_3(g) + N(s) —> TiCl(s) + NH_2(s) + HCl(g) + N(b)	$2.5\ 10^{22}$	7500
5.	TiCl(s) + NH_3(g) + N(s) —> Ti(s) + NH_2(s) + HCl(g) + N(b)	$2.5\ 10^{22}$	7500

Surface condensation:			
6.	$TiCl_3$(s) + NH_2(s) —> $TiCl_2$(s) + NH(s) + HCl(g)	$4\ 10^{13}$	7500
7.	$TiCl_3$(s) + NH(s) —> $TiCl_2$(s) + N(s) + HCl(g)	$4\ 10^{13}$	7500
8.	$TiCl_2$(s) + NH_2(s) —> TiCl(s) + NH(s) + HCl(g)	$4\ 10^{13}$	7500
9.	$TiCl_2$(s) + NH(s)—> TiCl(s) + N(s) + HCl(g)	$4\ 10^{13}$	7500
10.	TiCl(s) + NH_2(s) —> Ti(s) + NH(s) + HCl(g)	$4\ 10^{13}$	7500
11.	TiCl(s) + NH(s) —> Ti(s) + N(s) + HCl(g)	$4\ 10^{13}$	7500
Bond breaking:			
12.	Ti(s) + N(s) —> Ti^*(s) + N^*(s)	$11\ 10^{14}$	7500
13.	Ti(s)+N^*(s) —> Ti^*(s) + N^{**}(s)	$11\ 10^{14}$	7500
N_2 liberation:			
14.	2Ti(s) + 2N^{**}(s)+2N(b) —> 2Ti^*(s) + N_2(g) + 2N(s)	$9.3\ 10^{30}$	7500

M. D. Allendorf, A. Arsenlis, R. Bastasz, M. E. Colvin, G. Evans, G. Germann, C. L.. Janssen, R. S. Larson, C. F. Melius, T. H. Osterheld, D. A. Outka, M. L. Schulberg, P. Ho, and I. M. B. Nielsen, *Development of a process simulation capability for the formation of titanium nitride diffusion barriers,* Sandia National Laboratories, 1997, p. 40.

Stream Function CVD Reactor

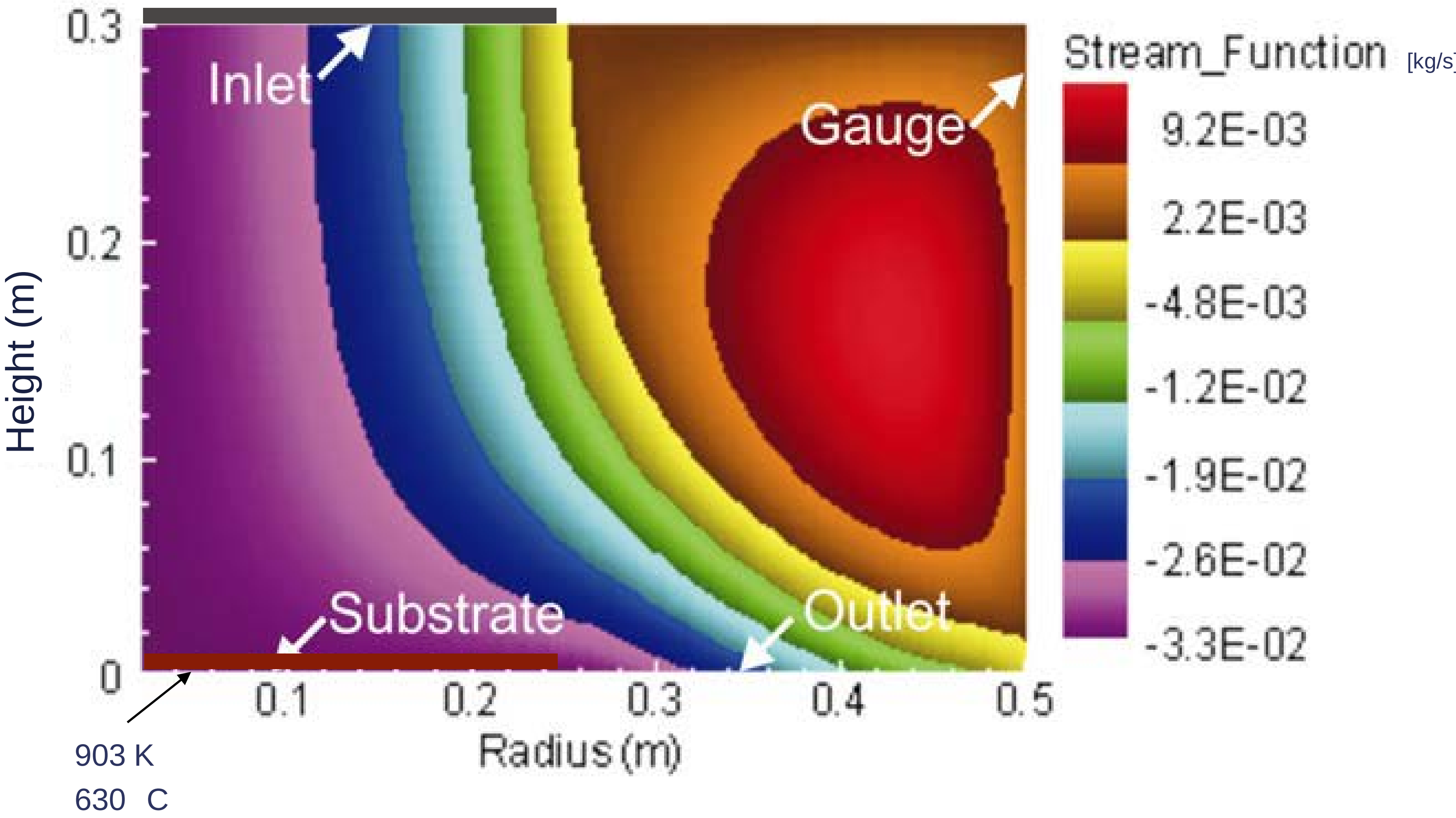

Profiles of Mass Fractions

$TiCl_4$

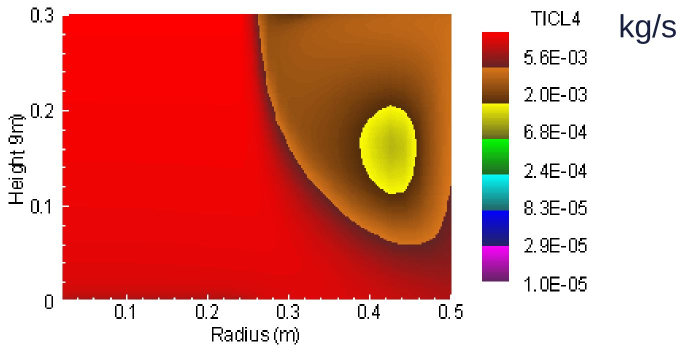

$TiCl_4{\cdot}2NH_3$

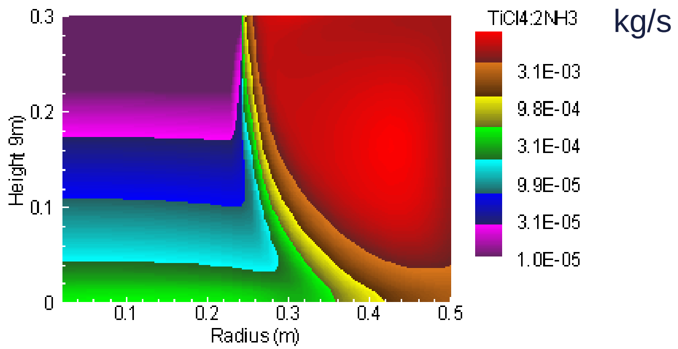

NH_4Cl

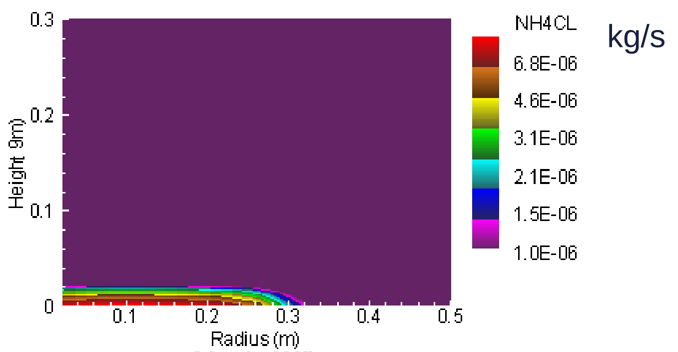

Validation Results

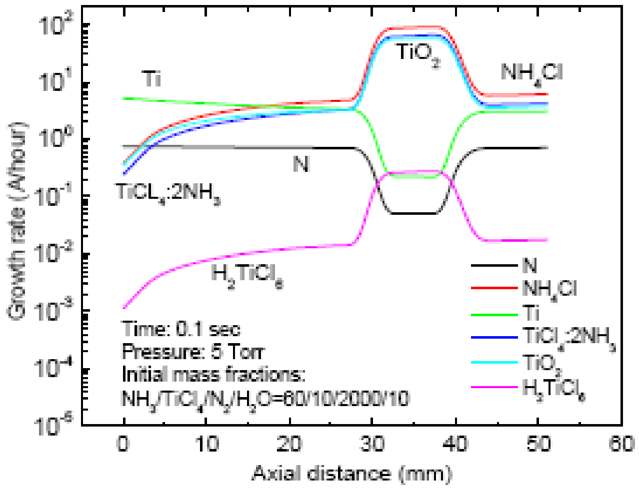

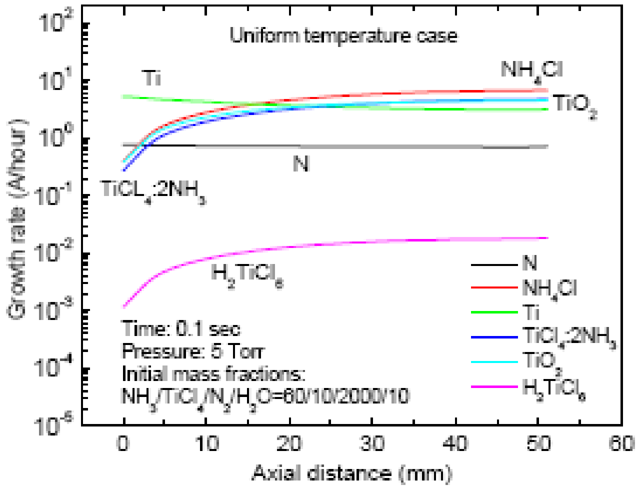

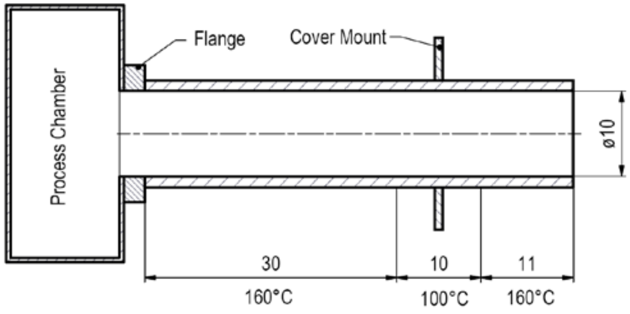

Validation Results

- The surface and gas-phase mechanisms for the TiN chemical vapor deposition process were developed based on literature data.
- Simulations were performed for a typical geometry and operating conditions of a CVD reactor and also for the transport and chemistry inside a gauge.
- The performed simulations indicate that powder deposition rate could be similar or even exceed the TiN deposition rate inside the gauge.
- Cold spot of 60 °C in gauge tube causes deposition of by-products.
    - Can reproduce deposition profile
- TiN etching by ClF_3 is not efficient since the products of etching quickly fill in the gauge and the etching stops. Cleaning is efficient only close to reactor wall.

Gauge Designs

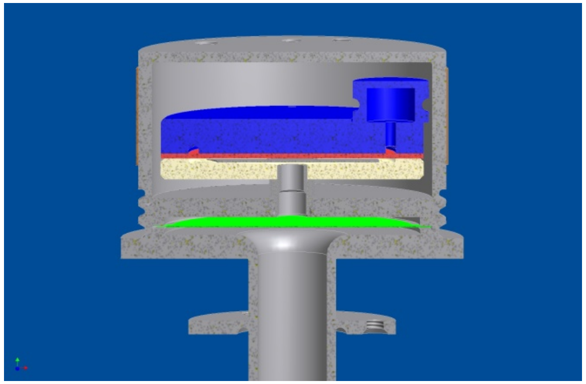

INFICON CDG160A

- Plasmashield
- Suprashield
- Crossshield

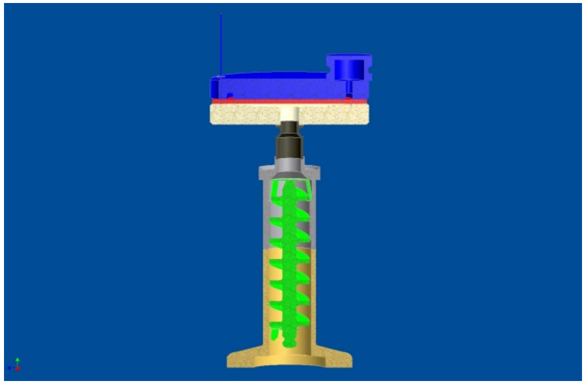

INFICON CDG160D

- Helix
- Crossshield

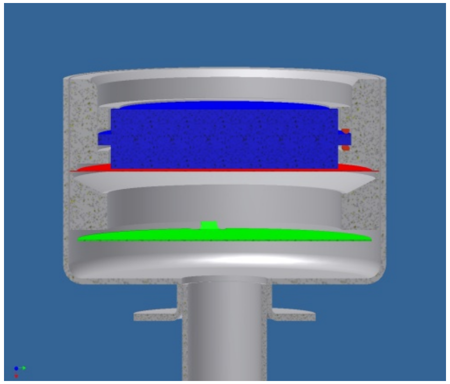

Competitor A

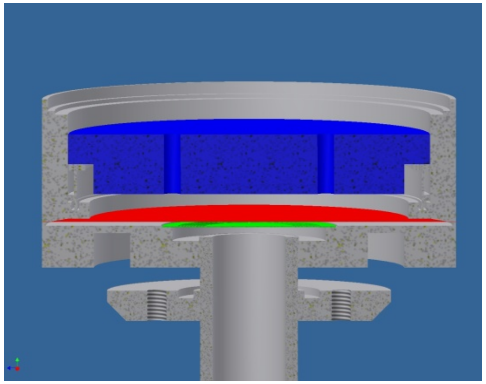

Competitor B

$TiCl_4$ + NH_3 Process in a CDG 160A with Plasma Shield
Spatial Mass Fraction Profiles

- Gas pressure 5 Torr
- Wall temperature 160 C
- Gauge filled with N_2 at start

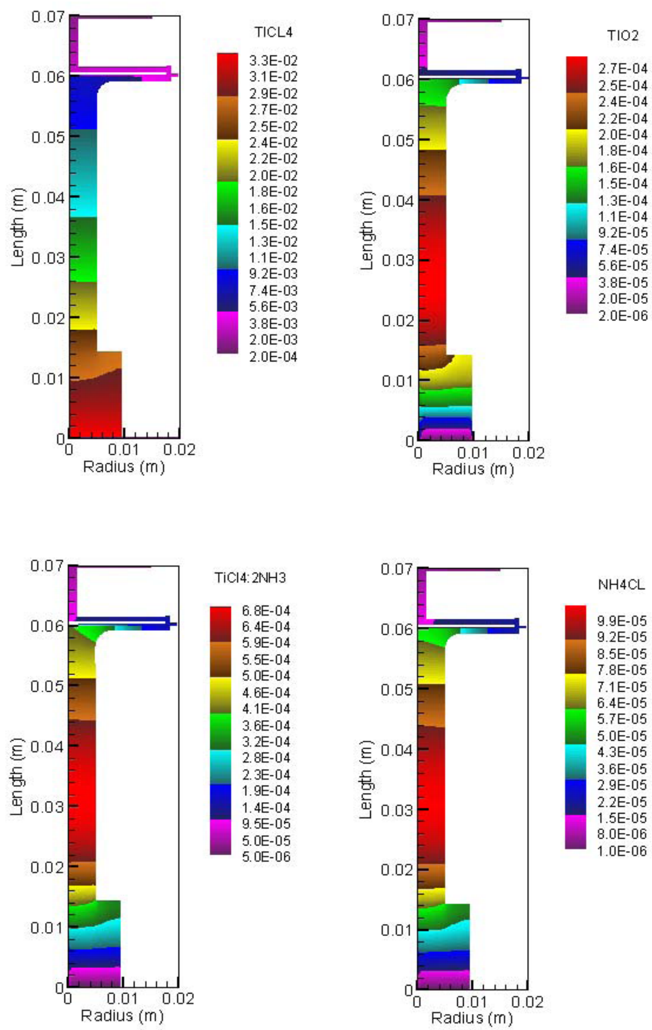

0.2 sec

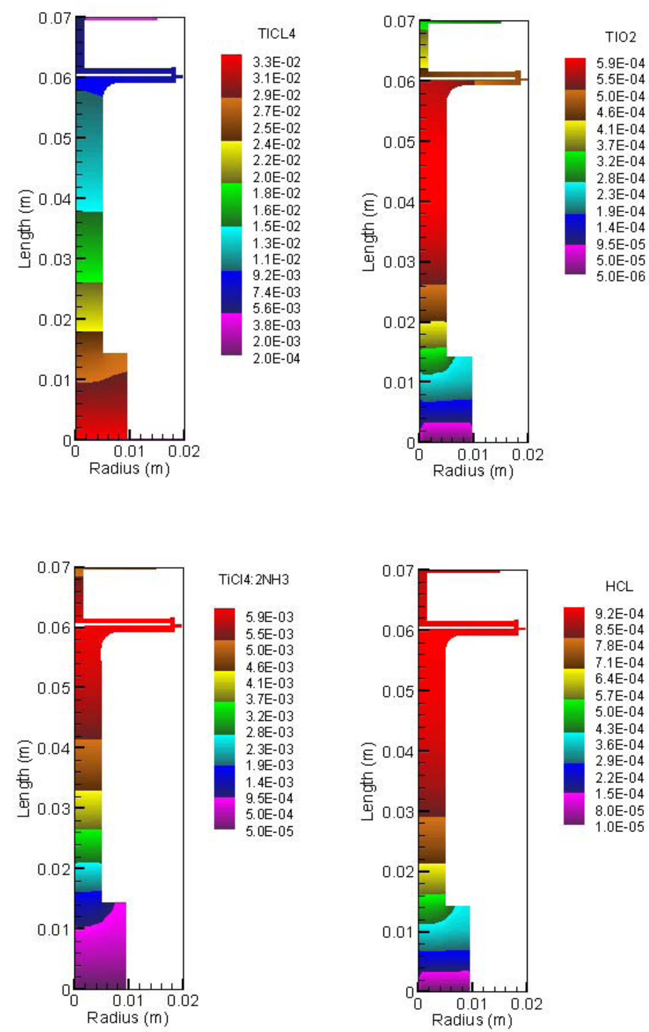

1 sec

Comparison Deposition Profile along Membrane

0.2 s

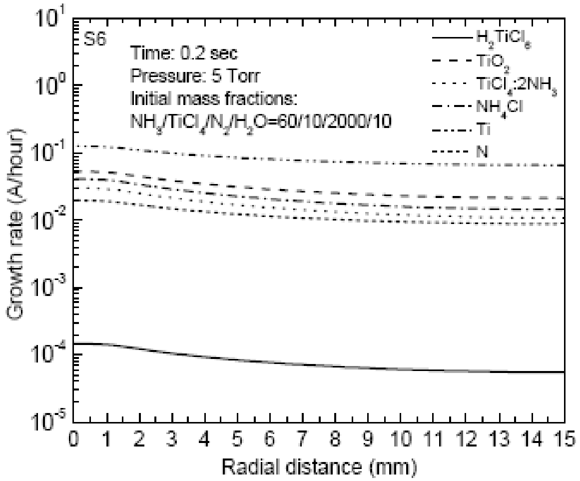

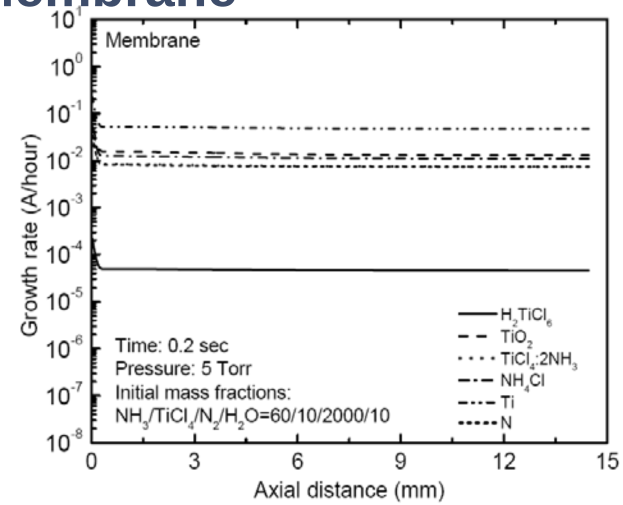

1s

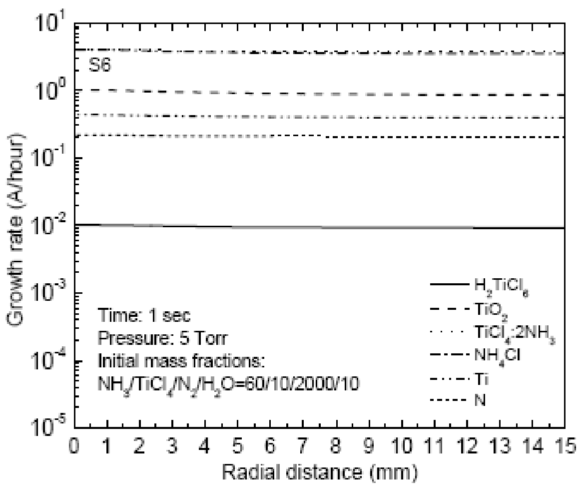

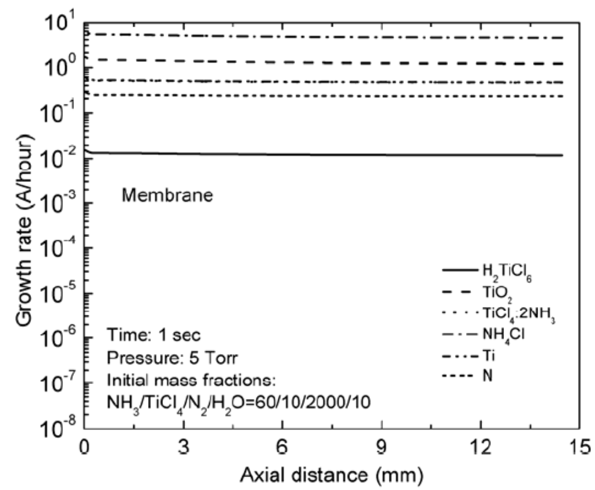

Plasmashield

Helix

3D Pressure Profile During Pressure Change
10^{-6} mbar to 1000 mbar in the Reactor

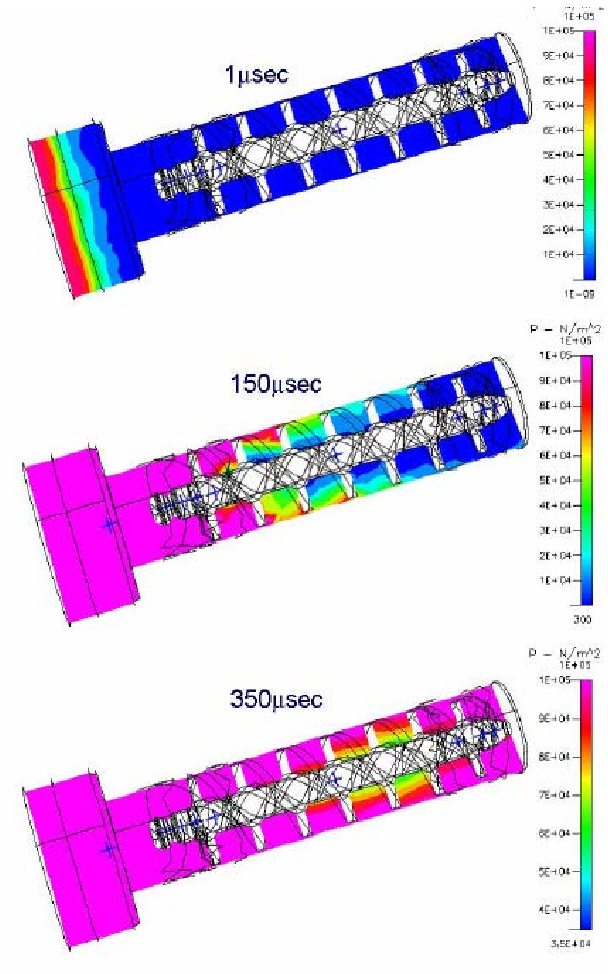

Pressure

1 ms to reach equilibrium at end of helix

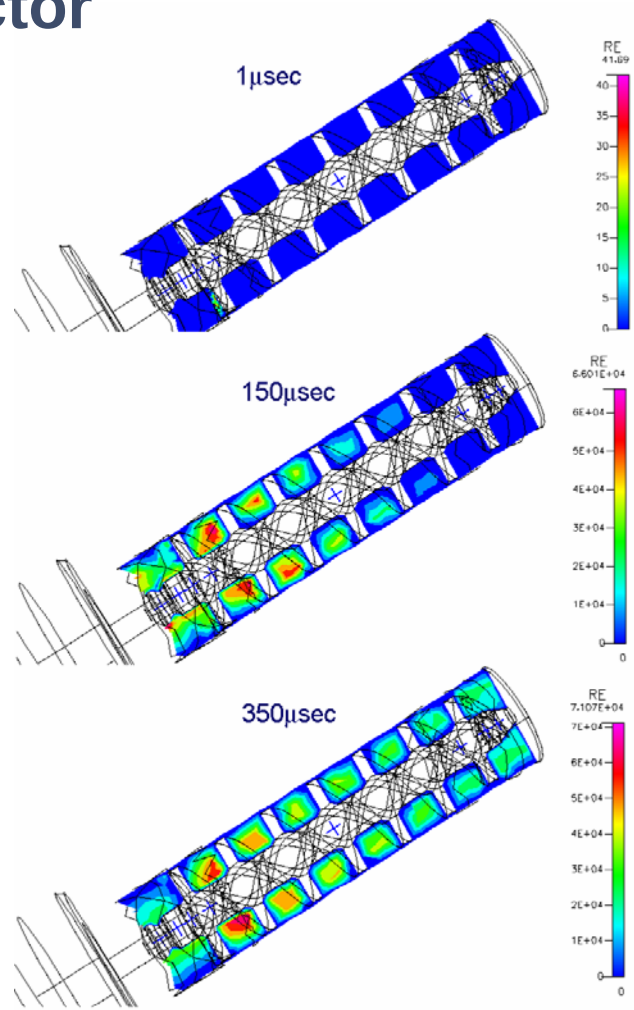

Re

Re < 2300 laminar

Re > 4000 turbulent

Stress on Membrane as Function of Time

Plasmashield

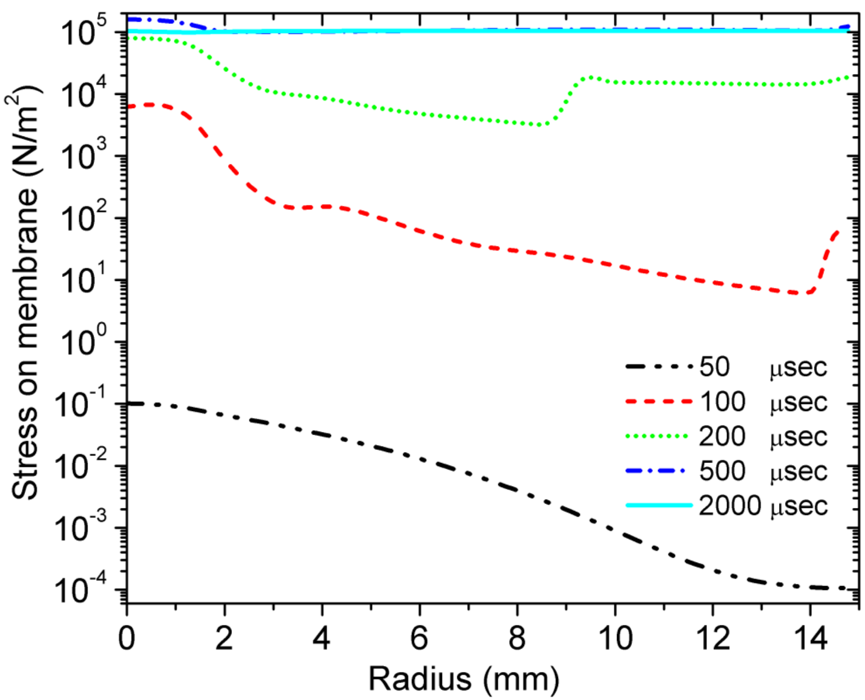

2 ms to reach equilibrium

Helix

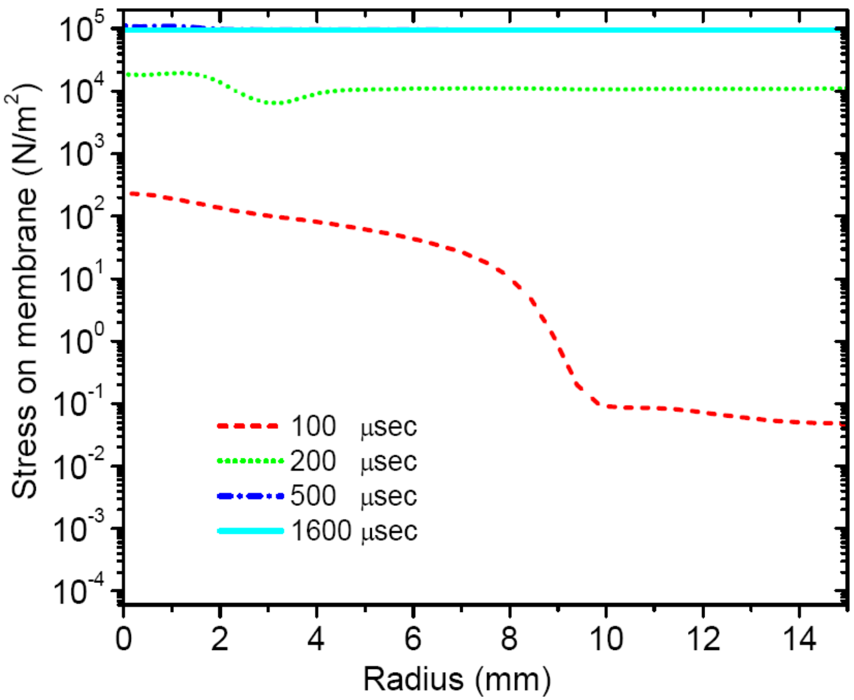

1.6 ms to reach equilibrium

2D Sim

Pressure/Knudsen Number (x, t)

Plasmashield

Solid curves - Pressure
Dashed curves - Kn

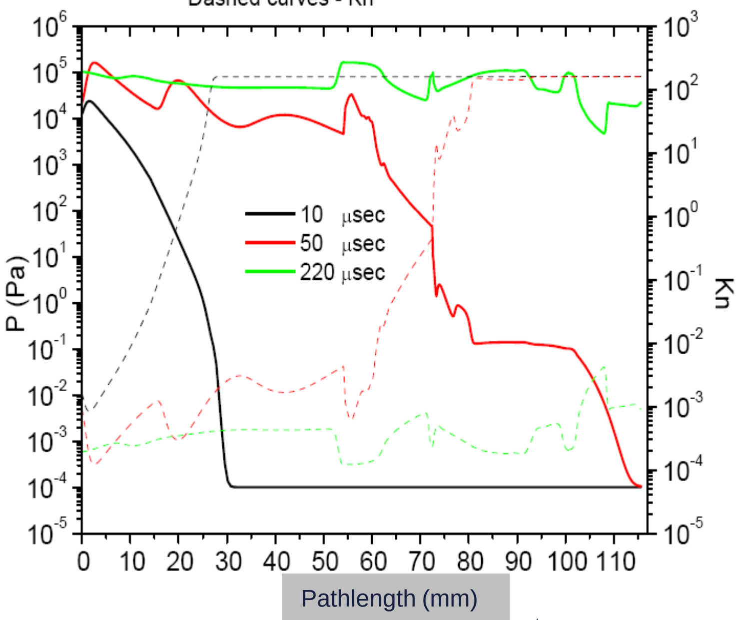

Plasma shield position

Extreme Front of Plasma shield

Center Back of Plasmashield

Helix

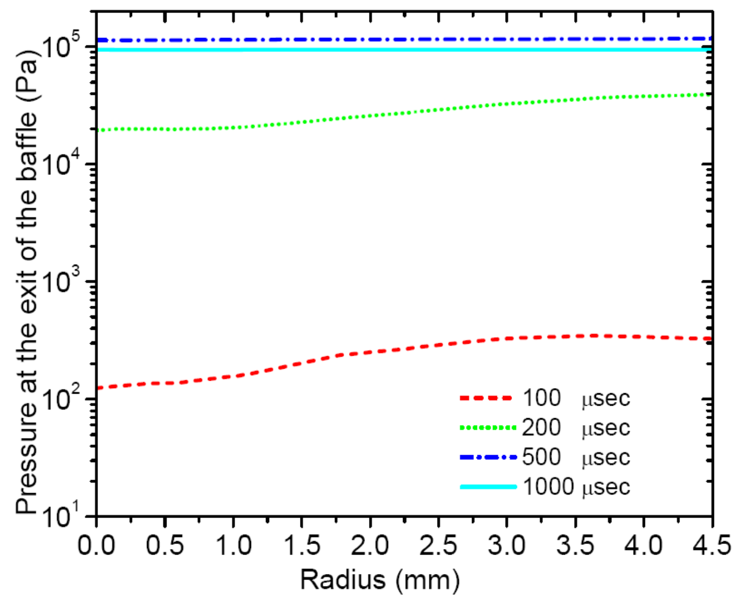

At Exit of Helix

3D Sim

Summary Dynamics

Response to step pressure change 10^{-6} mbar to ATM

Ranking	Name of the gauge	Time (µs)
1	**CDG160D with spiral baffle system**	**1600 (CFD-ACE)**
2	**CDG160A gauge with plasma shield**	**2000 (CFD-ACE)** **2000 (Fastran)** **2000 (UFS)**
3	**CDG160D gauge with a spiral baffling system and cross shield**	**2200 (CFD-ACE)**
4	**Competitor B gauge**	**3000 (CFD-ACE)**
5	**CDG160A gauge with plasma and supra shields**	**6000 (CFD-ACE)** **20000 (UFS)**
5	**Competitor A gauge**	**6000 (CFD-ACE)**

Significant difference between the results obtained with CFD-ACE and UFS for a CDG160A gauge with plasma and supra shields was attributed to different gas-surface models implemented in the codes.

Membrane Contamination

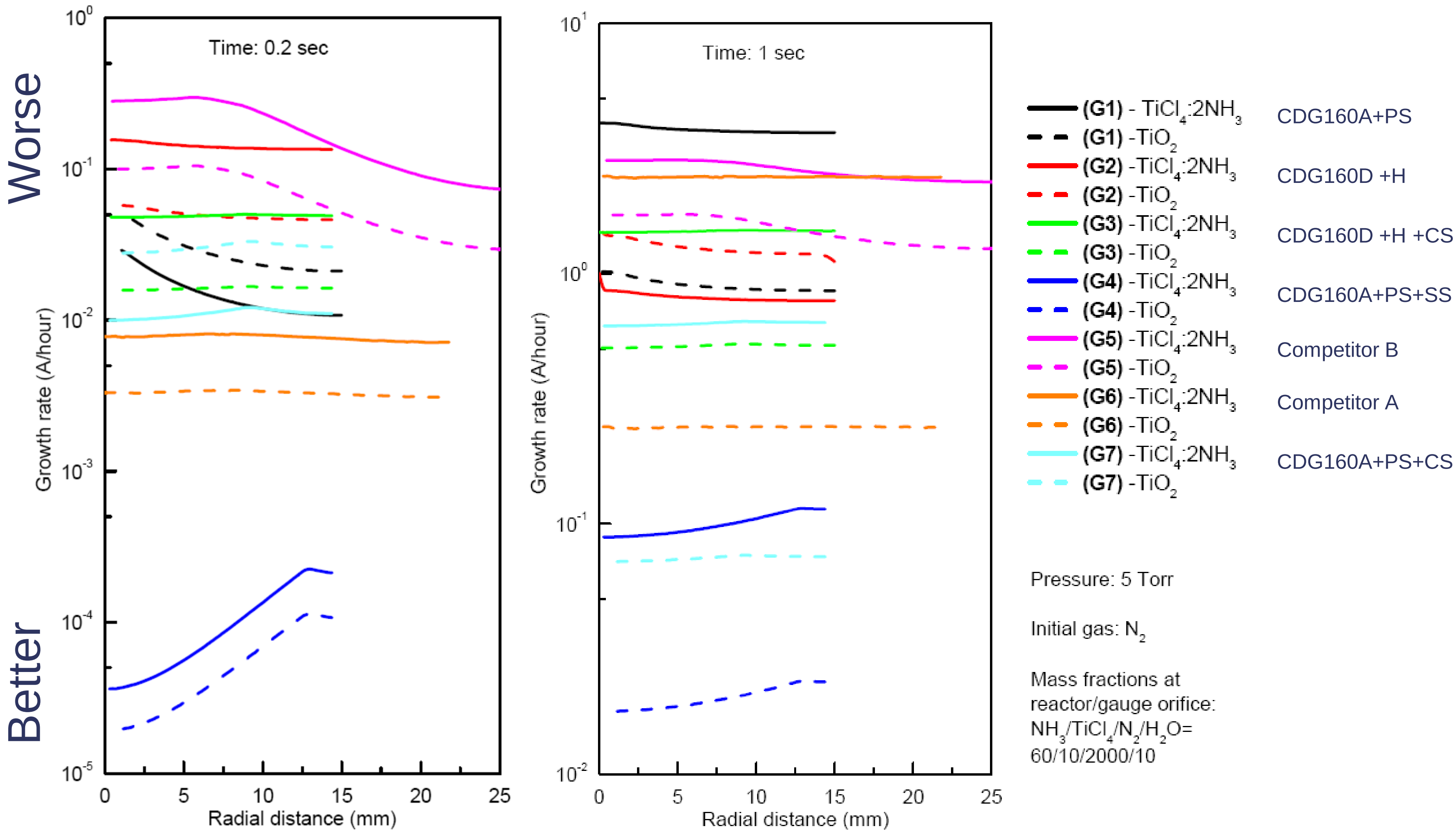

Best Membrane Protection

1. CDG160A with Plasmashield + Suprashield (G4 geometry)

   has the smallest powder deposition rates at both 0.2 s and 1 s.

2. CDG160A with Plasmashield + Cross shield (G7 geometry)
3. CDG025D + Helix (G2)
4. CDG025D + Helix + Cross shield (G3)
5. Competitor A (G6)
6. Competitor B (G5)

   largest at 0.2 s, but they are smaller than G1 at 1 s.

7. CDG160A + Plasmashield (G1)

Process Drift Improvement

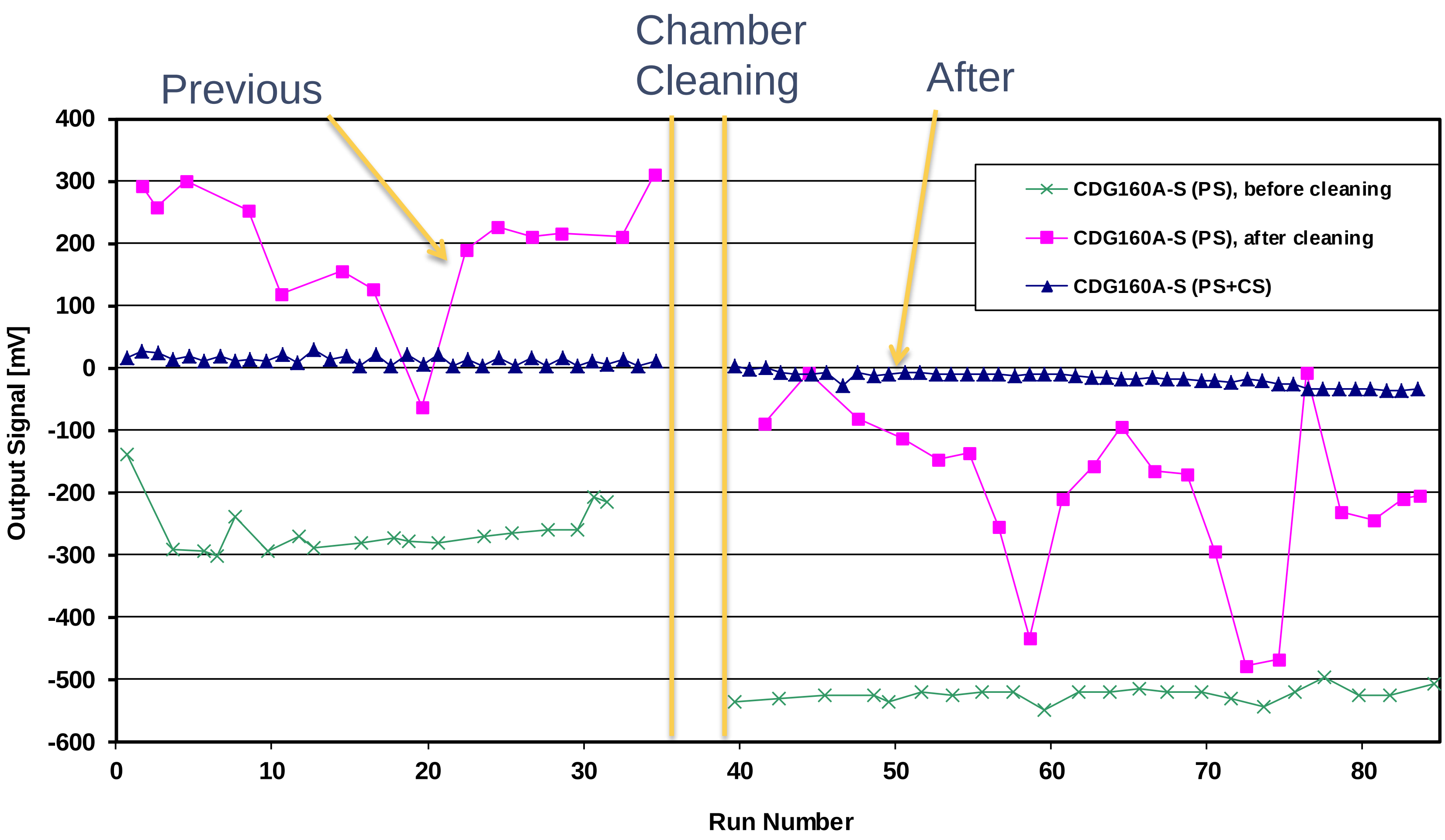

Summary of Simulation

- Using a CFD computer code we have investigated membrane contamination and gas dynamical response time in a TiN process for 7 different geometries.
- Position of gauge in process has great influence on chemistry seen by gauge.
- Baffle geometry and gas dynamics in a gauge have a strong effect on the contamination of the membrane and the speed of response.
- INFICON has best in class gauge protection available.

Small Scale CDGs

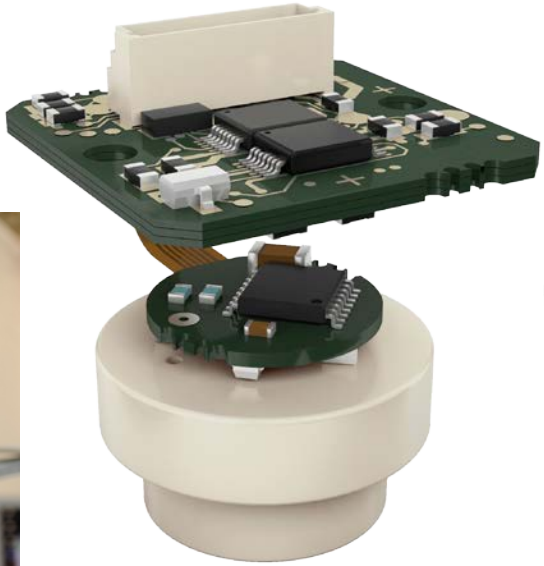

INFICON Spot CDS550D

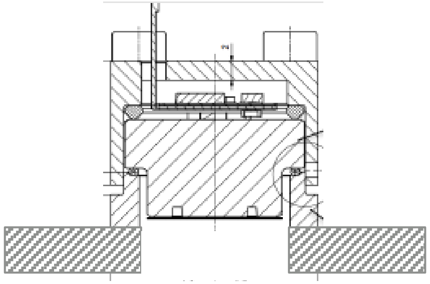

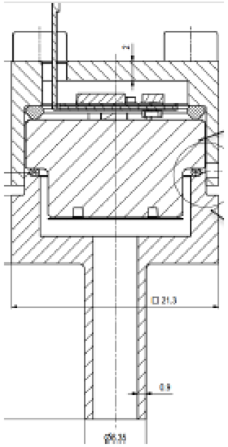


INFICON
CDG

Pirani

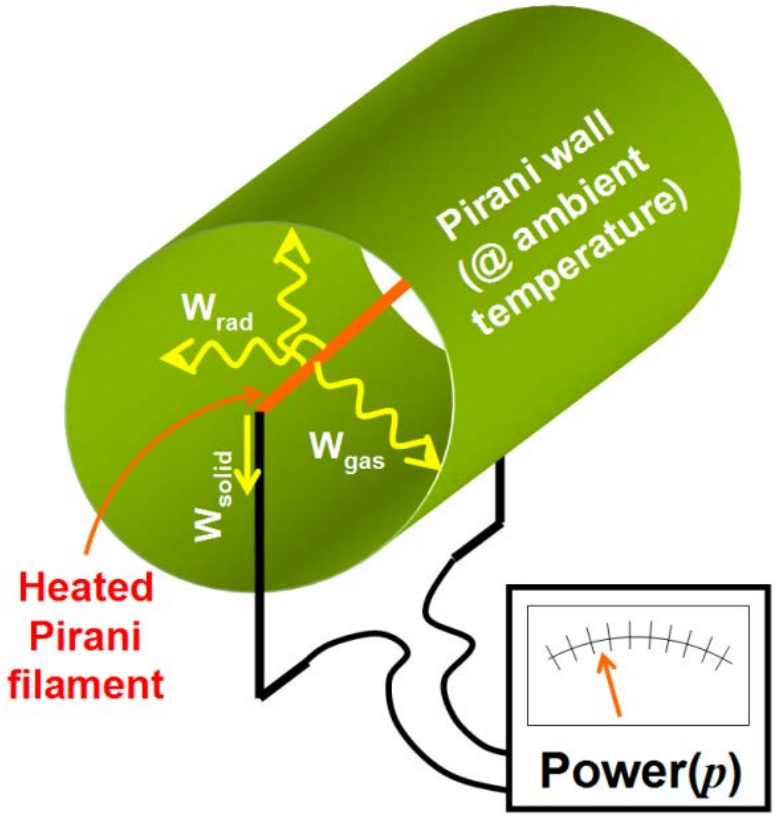

Pirani wall
(@ ambient
temperature)
W_{rad}
W_{solid}
W_{gas}
Heated
Pirani
filament
Power(p)

Thermal Conductivity Sensor

a) Heat loss through radiation

$$W_{gas,v} \propto f\left(\varepsilon_p, \varepsilon_W\right) \times \left(T_p^4 - T_W^4\right)$$

b) Heat conductance from filament to support

$$W_{solid} \propto \left.\frac{\partial T_p}{\partial x}\right|_{@ends}$$

c) Heat conductance through gas

- Molecular flow (Kn > 0.5)

$$W_{gas,m} \propto \frac{a_E}{\sqrt{m}} \frac{\left(T_p - T_W\right)}{\sqrt{T_W}} \times p$$

- Viscous flow (Kn < 0.01)

$$W_{gas,v} \propto \frac{\left(T_p - T_W\right)}{\sqrt{m}} \times f\left(d\right)$$

- Transition flow (0.01 < Kn < 0.5)

d) Heat transport through convection (Kn << 0.01)

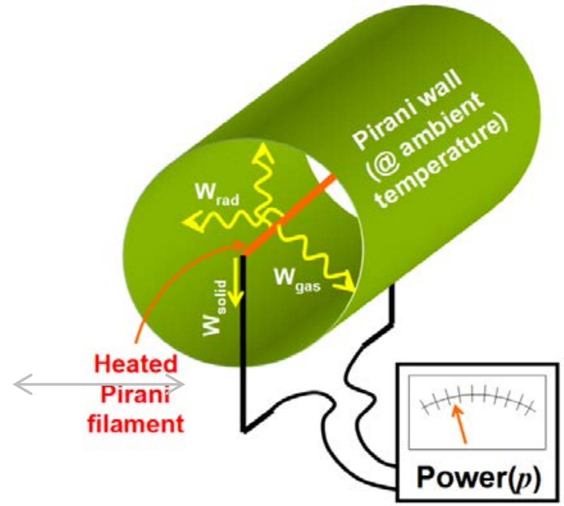

Pirani Sensor Elements

1970

TPR010

10^{-3} to 100 mbar

1995

TTR211/216

$5*10^{-4}$ mbar to ATM

1998

PSG400

$5*10^{-4}$ mbar to ATM

2004

PSG500

$5*10^{-5}$ mbar to ATM

2010

PSG550

$5*10^{-5}$ mbar to ATM

Issues

- Increase upper pressure limit
- Increase lower pressure limit
- Increase accuracy
- Increase process inertness
- Increase dynamics
- Decrease size

Range Extensions

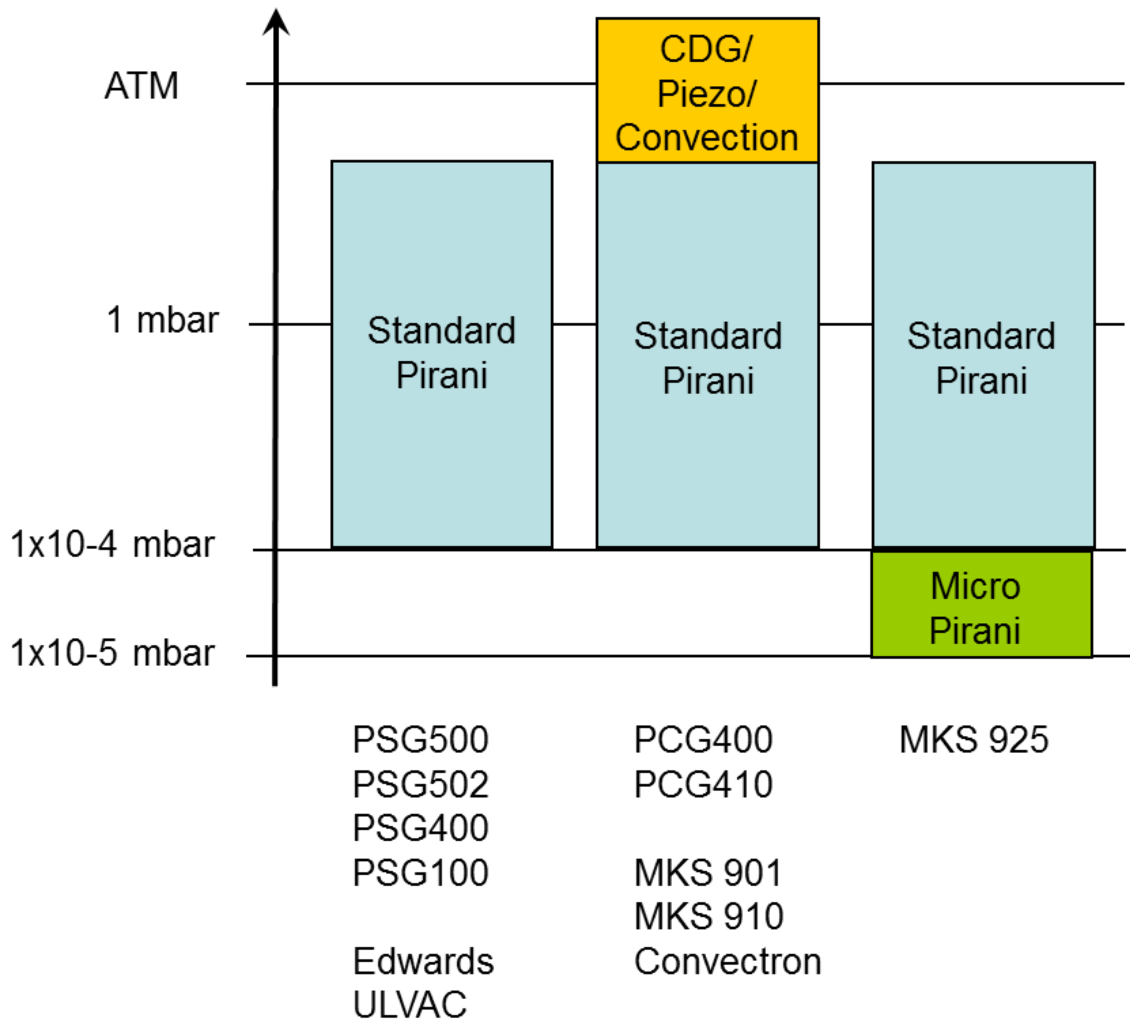

Increasing the Upper Pressure Limit:

1. **Use of convective transport**

Convection enhanced gauge

- ✓ Increased sensitivity at atmospheric pressure
- × Orientation dependence
- × Large volume needed
- × Slow dynamics

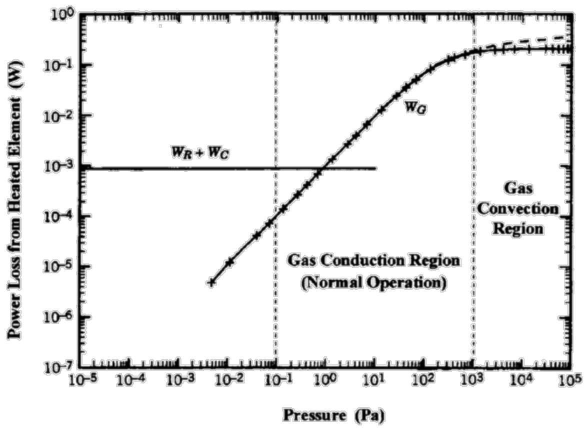

Ellefson and Miiller, JVSTA, 18, 2568-2577, 2000,

INFICON PGE050

Alternative designs, e.g. Edwards APGX

- ✓ Reduced orientation dependence
- — Smaller but still substantial volume
- × Slow dynamics

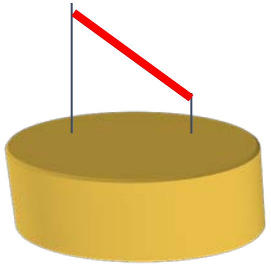

Pirani filament at tilted angle

Increasing the Upper Pressure Limit:

2. Reduce mean free path

Reduce distance Pirani – Wall → MEMS

- ✓ Increased sensitivity at atmospheric pressure
- ✓ Good dynamics
- ✗ Sensitive to contamination

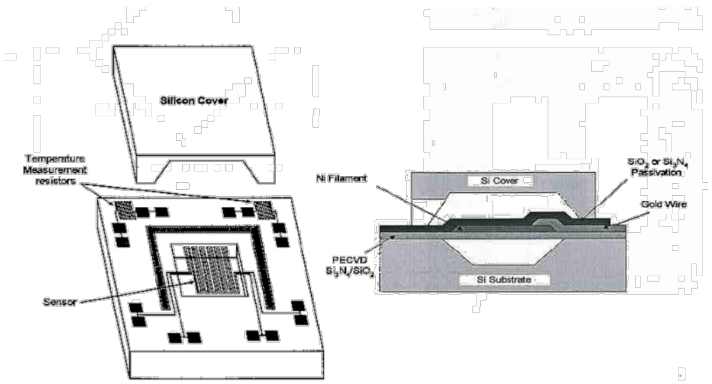

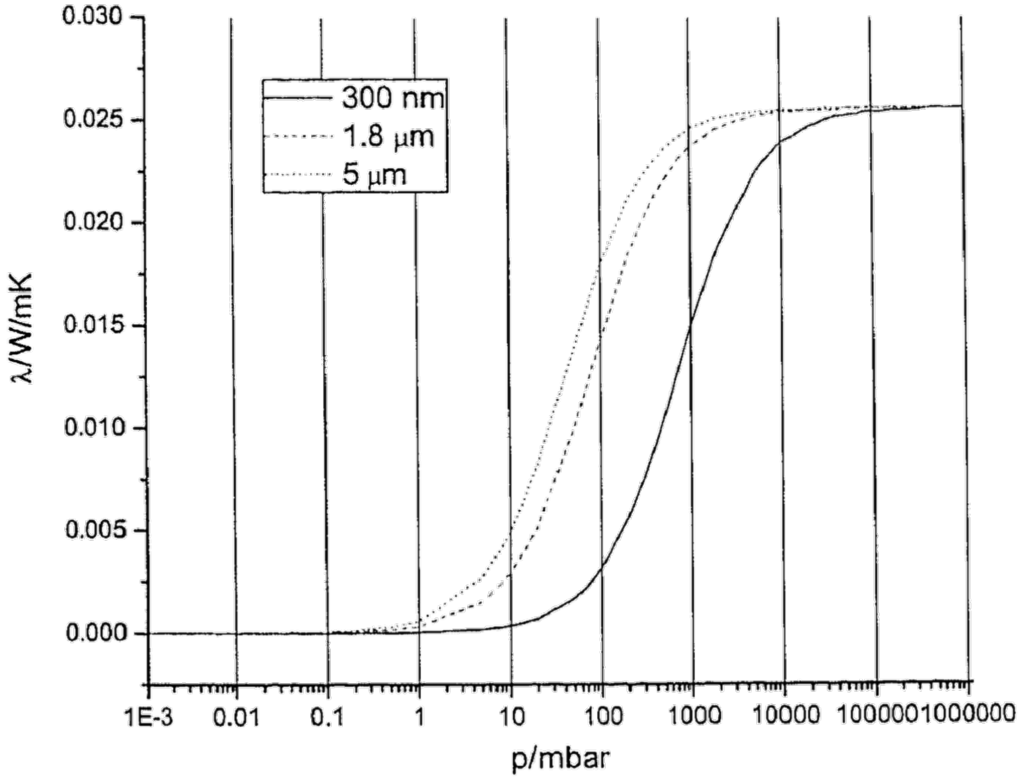

Doms et al., J. Micromech. Microeng., **15,** 1504-1510, 2005

Increasing the Upper Pressure Limit:

3. Measurement of gas' heat capacity

Use time variable Pirani temperature $T_p(t)$

a) Pulsed heating mode

Jitschin and Ludwig, Vacuum 75, 169-176, 2004

b) Superposition of AC temperature signal on stationary Tp

D.J. Seong et al., Key. Eng. Mat., **277-279**, 990-994, 2005.

✓ Conventional Pirani sensor may be used

✗ Medium to slow dynamics (1-10 Hz)

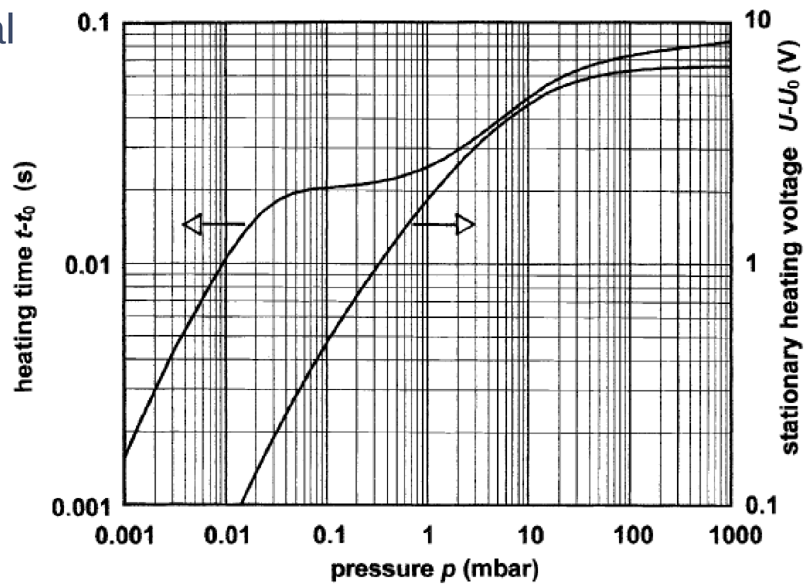

W. Jitschin et al., Vacuum, **75**, 169-176, 2004.

Reducing the Lower Pressure Limit

$$W_{gas} << W_{rad}\ ,\ W_{solid}$$

1) Radiation losses

- Reduce Pirani temperature
  - MEMS
  - use low emissivity materials

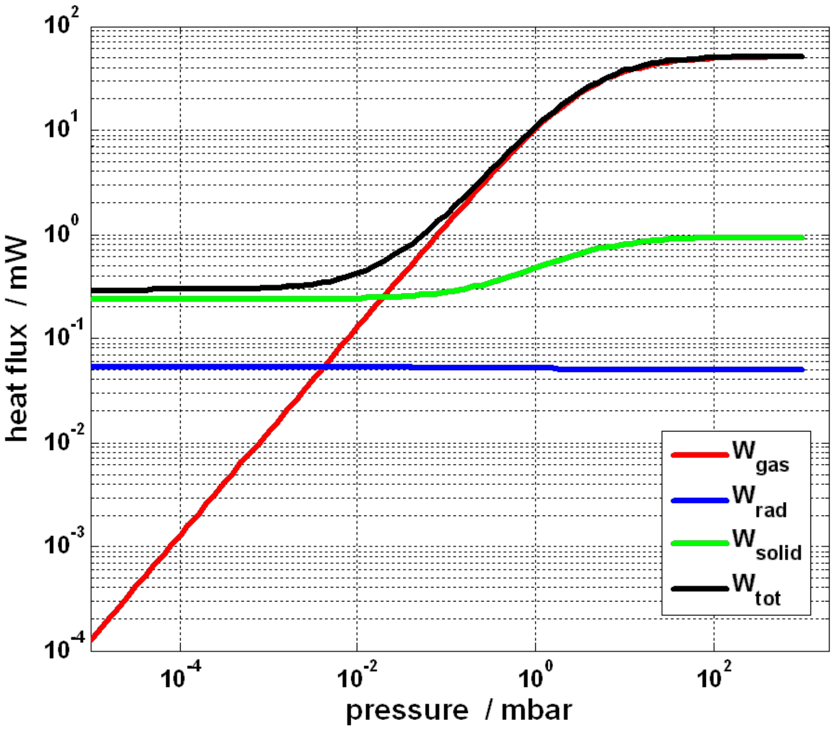

Reducing the Lower Pressure Limit

2. **Heat losses through Pirani filament ends**

- typically dominate over radiation losses

$$W_{solid} >> W_{rad}$$

- increase filament length
  - ➢ helicoidal filament
- inhibit thermal flux from heated Pirani element to support through bridges
  - ➢ high thermal resistance bridges between support and Pirani-membrane in MEMS-Pirani
  - ➢ heated bridges

A. W. Van Herwaarden et al., Sensors & Actuators, **14**, 259-268, 1988.

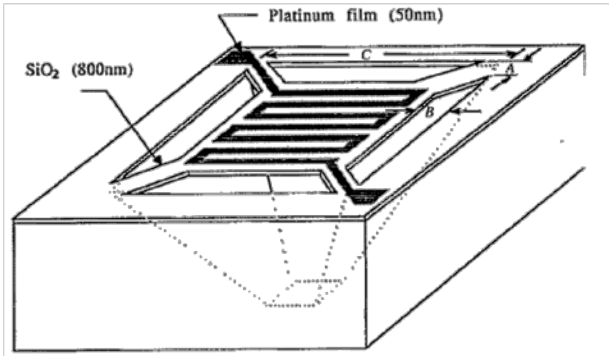

P. K. Weng et al., Rev. Sci. Instrum., **65**, 492-499, 1994.

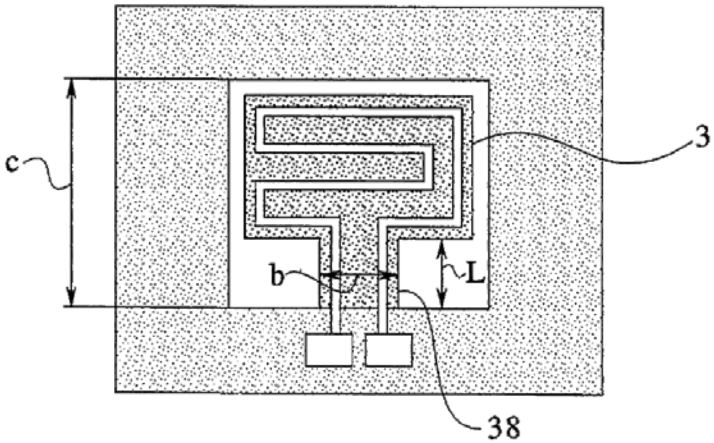

J. Schieferdecker et al., US005597957A

A Comparison

Conventional Pirani with helicoidal filament

- ✓ Robust and reliable
- ✓ Good long term stability
- ✓ Good dynamics
- ✓ Low price
- ✗ Limited sensitivity @ $p < 10^{-4}$ mbar and $p > 10^{2}$ mbar
- ✗ Gas type dependence

MEMS-Pirani

- ✓ Extended low pressure range when W_{solid} is reduced
- ✓ Better sensitivity at atmospheric pressure due to
- ✓ Small volume
- ✓ Good dynamics
- ✗ Price
- ✗ Contamination ➢ limited long term stability
- ✗ Gas type dependence

Convection enhanced Pirani

- ✓ Increased sensitivity at $p > 10^{2}$ mbar
- ✗ Large volume
- ✗ Slow dynamics
- ✗ Dependence on mounting orientation
- ✗ Gas type dependence

Heat capacity measuring Pirani

- ✓ Increased sensitivity at $p > 10^{2}$ mbar
- ✓ Low price as based on conventional Pirani
- ✗ Medium to slow dynamics
- ✗ Gas type dependence

Carbonized filament

Fluorine Etch of W Wire

Dry etch application: CHF_3, CF_4, C_4F_6, CH_2F_2, C_4F_8

W is not resistant to those gases.

-> Wire gets thinner

->Resistance increases

$$R = \rho \frac{l}{A} = \rho \frac{l}{\pi r^2}$$

Eventually gauge failure after 2 weeks

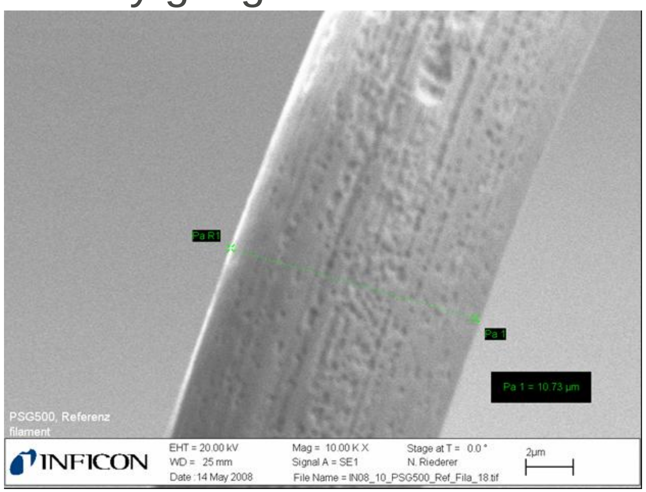

The measured diameter of a new W wire amounts to approx. 10.7µm (with tolerances)

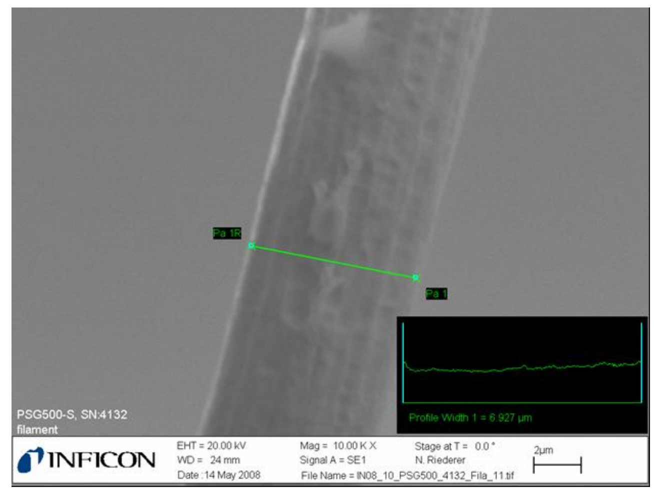

The measured diameter of the W wire of SN:4132 amounts to approx. 6.9 µm (with tolerances)

W Filament 10 min in 40% HF Solution

Prior

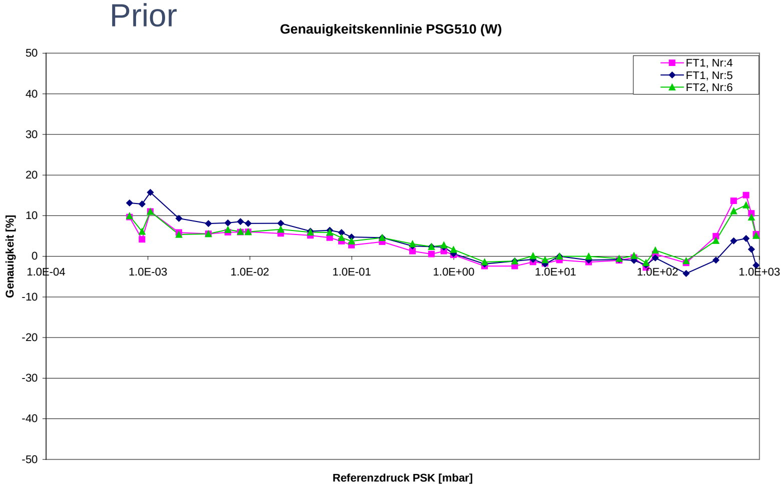

After

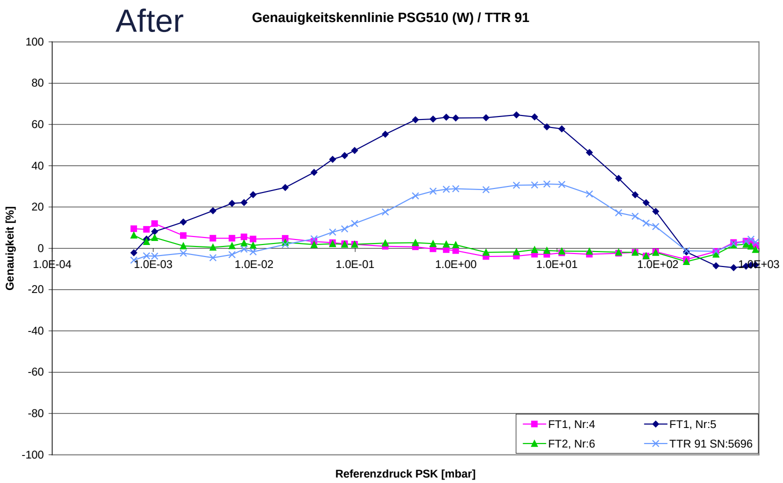

	Nr. 0	Nr. 5	Nr. 6
Filament Resistance after Test	41.46 Ω	40.39 Ω	39.7 Ω

PSG502 Ni Filament with HF

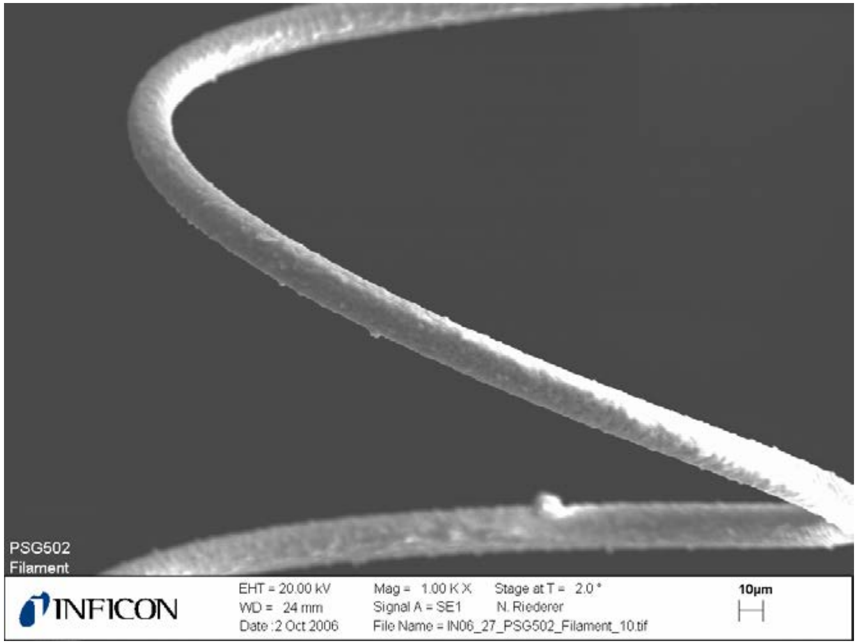

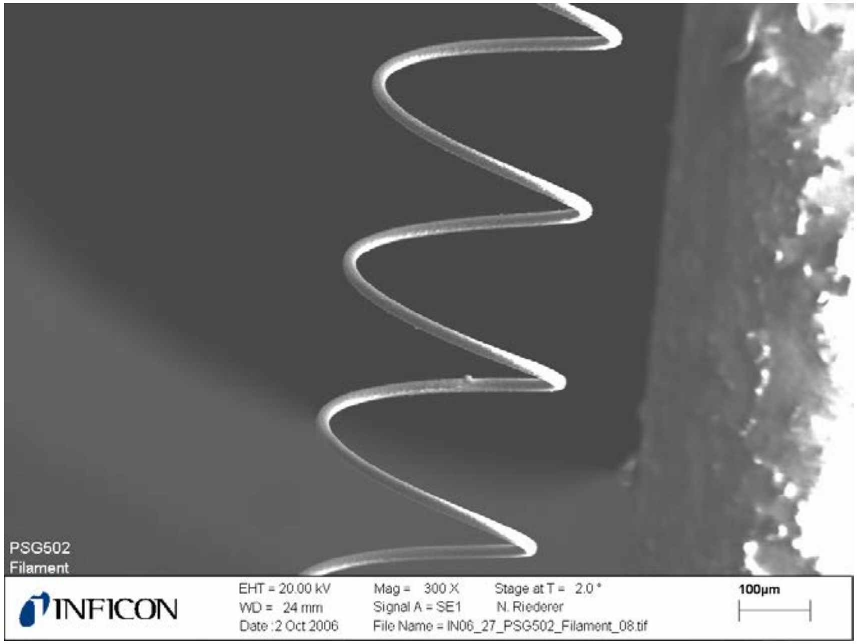

Pirani in liquid (!) HF

Nickel

Tungsten

Experiment conditions: HF 40% 10 minutes

Critical Materials: ZnO

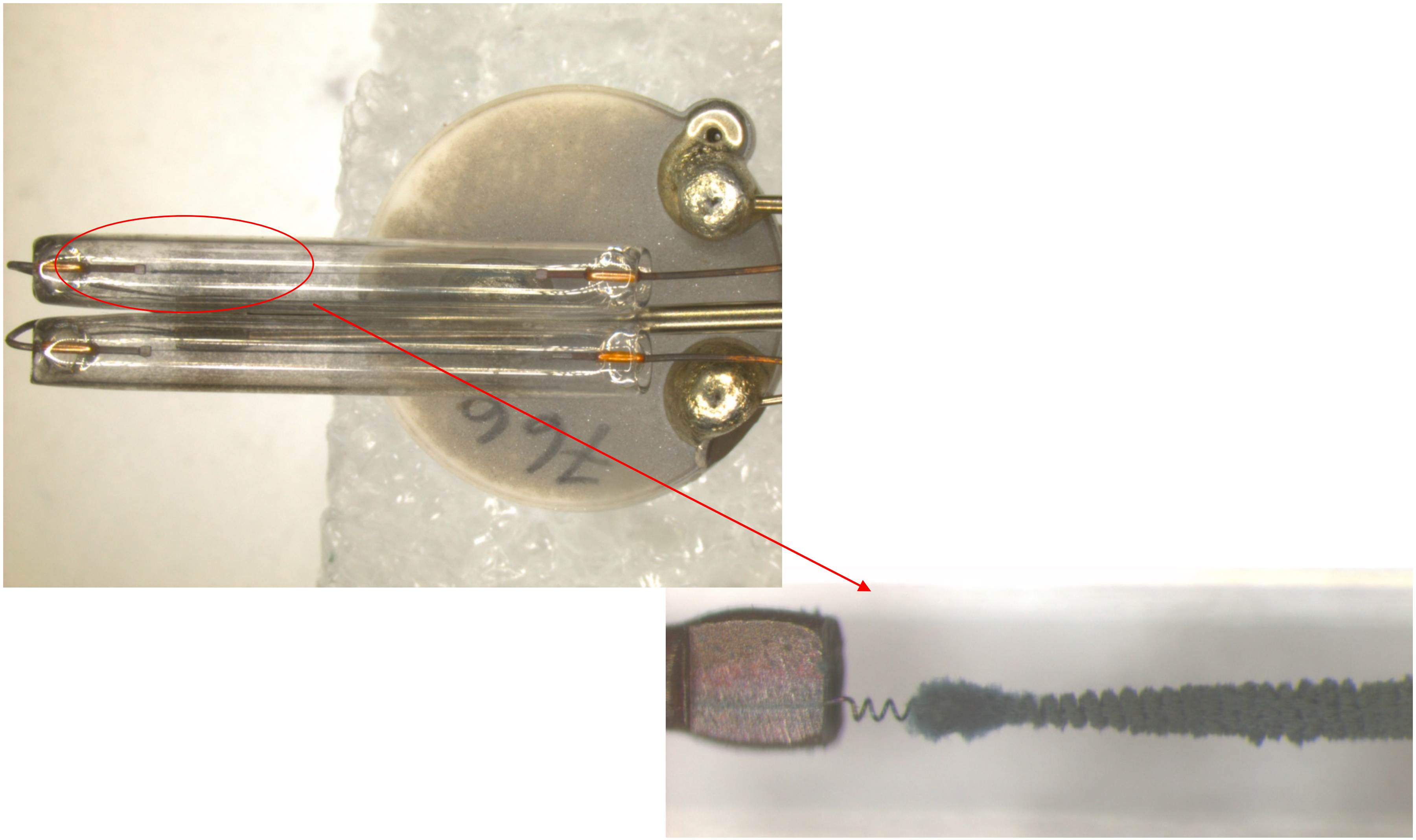

Accuracy PSG vs. PCG

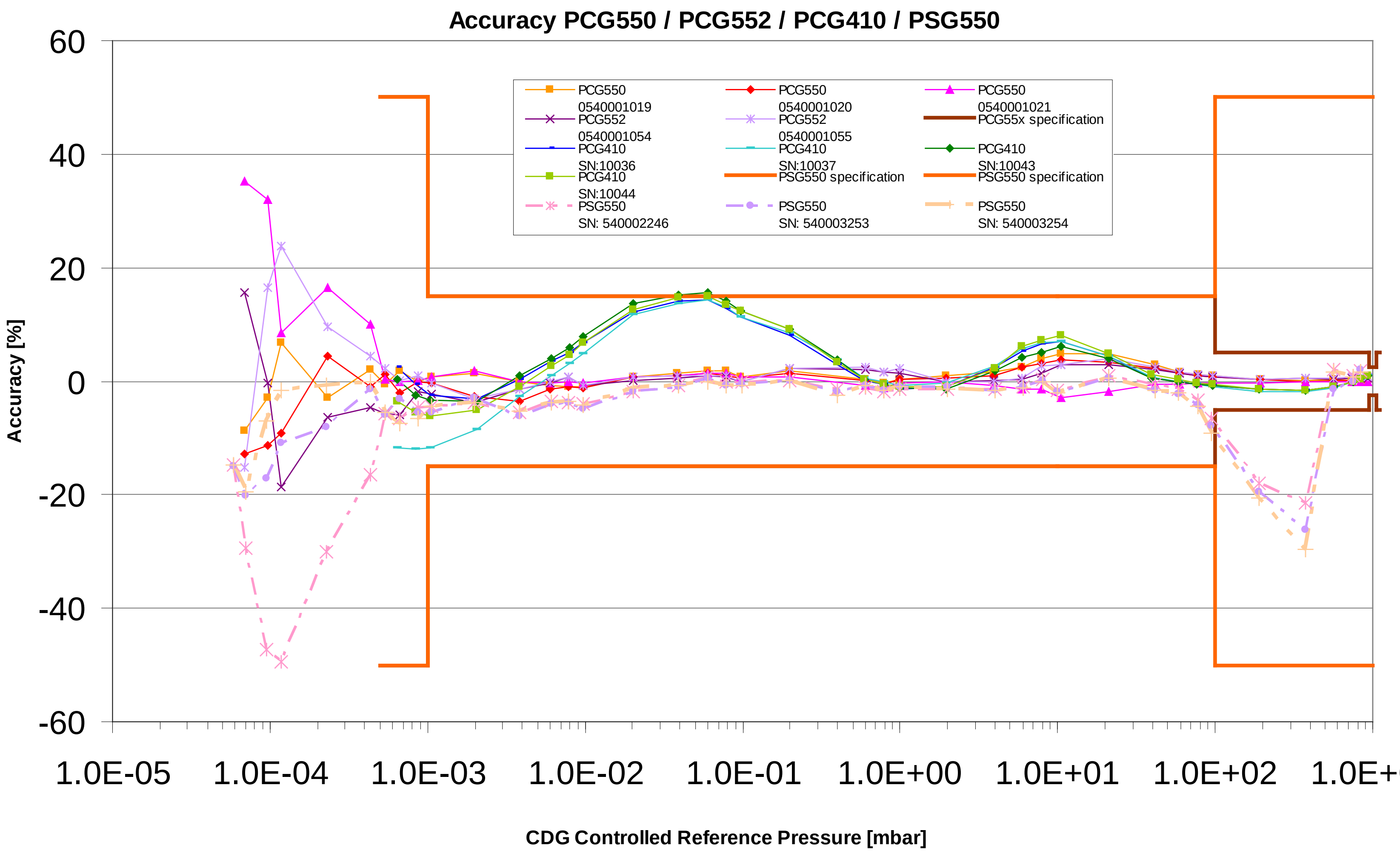

Insufficient Corrosion Resistance

What is the Ceramic Coated sensor?

The Ceramic Coated Pirani is a fully Al_2O_3 coated sensor. The ceramic coating prevents the sensor from corrosion in harsh environment.

W or Ni Version **Ceramic Coated**

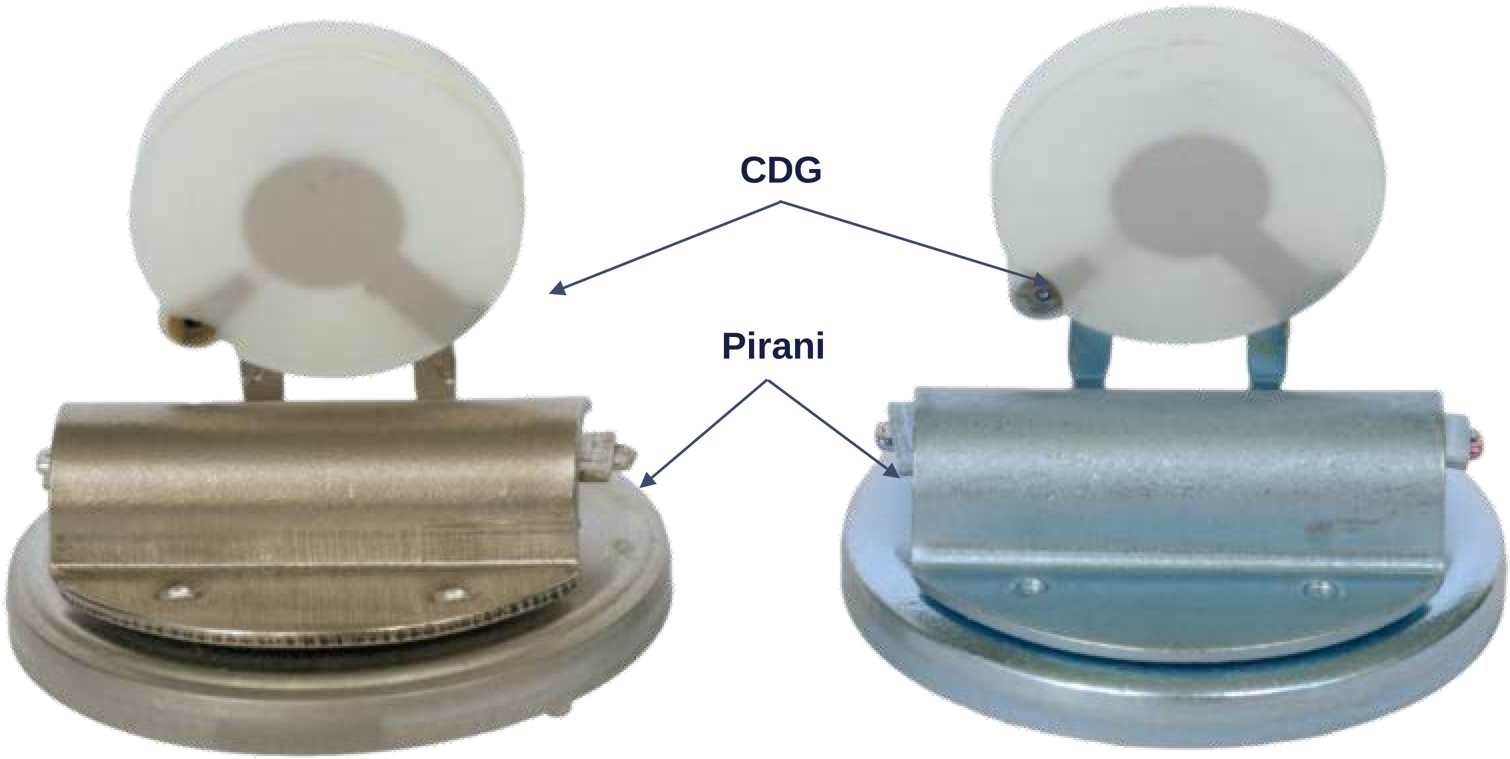

Testing

To investigate that the coating is sealed, we run tests with H_2O_2 and saw that the ceramic coated filament showed no dissolution or corrosion whatsoever.

Coated filament after 60 min in 50 % H_2O_2 at 25 °C

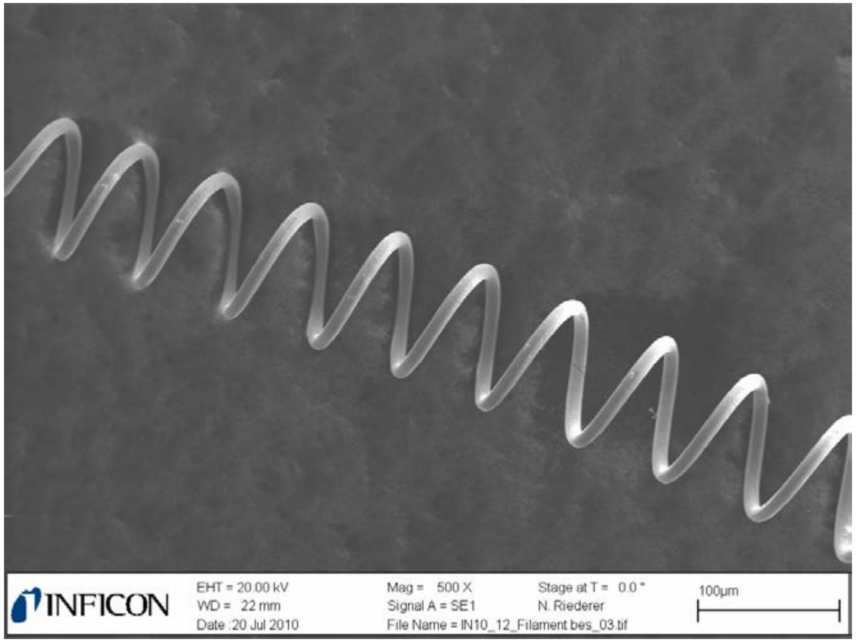

Uncoated tungsten filament after 60 min in 50 % H_2O_2 at 25 °C

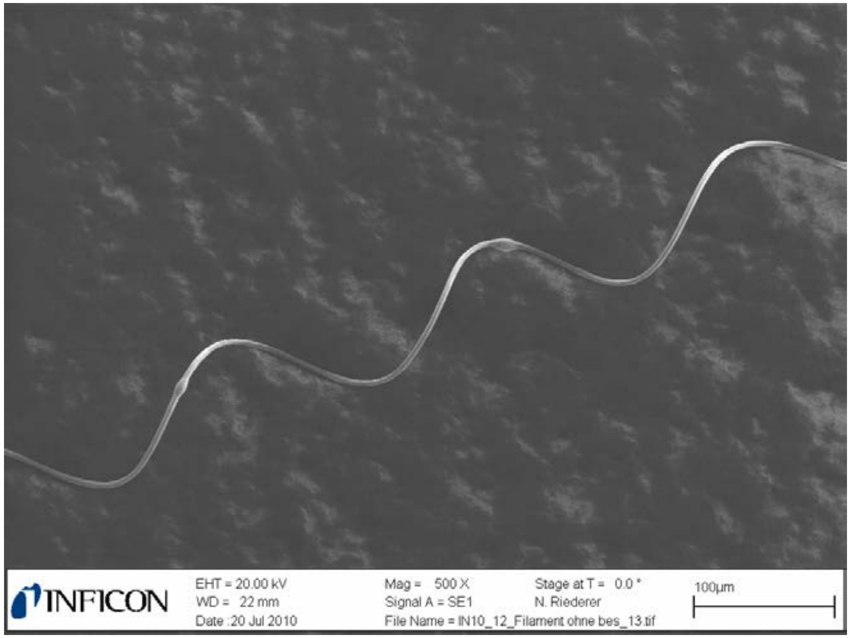

Testing

When moving closer into the SEM picture we see that the coated filament still has the exact same diameter then before the test. The uncoated filament has been eaten down to more then the half of the original diameter.

coated filament after 60 min in 50% H_2O_2 at 25 °C

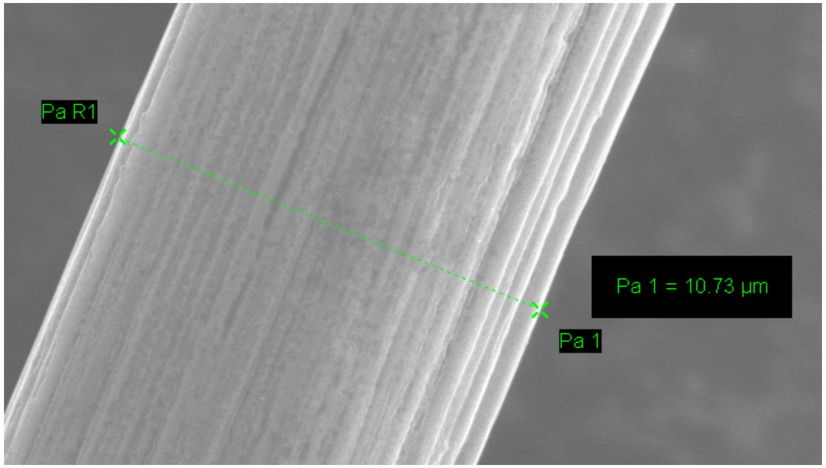

uncoated tungsten filament after 60 min in 50% H_2O_2 at 25 °C

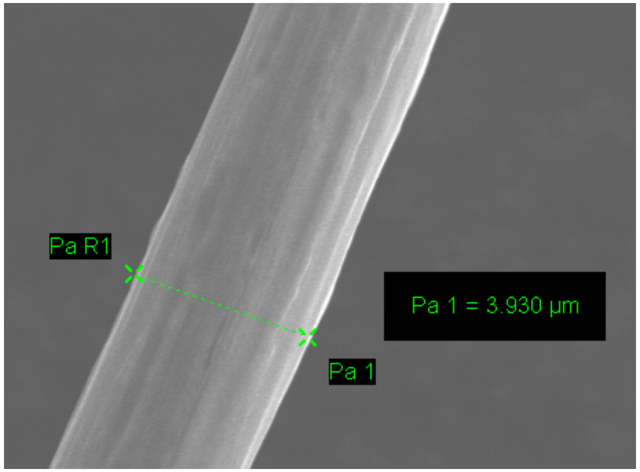

Original wire diameter = 10.6 µm
Coating thickness = 0.08 µm

Wireless Pressure Sensing

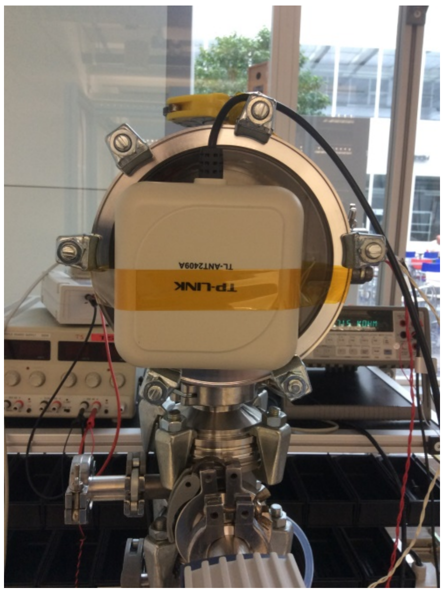

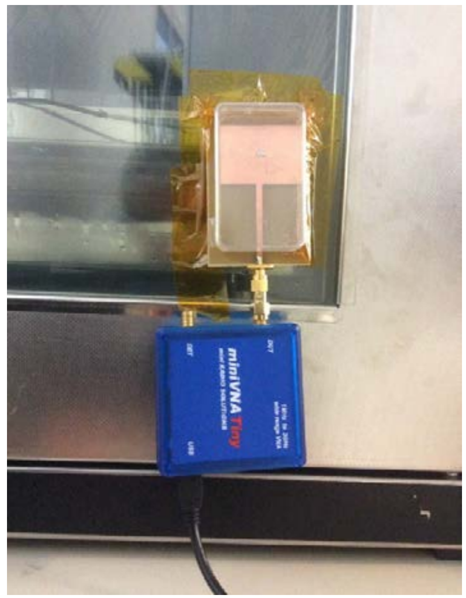

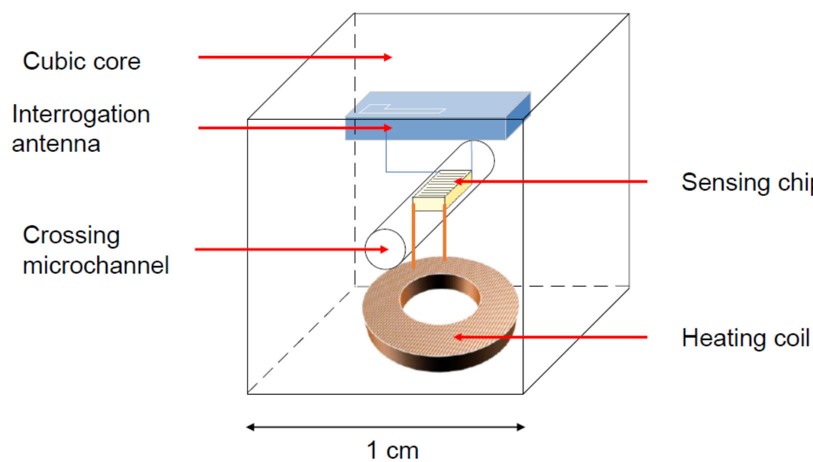

Sofia Toto, Ph.D. Thesis, Karlsruhe Institute of Technology, 2018

Manufacturing

Manufacturing: Automation

Manufacturing: SPC Pirani

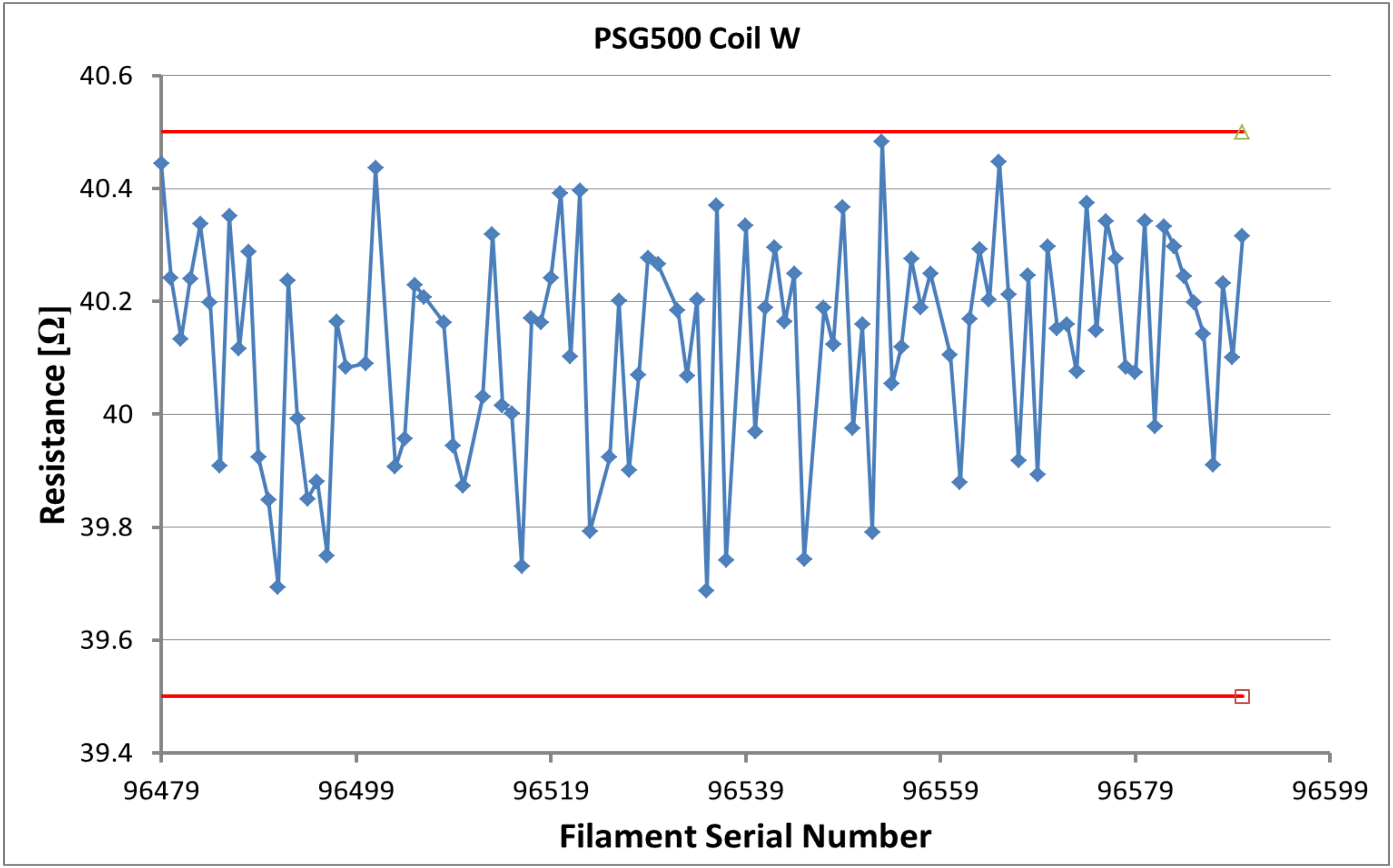

Manufacturing: Optical Inspection Tool

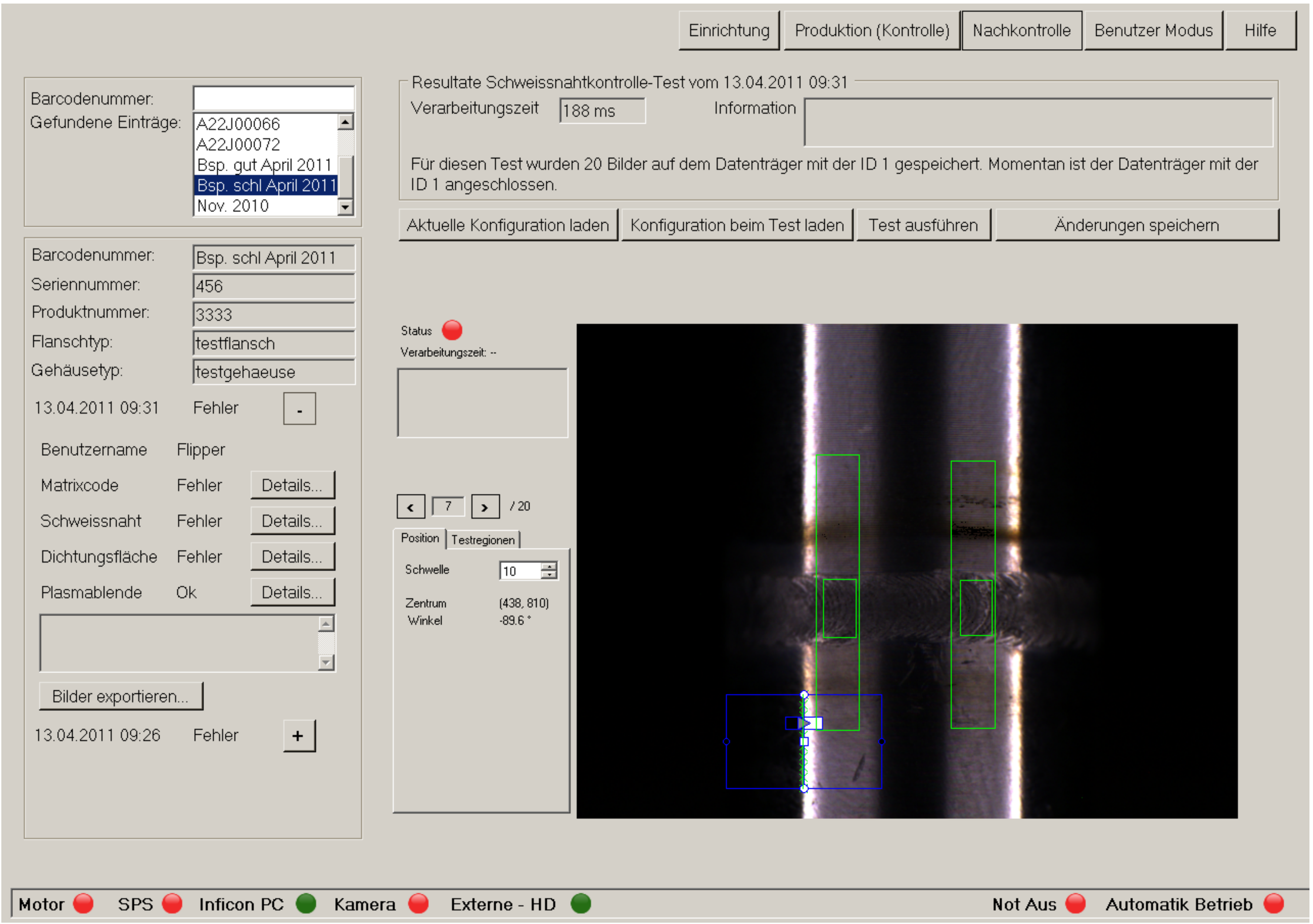

Factory Calibration

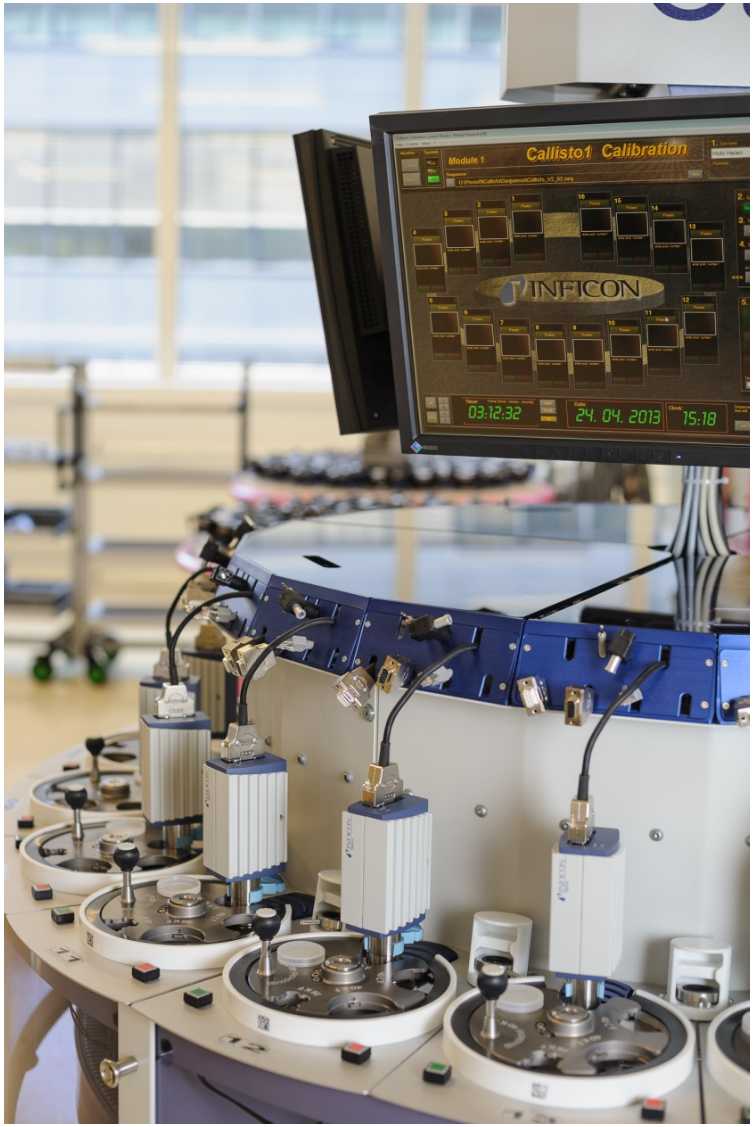

Optical Methods

INFICON Optical Diaphragm Gauge

NIST FLOC

$$\lambda_{gas} = \frac{c}{nf}$$

$$n - 1 \propto \frac{p}{k_B} T$$

The Fixed Length Optical Cavity
FLOC

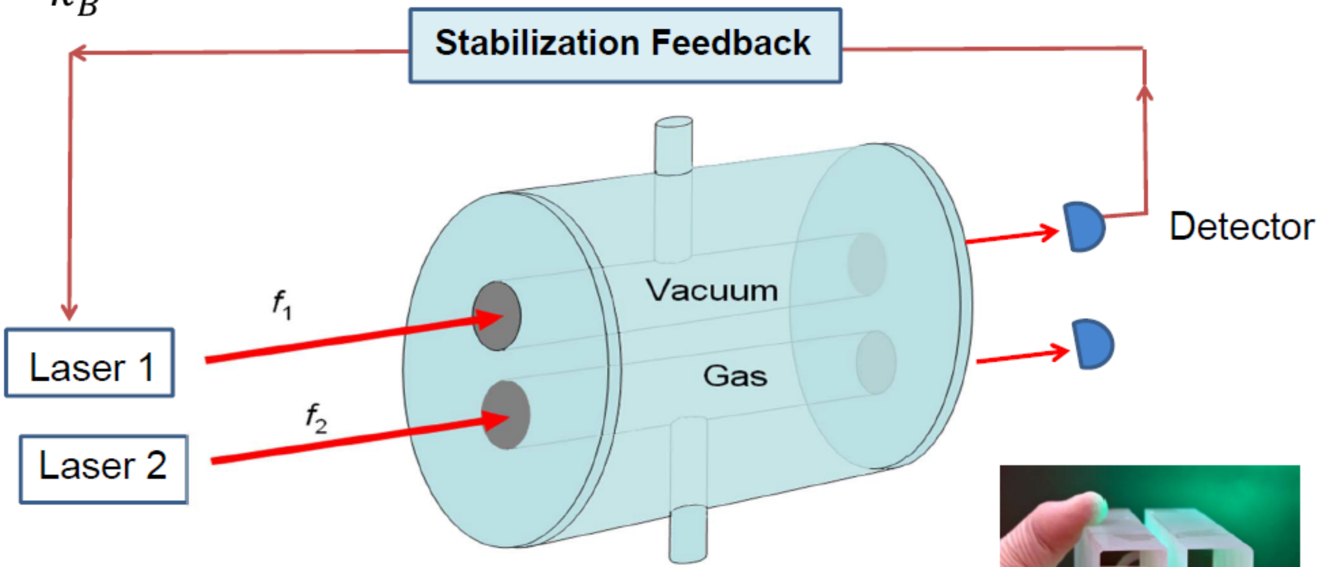

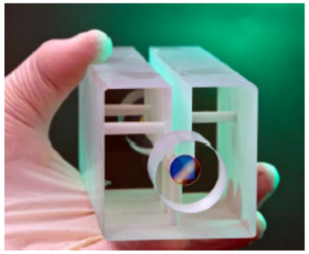

Pressure determined from $f_1 - f_2$

Uncertainty goal (k=1): 2.1 ppm at 1 atm

NIST

NIST FLOC

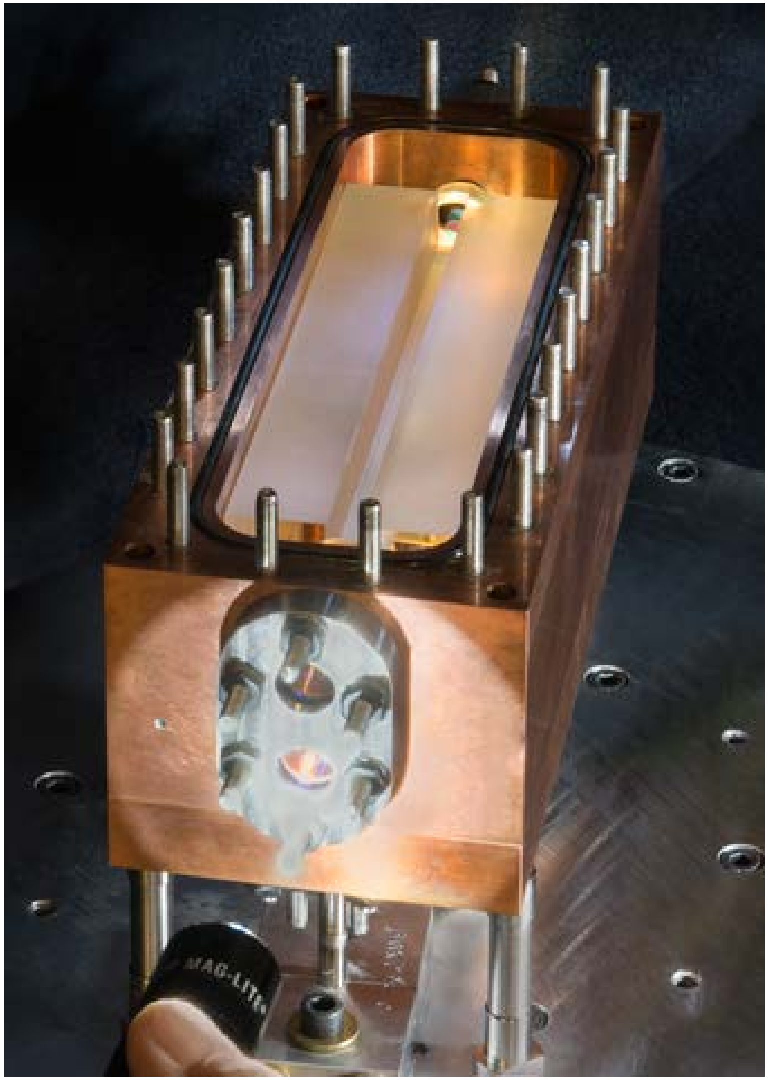

NIST FLOC

- Compared to NIST Hg Standard
  - 35x better resolution 0.1 mPa (10^{-6} mbar),
    Cube: 0.95 ppm F.S. = 9.6×10^{-4} mbar @ Atm)
  - 100 x faster
  - Covers 8 decades of pressure in one instrument
  - Negligible hysteresis 8 μPa/hr

- Customer calibrations will be done now on new system

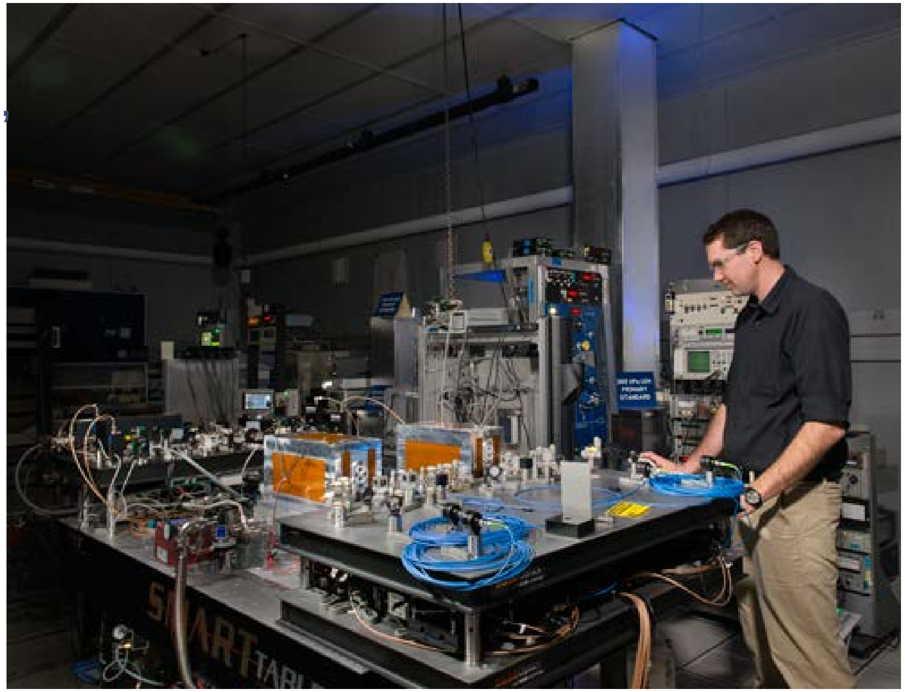

FLOC: 15.5 x 5 x 5 cm^3 + laser optics

Cube: 19.45 x 11.0 x 10.3 cm^3 incl. all electronics

University of Umea: GAMOR

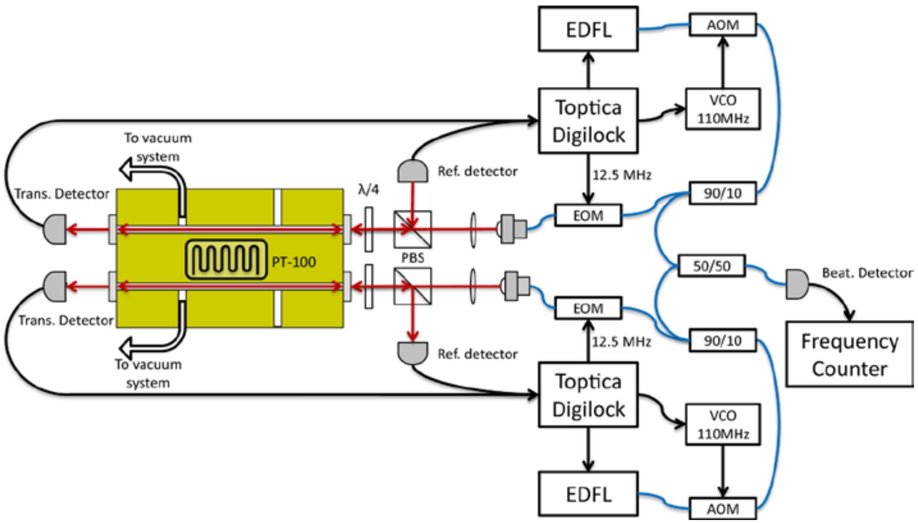

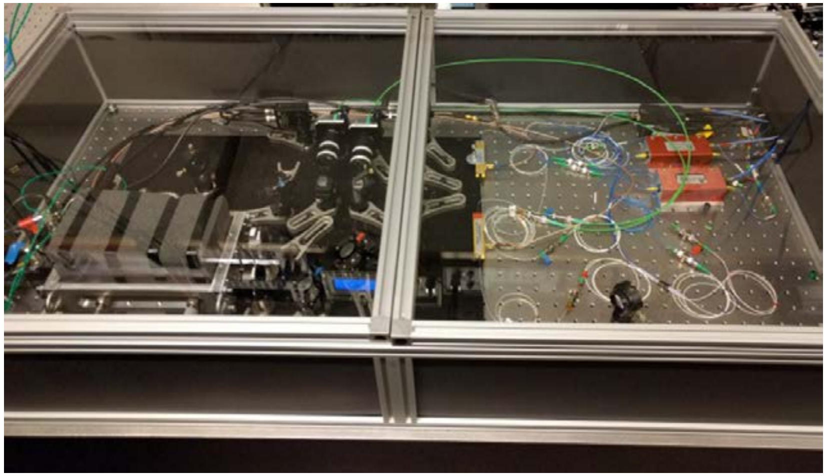

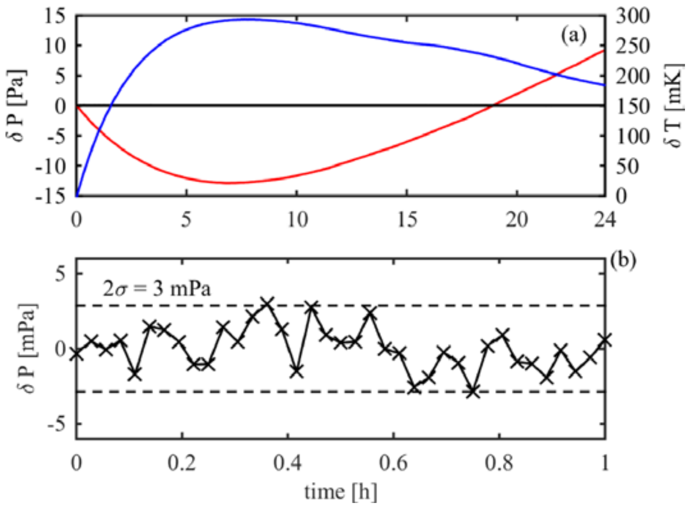

Silander et al., Gas modulation refractometry for high-precision assessment of pressure under non-temperature-stabilized conditions, JVST A36, 03E105 (2018)

Summary

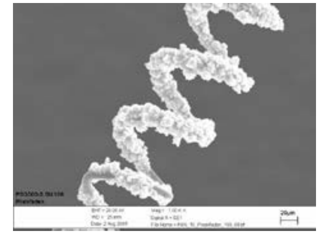

- Gauges are becoming more robust for industrial processes
- To achieve this requires a deep understanding of many different fields of science
- Optical methods are being established for standards laboratories

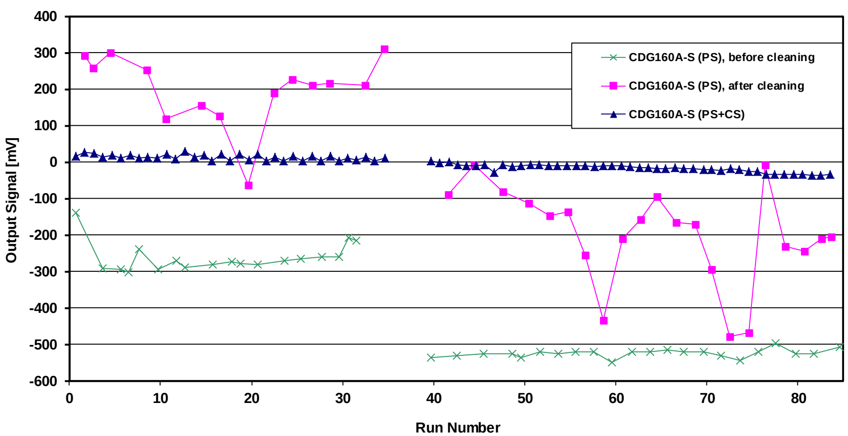

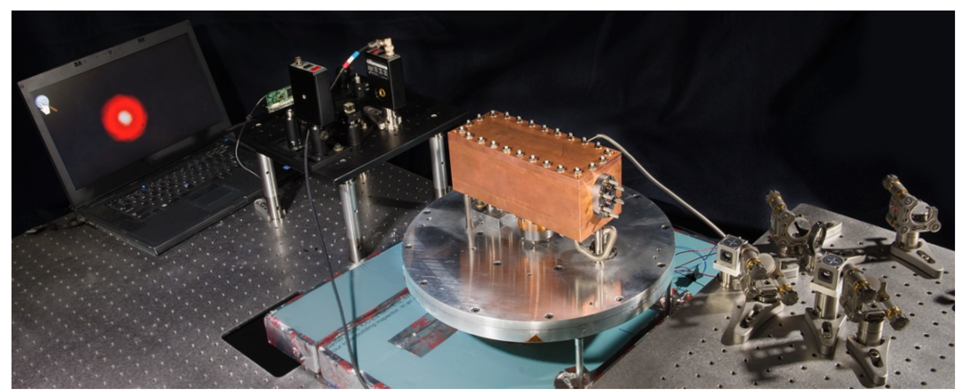

www.nist.gov/https://www.nist.gov/pml/nist-chip-photonic-sensors-pressure-and-light

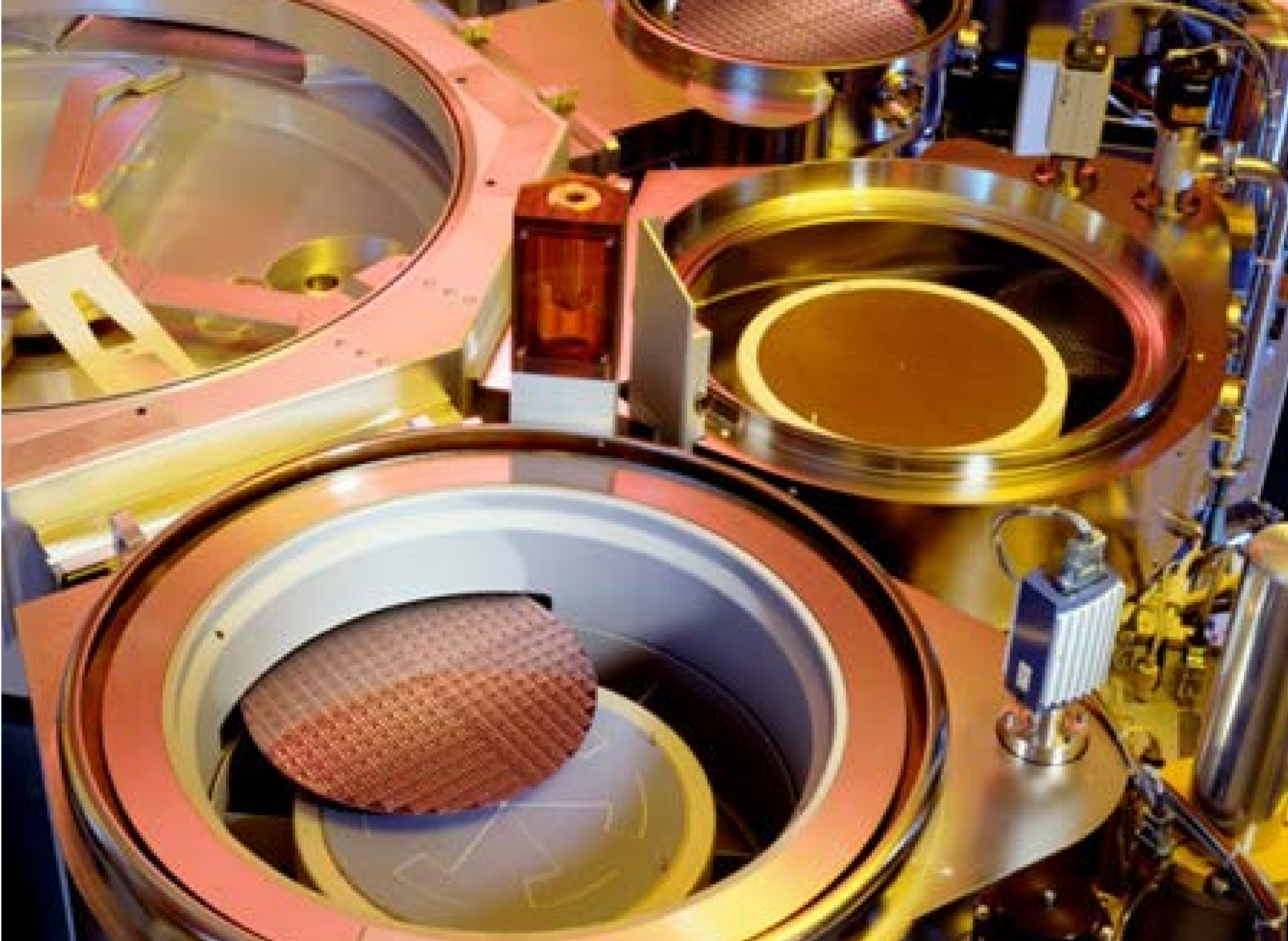

Vacuum Control in Liechtenstein